

**İSTANBUL TECHNICAL UNIVERSITY ★ INSTITUTE OF SCIENCE AND TECHNOLOGY**

**THE SYNTHESIS AND THERMAL PROPERTIES OF  
NOVEL ORGANIC PHASE CHANGE MATERIALS**

**Ph.D. Thesis by  
Ahmet Alper AYDIN**

**Department : Chemical Engineering**

**Programme : Chemical Engineering**

**JULY 2010**



**THE SYNTHESIS AND THERMAL PROPERTIES OF  
NOVEL ORGANIC PHASE CHANGE MATERIALS**

**Ph.D. Thesis by  
Ahmet Alper AYDIN  
(506052001)**

**Date of submission : 20 May 2010  
Date of defence examination: 01 July 2010**

**Supervisor (Chairman) : Prof. Dr. Hasancan OKUTAN (ITU)  
Members of the Examining Committee : Prof. Dr. A. Tuncer ERCİYES (ITU)  
Prof. Dr. Lütfi M. ÖVEÇOĞLU (ITU)  
Prof. Dr. Ersan KALAFATOĞLU (MU)  
Prof. Dr. Ahmet KAŞGÖZ (IU)**

**JULY 2010**



**İSTANBUL TEKNİK ÜNİVERSİTESİ ★ FEN BİLİMLERİ ENSTİTÜSÜ**

**YENİ ORGANİK FAZ DEĞİŞİM MALZEMELERİNİN SENTEZİ VE  
TERMAL ÖZELLİKLERİNİN BELİRLENMESİ**

**DOKTORA TEZİ  
Ahmet Alper AYDIN  
(506052001)**

**Tezin Enstitüye Verildiği Tarih : 20 Mayıs 2010**

**Tezin Savunulduğu Tarih : 01 Temmuz 2010**

**Tez Danışmanı : Prof. Dr. Hasancan OKUTAN (İTÜ)  
Diğer Jüri Üyeleri : Prof. Dr. A. Tuncer ERCİYES (İTÜ)  
Prof. Dr. Lütfi M. ÖVEÇOĞLU (İTÜ)  
Prof. Dr. Ersan KALAFATOĞLU (MÜ)  
Prof. Dr. Ahmet KAŞGÖZ (İÜ)**

**TEMMUZ 2010**



## **FOREWORD**

I would like to thank to my advisor Prof.Dr Hasancan Okutan for his kind guidance and support throughout this research. I would also like to express my gratitude to Prof.Dr. Tuncer Erciyes and Prof.Dr. Ersan Kalafatoğlu for serving on my committee.

I would like to thank to Istanbul Chamber of Industry (ICI) and members of Sectoral Committee of Manufacture of Basic Chemicals: Refik Sait Önür, Ak-Kim; Osman Şahit Kanuni, Deteks Kimya; Hüseyin Ergün, Linde Gas; Dr. Ercan Önür, Ak-Kim; Bora Uluğ, Linde Gas and Bora Değirmencioğlu, ICI.

I also thank to all members of the Chemical Engineering Department for their direct and indirect contribution.

Finally, I would like to dedicate my thesis to my dearest family. I cannot ignore their motivating attitudes and guidance throughout my thesis and my academic career.

This research has been financially supported by Istanbul Chamber of Industry, the 24<sup>th</sup> Group of Manufacture of Basic Chemicals and ITU, Institute of Science and Technology.

May 2010

Ahmet Alper AYDIN

Chemical Engineer, M.Sc.





## TABLE OF CONTENTS

	<u>Page</u>
<b>FOREWORD</b> .....	<b>v</b>
<b>TABLE OF CONTENTS</b> .....	<b>vii</b>
<b>ABBREVIATIONS</b> .....	<b>ix</b>
<b>LIST OF TABLES</b> .....	<b>xi</b>
<b>LIST OF FIGURES</b> .....	<b>xiii</b>
<b>SUMMARY</b> .....	<b>xv</b>
<b>ÖZET</b> .....	<b>xvii</b>
<b>1. INTRODUCTION</b> .....	<b>1</b>
1.1 Basic Thermodynamics of Thermal Energy Storage with Phase Change Materials.....	2
1.1.1 Latent heat of solid-liquid phase change.....	4
1.1.2 Latent heat of liquid-gas phase change .....	5
1.1.3 Latent heat of solid-solid phase change .....	5
1.1.4 Thermo-physical, chemical and economic requirements of PCMs .....	6
1.2 Major Applications of PCMs .....	7
1.2.1 Thermal storage of solar energy.....	8
1.2.2 Building applications .....	12
1.2.2.1 PCM trombe wall.....	12
1.2.2.2 PCM wallboards .....	13
1.2.2.3 Concrete blocks with impregnated PCM.....	14
1.2.3 Conservation and transportation of temperature sensitive materials .....	16
1.2.4 New PCM technological innovations .....	16
1.3 Scope of the PhD Research .....	18
<b>2. SOLID – LIQUID PCMs</b> .....	<b>19</b>
2.1 Classes of Materials .....	20
2.1.1 Inorganic phase change materials .....	20
2.1.2 Organic phase change materials.....	23
2.2 Commercial PCMs .....	28
2.3 Stability of PCMs under Extended Thermal Cycling .....	29
2.4 Encapsulation of PCMs.....	31
2.4.1 Macroencapsulation .....	32
2.4.2 Microencapsulation.....	33
<b>3. FATTY ACID ESTERS</b> .....	<b>35</b>
3.1 Esterification and Fatty Acid Esters.....	35
3.2 Esterification Reactions .....	36
3.2.1 Esterification without catalyst.....	36
3.2.1.1 Esterification without catalyst under vacuum .....	37
3.2.2 Fischer esterification.....	39
3.2.3 Mitsunobu reaction .....	41
3.2.4 Reaction with acyl halides .....	43

3.2.5 Reaction with acid anhydrides .....	43
3.2.6 Reaction with carboxylate salts .....	44
3.2.7 Steglich esterification .....	44
<b>4. POLYURETHANE .....</b>	<b>45</b>
4.1 Polyurethane Rigid Foam .....	48
<b>5. MATERIALS AND METHODS.....</b>	<b>53</b>
5.1 Materials .....	53
5.2 Instrumentation.....	54
5.2.1 Differential scanning calorimeter (DSC) .....	54
5.2.2 Thermogravimetric analysis (TGA) .....	55
5.2.3 DNA thermal cycler .....	55
5.2.4 Fourier transform infrared spectroscopy (FT-IR) analysis .....	56
5.2.5 Optical microscope imaging.....	56
5.2.6 Scanning electron microscope (SEM) imaging.....	56
5.2.7 X-ray diffraction (XRD).....	56
5.3 Synthesis.....	57
5.3.1 Synthesis of high-chain fatty acid esters .....	57
5.3.2 Synthesis of polyurethane rigid foam and composite .....	58
5.3.3 Characterization of high-chain fatty acid esters and polyurethane rigid foam with/without PCM.....	59
<b>6. RESULTS AND DISCUSSIONS .....</b>	<b>61</b>
6.1 Synthesis of High-Chain Fatty Acid Esters.....	61
6.2 Chemical and Thermal Characterization of High-Chain Fatty Acid Esters .....	62
6.2.1 FT-IR analysis .....	62
6.2.2 DSC analysis .....	65
6.2.2.1 Determination of phase change enthalpies and temperatures .....	65
6.2.2.2 The effect of ester bond on the thermal properties of the organics .....	71
6.2.2.3 Determination of change in thermal properties with extended cycling .....	76
6.2.2.4 Determination of specific heat capacity ( $C_p$ ) of the novel organic PCMs .....	80
6.2.3 Thermogravimetric analysis of the novel organic PCMs.....	84
6.2.3.1 The effect of the ester bond on gravimetric analyses of the organics... ..	87
6.3 Synthesis of Polyurethane Rigid Foam – PCM (PU – PCM) Composite .....	89
6.4 Chemical and Thermal Analyses of PU – PCM Composites .....	93
6.4.1 FT-IR analysis .....	93
6.4.2 DSC analysis .....	95
6.4.2.1 Total enthalpy change of composites in a specific temperature interval .....	99
6.4.3 Thermogravimetric analysis.....	101
6.5 Optical Microscope and SEM Images of PU – PCM Composites .....	102
6.6 X-Ray Diffraction of Cetiol MM .....	107
<b>7. CONCLUSION.....</b>	<b>109</b>
<b>REFERENCES .....</b>	<b>117</b>
<b>APPENDICES.....</b>	<b>127</b>
<b>CURRICULUM VITA.....</b>	<b>131</b>

## ABBREVIATIONS

<b>ICI</b>	: Istanbul Chamber of Industry
<b>PCM</b>	: Phase change material
<b>SEM</b>	: Scanning electron microscopy
<b>FT-IR</b>	: Fourier transform infrared spectrometry
<b>TGA</b>	: Thermogravimetric analysis
<b>DSC</b>	: Differential scanning calorimetry
<b>XRD</b>	: X-ray diffraction
<b>ISO</b>	: International Organization for Standardization
<b>ASTM</b>	: American Standard Test Method
<b>PU</b>	: Polyurethane
<b>C<sub>p</sub></b>	: Specific heat capacity
<b>THF</b>	: Tetrahydrofuran
<b>DNA</b>	: Deoksiribonükleik asit
<b>w/w</b>	: weight/weight
<b>SD</b>	: Standard deviation
<b>TDI</b>	: Toluen diisocyanate
<b>MDI</b>	: Diphenylmethane diisocyanate
<b>HDI</b>	: Hexamethylene diisocyanate
<b>IPDI</b>	: Isophorone diisocyanate
<b>DMC</b>	: Dimethyl carbamate
<b>MPC</b>	: Methyl phenyl carbamate
<b>MDC</b>	: Methyl diphenyl-4,4'-dicarbamate
<b>EG</b>	: Ethylene glycol
<b>BDO</b>	: 1,4-butanediol
<b>DEG</b>	: Diethylene glycol
<b>TMP</b>	: Trimethylol propane
<b>PO</b>	: Propylene oxide
<b>EO</b>	: Ethylene oxide
<b>DPG</b>	: Dipropylene glycol
<b>DMF</b>	: Dimethyl formamide
<b>DEAD</b>	: Diethyl azodicarboxylate



## LIST OF TABLES

	<b><u>Page</u></b>
<b>Table 1.1</b> : Brief comparison of different storage materials.....	3
<b>Table 1.2</b> : Basic thermal properties of some PCMs.....	5
<b>Table 1.3</b> : Thermal properties of some solid-solid phase change material.	6
<b>Table 1.4</b> : Applications of PCMs in thermal energy storage.....	8
<b>Table 2.1</b> : Thermal properties of several inorganic PCMs and their mixtures.....	22
<b>Table 2.2</b> : Thermal properties of several fatty acids and their mixtures.....	24
<b>Table 2.3</b> : Thermal properties of several paraffins and polyethylene glycols.....	26
<b>Table 2.4</b> : Thermal properties of several low-chain fatty acid esters.....	27
<b>Table 2.5</b> : Thermal properties of several commercial PCMs.....	29
<b>Table 2.6</b> : Latent heat values (kJ/kg) after repeated thermal cycles.....	30
<b>Table 3.1</b> : The yields of ester formation in the presence of catalyst.....	37
<b>Table 5.1</b> : High-chain fatty acid esters of myristyl alcohol.....	57
<b>Table 5.2</b> : Modified polyurethane rigid foam formulation with/without PCM. ....	59
<b>Table 6.1</b> : Phase change temperatures of the novel organic PCMs.....	65
<b>Table 6.2</b> : The phase change enthalpies of the novel organic PCMs.....	67
<b>Table 6.3</b> : Brief comparison of the selected PCMs with the results of the presented work.....	68
<b>Table 6.4</b> : Phase change temperatures of the n-alkanes and PCMs.....	74
<b>Table 6.5</b> : Phase change enthalpies of the n-alkanes and PCMs.....	75
<b>Table 6.6</b> : Comparison of the thermal properties of the selected fatty acids and the related fatty esters.....	76
<b>Table 6.7</b> : The percentage changes in the phase change temperatures after thermal cycling.....	77
<b>Table 6.8</b> : The percentage changes in the phase change enthalpies after thermal cycling.....	78
<b>Table 6.9</b> : Coefficients of the second order polynomials in solid state.....	83
<b>Table 6.10</b> : Coefficients of the second order polynomials in liquid state....	83
<b>Table 6.11</b> : Average specific heat capacity ( $C_p$ ) of solid and liquid phases..	84
<b>Table 6.12</b> : Thermal decomposition temperatures of high-chain fatty acid esters.....	85
<b>Table 6.13</b> : Onset decomposition temperatures of the materials.....	88
<b>Table 6.14</b> : Basic polyurethane rigid foam formulation.....	90
<b>Table 6.15</b> : The thermal properties of the PU – PCM composites.....	96
<b>Table 6.16</b> : The total heat absorbed by reference foam and PU – PCM composites.....	100
<b>Table 6.17</b> : TGA results of the PU – PCM composites.....	101



## LIST OF FIGURES

	<u>Page</u>
<b>Figure 1.1</b> : Several methods for thermal energy storage.....	2
<b>Figure 1.2</b> : Temperature – time diagram for heating of a material.....	3
<b>Figure 1.3</b> : Latent heat storage unit using flat containers for encapsulating the PCM.....	9
<b>Figure 1.4</b> : Simplified sketch of a thermal storage unit employing two types of PCM.....	9
<b>Figure 1.5</b> : Photograph of the air heating system. A, collector assembly with energy storage and air-heating subsystems; B, heated space.....	11
<b>Figure 1.6</b> : Cross-sectional view of the collector assembly.....	12
<b>Figure 1.7</b> : South wall temperature with and without PCM.....	15
<b>Figure 2.1</b> : Classes of PCMs and their range melting temperature and enthalpy.....	19
<b>Figure 2.2</b> : Heat flow curves of eutectic mixture and its components.....	25
<b>Figure 2.3</b> : Experimental PCM storage system using three waxes.....	32
<b>Figure 3.1</b> : Esterification apparatus; (A) thermometer, (B) thermometer, (C) reaction flask and (D) drying bulb.....	38
<b>Figure 3.2</b> : The mechanism of Fischer esterification.....	41
<b>Figure 3.3</b> : Mitsunobu reaction.....	41
<b>Figure 3.4</b> : The mechanism of Mitsunobu reaction.....	42
<b>Figure 3.5</b> : Ester formation with acid halides.....	43
<b>Figure 3.6</b> : Ester formation with acid anhydrides.....	43
<b>Figure 3.7</b> : Ester formation with carboxylate salts.....	44
<b>Figure 3.8</b> : Steglich esterification.....	44
<b>Figure 4.1</b> : Chemical structures of pure MDI.....	46
<b>Figure 4.2</b> : Overall reaction of polyurethane formation.....	47
<b>Figure 4.3</b> : Comparison of thermal insulation performance of several materials.....	49
<b>Figure 4.4</b> : General chemical structure of polymeric MDI.....	50
<b>Figure 6.1</b> : FT-IR spectra of (a) hexadecanoic acid and (b) tetradecanol....	63
<b>Figure 6.2</b> : FT-IR spectra of (a) Cetiol MM and (b) 14 – 14.....	64
<b>Figure 6.3</b> : FT-IR spectra of (a) 14 – 12, (b) 14 – 16 and (c) 14 – 17.....	64
<b>Figure 6.4</b> : Modified graph of Mehling and Cabeza (2008).....	69
<b>Figure 6.5</b> : Heat flow graphs of (a) 14 – 12, (b) 14 – 17 and (c) 14 - 16.....	70
<b>Figure 6.6</b> : Heat flow graphs of (a) Cetiol MM and (b) 14 – 14.....	71
<b>Figure 6.7</b> : The chemical structures of n-alkanes and fatty acid esters.....	72
<b>Figure 6.8</b> : Heat flow graphs of (a) 14 – 12 and (b) n-hexacosane.....	73
<b>Figure 6.9</b> : Heat flow graphs of (a) 14 – 16 and (b) n-triacontane.....	73
<b>Figure 6.10</b> : Heat flow graphs of (a) 14 – 18 aged and (b) 14 – 18.....	79
<b>Figure 6.11</b> : Heat flow graphs of (a) Cetiol MM and (b) Cetiol MM aged....	79

<b>Figure 6.12 :</b>	An example of specific heat analysis.....	81
<b>Figure 6.13 :</b>	The specific heat capacity analysis of 14 – 16: (a) specific heat change and (b) heat flow.....	81
<b>Figure 6.14 :</b>	The specific heat capacity analysis of 14 – 13: (a) specific heat change and (b) heat flow.....	82
<b>Figure 6.15 :</b>	Thermal decomposition graphs of (a) 14 – 14 and (b) Cetiol MM.....	86
<b>Figure 6.16 :</b>	Thermal decomposition graphs of (a) 14 – 12, (b) 14 – 16 and (c) 14 – 17.....	87
<b>Figure 6.17 :</b>	Thermal decomposition graphs of (a) 14 – 12 and (b) n-hexacosane.....	88
<b>Figure 6.18 :</b>	Thermal decomposition graphs of (a) n-triacontane and (b) 14 – 16.....	89
<b>Figure 6.19 :</b>	The PU – PCM composites: (a) reference, (b) 9.2 (w/w) %, (c) 13.9 (w/w) % and (d) 22.6 (w/w) % blocks.....	92
<b>Figure 6.20 :</b>	FT-IR spectra of (a) polymeric MDI, (b) polyether polyol and (c) reference.....	94
<b>Figure 6.21 :</b>	FT-IR spectra of (a) reference, (b) 9.2 (w/w) %, (c) 13.9 (w/w) %, (d) 22.6 (w/w) % PU – PCM composites and (e) Cetiol MM.....	95
<b>Figure 6.22 :</b>	Heat flow graphs of (a) reference and (b) 22.6 (w/w) % PU – PCM composite.....	97
<b>Figure 6.23 :</b>	Heat flow graphs of (a) 22.6 (w/w) %, (b) 13.9 (w/w) % and (c) 9.2 (w/w) % PU – PCM composites.....	99
<b>Figure 6.24 :</b>	Total enthalpy change of 22.6 (w/w) % PU – PCM composite: (a) specific heat change and (b) heat flow.....	100
<b>Figure 6.25 :</b>	Overlapped thermal decomposition graphs of (a) reference, (b) 9.2 (w/w) %, (c) 13.9 (w/w) % and (d) 22.6 (w/w) % PU – PCM composites.....	102
<b>Figure 6.26 :</b>	The optical microscope image of reference foam.....	103
<b>Figure 6.27 :</b>	The optical microscope image of 9.2 (w/w) % PU – PCM composite.....	103
<b>Figure 6.28 :</b>	The optical microscope image of 13.9 (w/w) % PU – PCM composite.....	104
<b>Figure 6.29 :</b>	The optical microscope image of 22.6 (w/w) % PU – PCM composite.....	104
<b>Figure 6.30 :</b>	SEM image of 9.2 (w/w) % PU – PCM composite.....	105
<b>Figure 6.31 :</b>	SEM image of 13.9 (w/w) % PU – PCM composite.....	106
<b>Figure 6.32 :</b>	SEM image of 22.6 (w/w) % PU – PCM composite.....	106
<b>Figure 6.33 :</b>	XRD spectra of Cetiol MM.....	107
<b>Figure A.1 :</b>	FT-IR spectra of (a) 14 – 13, (b) 14 – 15 and (c) 14 – 19.....	128
<b>Figure A.2 :</b>	FT-IR spectra of (a) 14 – 18 and (b) 14 – 20.....	128
<b>Figure A.3 :</b>	Heat flow graphs of (a) 14 – 13, (b) 14 – 15 and (c) 14 – 19.....	129
<b>Figure A.4 :</b>	Heat flow graphs of (a) 14 – 18 and (b) 14 – 20.....	129
<b>Figure A.5 :</b>	Thermal decomposition graphs of (a) 14 – 13, (b) 14 – 15 and (c) 14 – 19.....	130
<b>Figure A.6 :</b>	Thermal decomposition graphs of (a) 14 – 18 and (b) 14 – 20..	130



## **THE SYNTHESIS AND THERMAL PROPERTIES OF NOVEL ORGANIC PHASE CHANGE MATERIALS**

### **SUMMARY**

The energy consumption of the world's population increased drastically during the last decades with increased fossil fuel consumption and carbon dioxide emissions. However, world's limited crude oil reserves and rise in barrel prices triggered the researches on utilization of renewable energy sources and energy efficiency. Concerning the energy efficiency issue, "thermal energy storage" plays an important role in energy conservation and reducing the costs with less fuel consumption. Thermal energy storage is very important when there is a mismatch between the supply and consumption of energy. Thermal energy storage systems provide the potential to attain energy savings, which in turn reduce the environment impact, related to energy use. Thermal energy can be stored in media where materials with high phase change enthalpy incorporated to absorb heat at constant temperatures and release the same during the reverse process.

As being conscious of the energy problems and related environmental issues, this PhD research is consisted of the synthesis and thermal analyses of novel "organic phase change materials" and enhancement of the thermal properties of "polyurethane rigid foam" with PCM to improve its insulation property.

In this research, a new group of materials, which is high-chain fatty acid esters of myristyl alcohol, has been successfully introduced with related thermal and chemical analyses for thermal energy storage. High-chain fatty acid esters of myristyl alcohol have been synthesized according to the esterification method of Baykut and Aydın (1969) and analyzed to determine their thermal properties. The melting temperatures of the introduced materials and one commercial product are spread between 38°C and 53°C and the phase change enthalpy values vary between 201 kJ/kg and 220 kJ/kg which are quite high among the known organic and inorganic phase change materials. In addition to the determination of the latent thermal properties of the materials, thermal reliability analyses after 1000 extended thermal cycles show that the introduced high-chain fatty acid esters do not have any significant changes in the thermal properties. Also, the materials are found to be thermally stable with onset decomposition temperatures starting from 275°C under nitrogen atmosphere.

Besides the synthesis and determination of the thermal properties of the high-chain fatty acid esters, the effect of the ester bond on the thermal properties of the materials has also been investigated in this research to find out the contribution of the chemical structure. The effect of the ester bond on the thermal behavior during DSC and thermogravimetric analyses have been studied with respect to aliphatic n-alkanes with the same carbon number. The results show that the ester bond in the chemical structure makes the high-chain fatty acid esters suitable for thermal energy storage.

In addition to the investigation of a new group of organic phase change materials, utilization of the introduced commercial product in enhancement of the thermal properties of polyurethane rigid foam insulation material has also been studied. According to the analyses, the total heat absorption capacity is improved up to 34 % and it is directly proportional to the PCM content. This means that approximately 30 % thinner foam blocks can be used to maintain the same insulation performance.

The homogenous and fine distribution of the PCM content provides uniform thermal response in foam blocks when larger scale production is under consideration. Hence, it maintains the validity of the presented data for pilot scale production. The homogeneous distribution of the PCM content and the particle size distribution between 2 $\mu$ m and 4 $\mu$ m throughout the polymer matrix have been presented with x400 and x2000 optical microscope and SEM images, respectively.

# YENİ ORGANİK FAZ DEĞİŞİM MALZEMELERİNİN SENTEZİ VE TERMAL ÖZELLİKLERİNİN BELİRLENMESİ

## ÖZET

Son on yılda artan dünya enerji talebi ve bu enerji talebini karşılamaya yönelik enerji arzının sınırlı olmasına karşılık artan fosil kaynaklı yakıt kullanımı sera gazı emisyonlarının artmasına sebep olmaktadır. Ancak, çevresel faktörler, dünya petrol rezervinin sınırlı olması ve bununla beraber yükselen ham petrol varil fiyatları, araştırmacıları yenilenebilir enerji kaynaklarının kullanılması ve enerji verimliliği konularına yöneltmiştir. Fosil yakıtlarına bağımlılığın azaltılmaya çalışıldığı günümüzde yenilenebilir enerji ve enerji verimliliği iki önemli konudur. Enerji kayıplarının azaltılarak enerjinin daha verimli kullanılması enerji tüketimini azaltarak enerji maliyetlerini düşürmeye önemli ölçüde yardımcı olmakta ve dolayısıyla sera gazı emisyonlarının ve hava kirliliğinin azaltılmasına önemli destek vermektedir.

Yaşanan enerji dar boğazı ve buna bağlı çevresel konulardan ötürü bu doktora tezinde, yeni “organik faz değişim malzemeleri”nin sentezi ve termal özelliklerinin belirlenmesi ile en yaygın yalıtım malzemelerinden biri olan “poliüretan rijit köpük” malzemesinin termal özelliklerinin iyileştirilmesi üzerine çalışılmıştır.

Bu çalışmada, ısı enerjisinin depolanmasına yönelik olarak yeni bir madde grubu olan tetradekanol yüksek esterlerinin sentezi ile termal ve kimyasal analizleri başarı ile tamamlanmıştır. 9 adet tetradekanol yüksek esteri Baykut ve Aydın (1969) tarafından geliştirilen esterleşme metoduna göre sentezlenmiş ve 1 adet ticari ürün ile beraber termal özellikleri detaylı olarak incelenmiştir. Tez kapsamında sunulan malzemelerin faz değiştirme sıcaklıkları 38°C ve 53°C arasında ve faz değiştirme entalpileri 201 kJ/kg ve 220 kJ/kg arasında değişmektedir. Bu entalpi değerleri literatürde bilinen organik ve inorganik faz değişim malzemeleri arasında oldukça yüksektir. Malzemelerin 1000 termal döngü sonrasında termal değerlerinin güvenilirliğinin tespiti için yapılan analizler tetradekanol yüksek esterlerinin özelliklerinde belirgin değişikliklerin olmadığını göstermiştir. Ayrıca, yapılan thermal dayanıklılık analizlerine göre de malzemeler azot ortamında oldukça dayanıklıdır ve termal bozunma onset sıcaklıkları 275°C’den başlamaktadır.

Yüksek zincir yağ asidi esterlerinin sentezi ve termal özelliklerinin belirlenmesine ek olarak, ester yapısında bulunan ester bağının termal özelliklerde yaptığı etki incelenerek kimyasal yapının analiz sonuçlarına katkılarının neler olduğuna da açıklık getirilmiştir. Ester bağının termal davranımdaki etkisi DSC ve termogravimetrik analizler ile aynı karbon sayısına sahip alifatik n-alkanlara karşılaştırılarak araştırılmıştır. Bulunan sonuçlar ışığında, yapıda bulunan ester bağının malzemelerin ısı depolamada kullanılabilmelerini sağlayacak özellikler kattığı bulunmuştur.

Ayrıca, bu doktora çalışması kapsamında sunulan yeni organik faz değişim malzemelerinden ticari olan madde, dünya üzerindeki en yaygın yalıtım malzemelerinden biri olan poliüretan rijit köpüğün termal özelliklerinin iyileştirilmesinde kullanılmıştır. Yapılan analizler sonucunda kompozit malzemenin ısı depolama kapasitesinin % 34'e kadar artış gösterdiği belirlenmiş ve bu artışın faz değişim malzemesi ile doğrudan orantılı olduğu görülmüştür. Bu iyileşme yaklaşık % 30 daha ince köpük katmanının benzer yalıtım kabiliyeti gösterebileceğini belirtmektedir.

Daha büyük boyutta üretim söz konusu olduğunda, faz değişim malzemesinin yapıda homojen ve ince dağılmış olması köpük bloklarının düzgün termal davranım göstermesini sağlayacaktır. Ayrıca, bu sayede bu çalışmada sunulan analiz sonuçlarının pilot ölçek üretim için de geçerli olabileceği sonucunu ortaya çıkaracaktır. Sentezlenmiş olan kompozit malzemelerde faz değişim malzemesinin yapıda homojen dağıldığı ve partikül boyutu dağılımının 2µm ve 4µm arasında olduğu x400 ve x2000 optik mikroskop ve SEM görüntüleri ile çalışmada sunulmuştur.

## **1. INTRODUCTION**

The increase in fuel prices and level of greenhouse gas emissions lead scientists to search of new and renewable energy sources. In today's world, utilization of renewable energy sources and enhanced energy efficiency are very important issues to cut down the dependency on the supply countries of fossil fuels and to reduce the carbon dioxide emissions. More efficient utilization of various sources of energy makes the systems more cost-effective by reducing the loss of energy with the help of energy storage. Therefore, development of energy storage devices is as important as utilization of renewable energy sources.

Thermal energy storage is very important when there is a mismatch between the supply and consumption of energy. Thermal energy storage systems provide the potential to attain energy savings, which in turn reduce the environment impact, related to energy use. In fact, these systems provide a valuable solution for correcting the mismatch and today, there is increasing interest related to thermal applications such as space and water heating, waste heat utilization, cooling and air-conditioning (Prakash, 1985; Maruoka, 2003; Wang, 2008).

The best known method of thermal energy storage is by changing the temperature of a material, which is called sensible heat storage. In space heating with hot water circulating radiators or under floor heating systems, the surrounding walls or floor and tiles are very good examples of sensible heat storage volumes. Even though sensible heat storage is a very common daily operation, thermal storage with changing phase of a material is more effective and advantageous, in terms of the amount of energy stored in the material. As the material melts or solidifies at a constant temperature, the stored energy is gained or released at that particular temperature in greater extent. This type of energy storage is called "latent heat storage", because it cannot be felt due to the constant phase change temperature. The best and the oldest examples are cold storage with ice and snow which were intensively used by ancient civilizations.

## 1.1 Basic Thermodynamics of Thermal Energy Storage with Phase Change Materials

A Phase Change Material (PCM) is a substance with high latent heat of fusion which is capable of storing or releasing large amounts of energy during melting and freezing at certain temperatures.

Thermal energy storage can be accomplished either by using sensible heat storage or latent heat storage. Sensible heat storage has been used for centuries in buildings to store thermal energy, but much larger volume of material is required to store the same amount of energy, compared to latent heat storage. Several methods for thermal energy storage are schematically summarized in Figure 1.1.

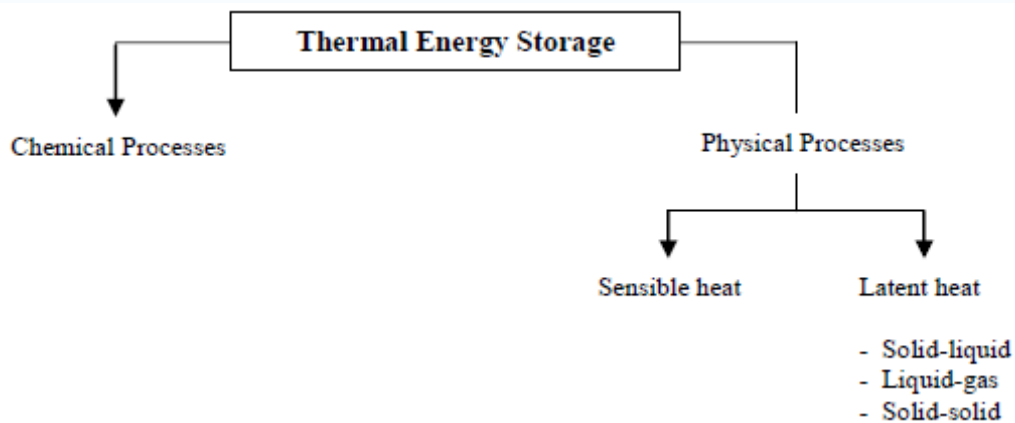


**Figure 1.1** : Several methods for thermal energy storage (Sharma, 2009).

During physical processes of thermal energy storage, temperature of a PCM rises initially as it absorbs heat; it performs like conventional storage materials. However, unlike conventional storage materials, when it reaches the temperature at which it changes phase, it absorbs large amounts of heat without a significant rise in temperature. When the ambient temperature around the material falls, the PCM releases its stored latent heat. They store much more heat per unit volume than conventional storage materials such as water, masonry, or rock (Hasnain, 1998). The comparison of conventional storage materials and phase change materials is given in Table 1.1.

**Table 1.1 :** Brief comparison of different storage materials (Hasnain, 1998).

Property	Rock	Water	An Organic PCM	An Inorganic PCM
Density, kg/m <sup>3</sup>	2240	1000	800	1600
Specific Heat, kJ/kg.K	1	4.2	2	2
Latent Heat, kJ/kg	-	-	190	230
Latent Heat, kJ/m <sup>3</sup>	-	-	152	368
Storage Mass for 10 <sup>6</sup> J, kg	67000	16000	5300	4350
Storage Volume for 10 <sup>6</sup> J, kg	30	16	6.6	2.7
Relative Storage Mass	15	4	1.25	1
Relative Storage Volume	11	6	2.5	1

Fig. 1.2 shows the change in temperature with time during heat transfer to the material. The total amount of heat energy stored in the material can be written as following:

$$Q = m \left[ \int_{T_A}^{T_B} C_{ps}(T) dT + L_p + L + \int_{T_C}^{T_D} C_{pl}(T) dT + L_g + \int_{T_E}^{T_F} C_{pg}(T) dT \right] \quad (1.1)$$

where  $m$  is the mass of material,  $C_{ps}$  is specific heat of material in solid phase,  $C_{pl}$  is specific heat of material in liquid phase,  $C_{pg}$  is specific heat of material in gas phase,  $L_p$  is latent heat of solid-solid phase change,  $L$  is latent heat of solid-liquid phase change and  $L_g$  is the latent heat of liquid-gas phase change.

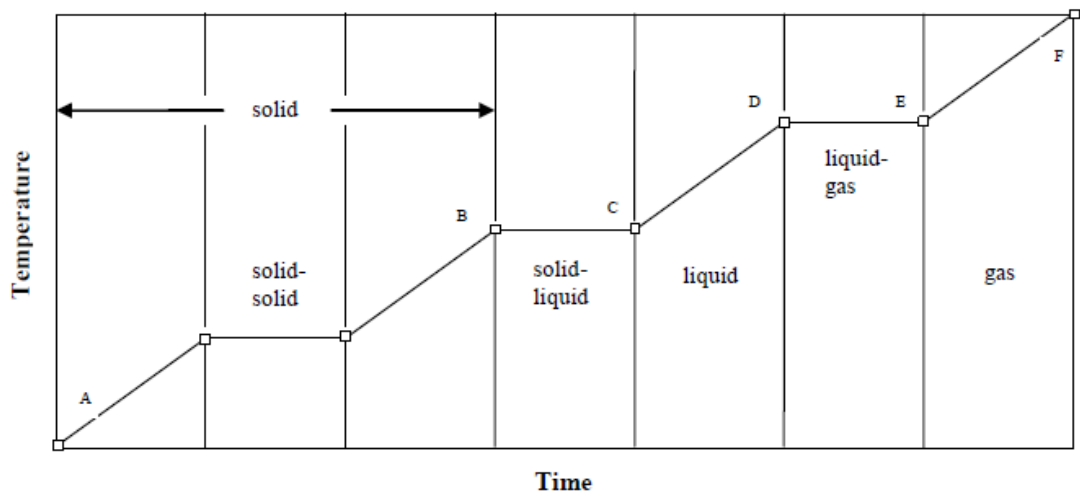


**Figure 1.2 :** Temperature – time diagram for heating of a material (Regin, 2008).

As seen from Figure 1.2, heat transferred to the storage medium as sensible heat leads to temperature increase which can be detected by sensors. Solid, liquid and gas phase specific heat capacities are usually given with respect to mass, volume or mole of material. Solids and liquids are often considered as sensible heat storage materials. On the other hand, gases cannot be used as sensible heat storage medium due to very low volumetric specific heat capacity (Hasnain, 1998; Mehling and Cabeza, 2008).

Unlike sensible heat, latent heat cannot be detected from temperature difference because phase change occurs at a constant temperature. Therefore, it is calculated from the enthalpy difference between two phases. Materials, which have high phase change enthalpy, are commonly referred to as “Phase Change Material”.

### **1.1.1 Latent heat of solid-liquid phase change**

Solid-liquid PCMs perform like conventional storage materials at the beginning; their temperature rises as they absorb heat. However, when they reach the melting temperature at which they melt, they absorb much larger amount of heat without significant rise in temperature. If heating is continued after phase change is completed, the further heat transferred is stored as sensible heat in the material. This method of storage is reversible for continuous storage of heat or cold.

It is important to clarify that the reversible process of heat storage must be continuous for long periods of time and this property is crucial for utilization of materials. Therefore, extended thermal cycling test results must be taken into consideration before decision making. Extended thermal cycling test is explained in detail in the following chapters.

There are many solid-liquid phase change materials with different melting temperatures and latent heat capacities to be used in different applications. Some examples of the materials with different chemical structures are given in Table 1.2 to show the broad diversity of the basic thermal properties.



**Table 1.2 :** Basic thermal properties of some PCMs.

	<b>Melting Temperature (°C)</b>	<b>Latent Heat (kJ/kg)</b>
Na <sub>2</sub> S <sub>2</sub> O <sub>3</sub> .5H <sub>2</sub> O (Naumann, 1989)	48	201.0
Ba(OH) <sub>2</sub> .8H <sub>2</sub> O (Lane, 1980)	78	265.7
MgCl <sub>2</sub> .6H <sub>2</sub> O (Lane, 1980)	117	168.6
Polyglycol E600 (Lane, 1980)	22	127.2
Erythritol (Kakuichi, 1998)	118	339.8
Capric Acid (Lane, 1980)	32	152.7

### **1.1.2 Latent heat of liquid-gas phase change**

Despite higher latent heat capacities, liquid-gas phase change is not employed in heat storage. Large changes in volume cause large, complex and impractical designs for constant pressure systems (Mehling and Cabeza, 2008). On the other hand, vapor pressure increases drastically in a closed system with constant volume.

### **1.1.3 Latent heat of solid-solid phase change**

In solid-solid phase changes, latent heat is accommodated with change in crystalline form of the material. Heat is stored or released as the material is transformed from one crystalline form to another. However, this type of phase change has generally less latent heat capacity, compared to solid-liquid phase change.

Some hydrocarbon molecular crystals show reversible solid phase transformations by absorbing heat. Some of these materials have potential usage in solar heated buildings. Pentaerythritol, pentaglycerine and neopentyl glycol can reversibly absorb heat with solid state crystalline transformations. These compounds have promising thermal properties to be used in thermal energy storage systems for solar applications (Benson, 1986). Thermal properties of pentaerythritol, pentaglycerine and neopentyl glycol are given in Table 1.3.

**Table 1.3 :** Thermal properties of some solid-solid phase change materials (Benson, 1986).

<b>Compound</b>	<b>Solid-state Transition Temp. (°C)</b>	<b>Latent Heat (kJ/kg)</b>
<b>Pentaerythritol</b>	187	269
<b>Pentaglycerin</b>	82	174
<b>Neopentyl Glycol</b>	48	139

Hyperbranched polyurethanes are one of the most recent polymeric solid-solid phase change systems which have been investigated by some researchers for thermal energy storage since the last decade. Several polyethylene glycol blends with different average molecular weights have been used as the soft segment of the polyurethane systems with aliphatic or aromatic diisocyanates as the hard segment. Even though these hyperbranched polyurethane systems have sharp phase change peaks at particular temperatures, the latent heat values are lower than that of polyethylene glycol, which is a drawback of solid-solid systems (Cao, 2006).

#### **1.1.4 Thermo-physical, chemical and economic requirements of PCMs**

High latent heat enthalpy and suitable melting/freezing temperatures are two fundamental requirements that a desirable PCM has to fulfill. These two properties determine the limits of the material in basic thermo-physical means (Mehling, 2008). However, there are more requirements that can be classified into thermo-physical, chemical and economic sub-groups.

Thermo-physical requirements:

- Melting temperature in the desired operating temperature range,
- High latent heat of fusion per unit volume/mass so that the required volume of the container to store a given amount of energy is less,
- High specific heat to provide additional significant sensible heat storage,
- High thermal conductivity of both solid and liquid phases to assist the charging and discharging energy of the storage system,
- Small volume change on phase transformation and small vapor pressure at operating temperature to reduce the containment problem,

- Congruent melting of the phase change material for a constant storage capacity of the material with each melting/freezing cycle
- High nucleation rate to avoid supercooling of the liquid phase,
- High rate of crystal growth, so that the system can meet demand of heat recovery from the storage system (Tyagi, 2007; Sharma, 2009).

Chemical requirements:

- Complete reversible freeze/melt cycle,
- No degradation after a large number of freeze/melt cycle,
- No corrosiveness to the construction material,
- Non-toxic, non-flammable and non-explosive material for safety (Tyagi, 2007).

Economic requirements:

- Low price
- Good recyclability for environmental and economic reasons
- Easy availability (Kennisarín, 2007; Mehling and Cabeza, 2008).

## **1.2 Major Applications of PCMs**

Today, there are many research activities to introduce new materials to the literature which have desirable properties for different thermal applications. However, there are also some materials which fulfill the requirements of different applications and researches are conducted to generate new designs for utilization of the present materials.

The applications are summarized in groups in Table 1.4 to give brief knowledge of the potential usage of PCMs and to call attention to the areas where heat efficiency can be increased with utilization of PCMs. Some of these groups are investigated in detail in the following sections.

**Table 1.4 :** Applications of PCMs in thermal energy storage  
(Zalba, 2003; Kenisarin, 2007).

1	Cooling: Reduction of installed power
2	Cooling of food, wine, daily products
3	Cooling of engines: electric and combustion engines
4	Heating and sanitary hot water
5	Medical applications: transport of blood, medicines, etc.
6	Passive storage in buildings
7	Temperature level maintenance in living places
8	Smoothing exothermic temperature peaks in chemical reactions
9	Thermal storage of solar energy
10	Thermal comfort in vehicles
11	Thermal protection of electronic devices
12	Space craft thermal applications
13	Cold or hot climate outfits

### 1.2.1 Thermal storage of solar energy

Worldwide increase in energy demands, fossil fuel shortage and concerns on the environmental issues have provided attention on the development of renewable energy sources. As a major renewable energy resource, solar energy needs efficient and effective storage systems. If no energy storage is used in solar energy systems, the major part of the energy demand will be met by the backup energy.

Extensive efforts have been made to apply the latent heat storage method to solar energy systems, where heat is required to be stored during the day for use at night. During sunshine, the heat transfer fluid gets warmer which in turn transfers heat to the PCM in contact. The PCM collects the heat energy in the form of latent heat and melts. At cloudy hours and nights, the temperature of the hot heat transfer fluid is kept stable with the energy released by the surrounding PCM layers as they change phase from liquid to solid.

The studies vary from those related to the fundamentals of heat transfer to those in which the PCM is tested in full size heat storage units. The PCM can be contained in thin flat containers, similar to plate type heat exchangers or it may be contained in small diameter tubes or honeycomb structure with the heat transfer fluid flowing along or across the tubes or it can be even more complex with utilization of two different PCMs (Lacroix, 1993; Abe, 1986; Riahi, 1993; Ismail, 1999; Farid, 1986). Figure 1.3 and 1.4 show simplified sketches of utilization of PCMs in heat transfer units.

The operational temperature range for low-temperature solar units and devices is in the temperature interval of 20°C and 80°C (Hasnain, 1998).

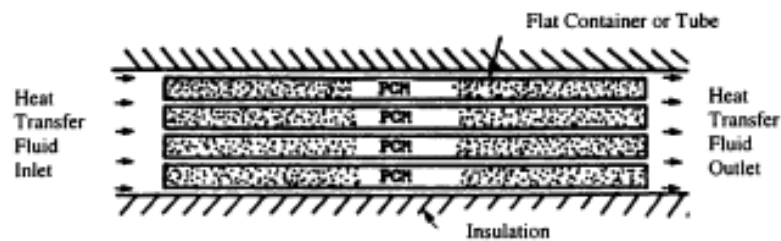


**Figure 1.3 :** Latent heat storage unit using flat containers for encapsulating the PCM (Bailey, 1976).

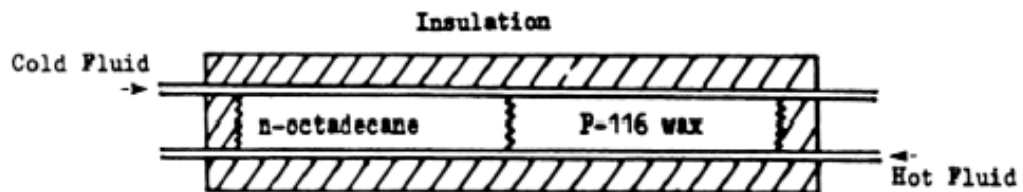


**Figure 1.4 :** Simplified sketch of a thermal storage unit employing two types of PCM (Farid, 1986).

In order to compare the solar energy storage systems based on latent heat and sensible heat storage, several researchs have been conducted to determine the contribution of PCMs. A comparative study has been carried out with two identical storage units, one containing paraffin wax as the storage material, packed in a heat exchanger made of aluminum tubes and another identical conventional storage unit with water. Both units have been separately charged by solar energy with the use of identical flat plate solar collectors. This research showed that the modified heat storage unit yields more hot water on the next day morning as compared to the conventional storage unit (Chaurasia, 2000).

Solar collectors which perform as solar energy absorbing medium and latent storage units have also been studied by researchers. In these systems, solar energy is first stored in PCM layers in the solar collector and then it is transferred to the water circulating pipes located inside the PCM.

Mettawee and Assassa (2006) investigated the thermal performance of compact phase change material solar collector. In this research, the temperature changes were recorded continuously during charging and discharging processes of heat with the change in solar intensity during the day. The effect of the water flow rate on the useful heat gain and the total heat transfer coefficients were calculated. The experimental results showed that in the charging process, the average heat transfer coefficient increases sharply with increasing PCM layer thickness as a result of increased natural convection. The useful heat gain was found to increase as the water mass flow rate increases during the discharge process.

Solar thermal storage systems can also be designed according to the utilization of air as the heat transfer fluid. Air based solar heating systems have been intensively studied to determine the thermal performance and to make comments on suitable material selection.

Morrison (1978), Khalik and Jurinak (1979) evaluated the performance of air based solar heating systems with phase change storage units. The main objective of the two works was to determine the effect of PCM latent heat and melting temperature on the thermal performance of air based solar heating systems. They concluded that the PCM should be selected on the basis of melting temperature rather than its latent heat and they also determined that utilizing sodium sulphate decahydrate as PCM requires roughly one-fourth storage volume of a pebble bed and one-half storage volume of a water tank.

Enibe (2002) tested the daytime performance of a natural convection solar air heater system with phase change material storage unit under ambient conditions involving ambient temperature variations between 19°C and 41°C and daily global radiation in the range of 4.9 – 19.9 MJ.m<sup>-2</sup>. The system was composed of a collector assembly with energy storage and air heating systems and a heated volume. Peak temperature rise of the heated air was found to be approximately 15°C with peak total efficiency of about 50%. Such a system is useful as a crop dryer for aromatic herbs, medical plants, which are sensitive to direct exposure to sunlight. Figure 1.5 and 1.6 shows a photograph and cross-sectional view of the experimental setup.



**Figure 1.5 :** Photograph of the air heating system. A, collector assembly with energy storage and air-heating subsystems; B, heated space (Enibe, 2002).

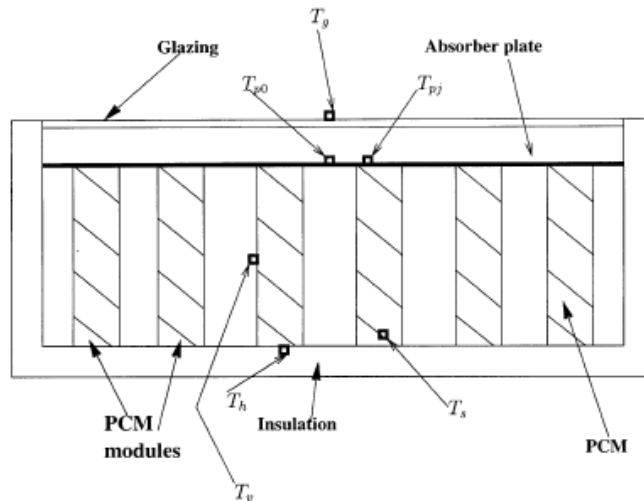


**Figure 1.6 :** Cross-sectional view of the collector assembly (Enibe, 2002).

## 1.2.2 Building applications

The utilization of PCMs in buildings can have two different goals; using natural heat that is solar energy for heating or night cold for cooling and using heat and cold sources, like heaters or air-conditioners. In any case, storage of heat or cold is necessary to match availability and demand with respect to time and power. Basically, three different options are available to use PCMs for heating and cooling of buildings.

- (i) PCMs in building walls
- (ii) PCMs in other building components
- (iii) PCMs in hot and cold storage units

### 1.2.2.1 PCM trombe wall

A trombe wall is a primary example of an indirect gain approach. It consists of a thick masonry wall on the sun-facing side of a house. A single or double layer of glass or plastic glazing is mounted in front of the wall's surface. Solar heat is collected in the space between the wall and glazing. The outside of the wall is usually black to absorb heat, which is then stored in the wall's mass. When the indoor temperature falls below that of the wall's surface, heat begins to radiate into the room.



Traditional tromble walls rely on sensible heat storage. However, PCM tromble wall is a promising concept due to greater heat storage per unit mass. A wall filled with PCM and placed on the south side of the house absorbs heat by radiation. The PCM inside the wall starts to melt and absorbs heat as the surface temperature reaches the phase change temperature of the material. Therefore, the volume required for a given amount of heat storage is less than traditional tromble walls. The total heat storage capacity is the cumulative of the sensible heat storage amount of the wall material and the latent heat of the embedded PCM bulk material.

Bourdeau (1980) tested passive storage collector walls using calcium chloride hexahydrate as a phase change material. The results showed that 8.1 cm thick PCM wall has better performance than 40 cm thick masonry wall. Several experimental and theoretical tests were conducted to investigate the reliability of PCMs in sun-facing trombe walls and it has been reported that thinner tromble walls with PCM are more desirable in comparison with traditional tromble walls for providing efficient thermal energy storage (Swet, 1980; Ghoneim, 1991; Chandra, 1985; Knowler, 1983).

#### **1.2.2.2 PCM wallboards**

The wallboards are widely used in construction of light weight buildings. Therefore, incorporation of PCM into wallboards is advantageous to increase the thermal properties of such buildings.

Kedl and Stovall (1989) and Salyer and Sircar (1990) used paraffin wax impregnated wallboard for passive solar application. They successfully demonstrated the processes in which PCM could be incorporated into wallboard either by post-manufacturing imbibing of liquid PCM into the pore space of the wallboard or by addition in the wet stage of wallboard manufacture.

Kissock et al. (1998) presented the results of an experimental study on the thermal performance of wallboards with 30 (w/w) % of commercial paraffin content. The results showed that peak temperature in the phase change test cell was up to 10°C less than the control test cell during sunny days.

Neeper (2000) investigated the thermal dynamics of PCM wallboard under daily temperature variations to provide guidelines for selecting the PCM and estimating its benefits. This research stated that the daily storage capacity is limited to 300 – 400 kJ/m<sup>2</sup>, even if the wallboard has a greater latent heat capacity. It is also stated that more PCM content might not be able to melt and solidify in a daily temperature cycle.

The companies Knauf and BASF developed a solution, which assures all the necessary properties for a commercial product and a suitable production process. These investigations were funded by the German Ministry of Economics between 1998 and 2004 under two research projects. Today, the wallboard with microencapsulated paraffin is commercially available from BTC Specialty Chemical Distribution GmbH (member of the BASF Group) with the brand name of “Micronal PCM Smartboard”. The standard size wallboard has dimensions of 2.0 m x 1.25 m x 15 mm and a weight of 11.5 kg/m<sup>2</sup>. The mass percentage of incorporated PCM is 26 wt % with storage capacity of 28.7 kJ/kg. This much of heat storage capacity makes a 1.5 cm thick wallboard equivalent to a 9 cm thick concrete wall or a 12 cm thick wall of bricks (Mehling and Cabeza, 2008).

### **1.2.2.3 Concrete blocks with impregnated PCM**

Collier and Grimmer (1979) showed that a macroencapsulated cement material within masonry building blocks results in significant thermal capacity increase compared to equivalent volume of concrete.

Hadjieva et al. (2000) investigated the heat storage capacity and thermal cycling stability of PCM-concrete composite systems with sodium thiosulphate pentahydrate as the PCM segment. They concluded that large absorption area of porous concrete serves as a good supporting matrix and improves thermal cycling stability.

Cabeza et al. (2007) presented results of two real size concrete test buildings. The PCM used in this study is Micronal from BASF with melting temperature of 26°C and phase change enthalpy of 110 kJ/kg. Each concrete panel contains 5 (w/w) % of Micronal PCM. A second test building with standard concrete was built next to the other as the reference. According to the results of this study, a temperature reduction of up to 4°C was achieved as the PCM melts and solidifies in every cycle during summer and autumn 2005. Figure 1.7 shows temperature fluctuation of the south wall with closed windows in June, 2005.

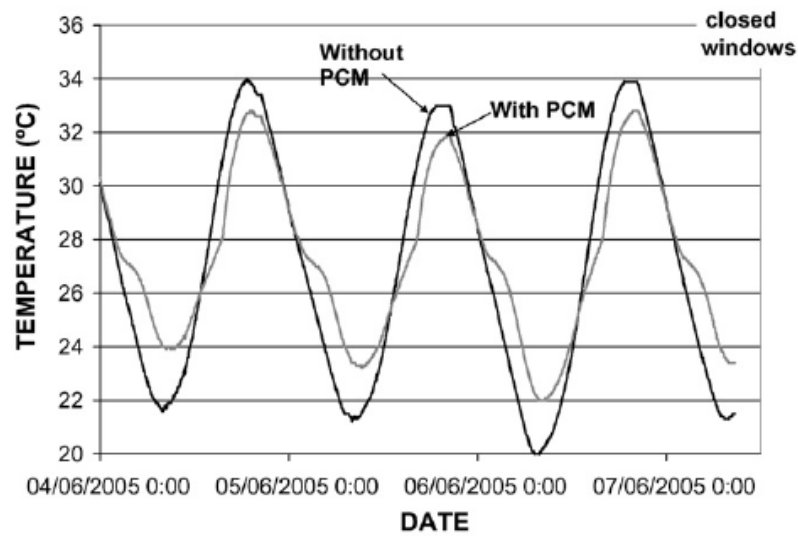


**Figure 1.7 :** South wall temperature with and without PCM (Cabeza, 2007).

### **1.2.3 Conservation and transportation of temperature sensitive materials**

In many cases of food transportation, the food temperature must be kept between certain temperature intervals. The situation is similar in transportation of sensitive medicines. Both applications are suitable for utilization of PCMs to store heat and cold in a range of several degrees. Many companies like Rubitherm GmbH and Sofrigam are in the market with different size transport boxes (Url-1; Url-2).

Electronic components tend to age and fail very fast when their operating temperature rises above a critical point. Utilization of PCMs seems to be very suitable to restrict the maximum temperature of electronic components as they act as passive materials and do not require any additional energy source (Pal and Joshi, 1996; Bellettre, 1997) For example, some batteries can show significant power drop when the operating temperature is too low, or fail when they get too hot. PCMs can be useful to maintain constant operating temperature by absorbing peak or cyclic heat loads. Jackets filled with PCM might help to minimize the effects of peak heat loads in the day when they are wrapped around batteries (Mehling and Cabeza, 2008).

### **1.2.4 New PCM technological innovations**

Scientists from Purdue University, USA have devised a new method for satellite power testing using PCMs. There are series of metal cells which contain a PCM that is liquid at high temperatures, which then freezes during hours of cold darkness, releasing its latent heat. The released heat can then be used to generate electricity by driving thermoelectric units. Because the systems generate at least three times more power than batteries of comparable size, they are seen as a possible alternative to conventional satellite solar power systems that rely on batteries (Url-3).

By having a hot converter at the start of a trip, auto emissions can be reduced up to 80%. National Renewable Energy Laboratory of USA developed a catalytic converter by using PCMs to absorb, store and release the needed heat. They modified the catalytic converter of a Ford Taurus and managed to keep it at an efficient operating temperature for up to 24 hours after the engine is shut off (Url-4).

Another interesting new innovation is utilization of PCMs in car interiors. On hot summer days, the temperature inside the passenger compartment of an automobile can rise substantially, especially when the car is parked outside and is exposed to direct sun irradiation. In order to stabilize the interior temperature while driving the car, many models are equipped with air-conditioning systems; however, providing a sufficient cooling capacity requires a lot of energy. Headliner, instrument panel and seats are suitable locations for PCM application.

In a closed passenger compartment, hot air, due to the exposure to sunlight through the windows, moves to the top and heats up the headliner. As a result, the headliner's temperature rises continuously. If PCM is applied to the headliner, it will absorb the heat without a further rise in its temperature until the PCM's melting point is reached. Based on the latent heat absorption by the PCM, the normal rise in the headliner's temperature is delayed significantly.

The thermal control feature of the PCM keeps the temperature inside the passenger compartment at a comfortable level without the need for an external energy supply. This is especially beneficial when the car is parked outside and exposed to direct sun irradiation. During the parking period, the passenger compartment in which PCM is applied to the headliner does not overheat. As a result, a lower cooling capacity is needed at the beginning of the driving process, which especially helps to save energy.

By the PCM application to a car seat, the thermal seating comfort is improved significantly, especially on hot summer days. The PCM absorbs surplus heat stored in the seat cover and heat released from the driver's body as soon as the driver starts occupying the seat. The heat transfer away from the seat's surface and the heat absorption by the PCM arranged inside the seat leads to an instant drop in the microclimate temperature until a comfortable level is reached and is maintained (Url-5).

### 1.3 Scope of the PhD Research

As the energy requirements increased greatly today, limited reserves of fossil fuels have led to a surge of interest with energy efficient applications. Efficient utilization of energy sources with new technologies can be the solution of the world's energy crisis to reduce the dependency on fossil fuels. Proper technologies that can be used to store large amounts of heat in a definite volume are the subject of researchers since decades. Energy storage plays an important role in energy conservation and reducing the costs, which is assisted by the latent heat storage. "Phase change materials" are one of the thermal storage devices which can be used to reduce costs.

In this research, the synthesis and thermal analyses of novel "organic phase change materials" for thermal energy storage at temperatures below 80°C is the core subject. The chosen temperature limit is suitable for utilization of the materials in solar units and devices and in applications which are related to thermal insulation.

The high-chain fatty acid esters of myristyl alcohol were chosen according to the preliminary analyses of some of the selected aliphatic higher esters among the synthesized and reported 84 high-chain fatty acid esters of Baykut and Aydın (1969) at the beginning of the PhD research. In addition to the promising preliminary results, it is interesting to point out that there are no thermal data available for high-chain fatty acid esters in literature except the low-chain fatty acid esters of methyl, ethyl and butyl alcohols. As a result, the main aim of this research is to investigate high-chain fatty acid esters of myristyl alcohol as novel organic phase change materials, nine of which were synthesized in laboratory at high purity and one commercial product.

In addition to the investigation of novel organic phase change materials, utilization of the introduced commercial product in enhancement of the thermal properties of the polyurethane rigid foam is the secondary goal of this research. The purpose of such a research is to find out if it is possible to combine the heat absorption properties of PCMs and polyurethane rigid foam to use thinner insulation panels of polyurethane rigid foam – PCM composites instead of the conventional ones.

## 2. SOLID – LIQUID PCMs

The oldest and a very well-known PCM over thousands of years is “ice”. Ice melts at 0°C and it has latent heat of 333.5 kJ/kg. Cold storage with ice is very effective in terms of the large amount of latent heat capacity and today, it is still being used. For temperatures below 0°C, usually water-salt eutectic mixtures are used.

In the 19th century, use of PCMs expanded to space heating in transport vehicles and in railway cars (Lane, 1983) and towards the end of 19th century, they appeared as an alternative to heating of cold spaces by fire-heated bricks or stones.

Several material classes cover the temperature range from 0°C to 150°C, such as fatty acids, paraffins, sugar alcohols as organic materials and salt hydrates with large amount of crystal water as inorganic materials. Figure 2.1 shows classes of materials that can be used as PCM with their range of temperature and enthalpy.

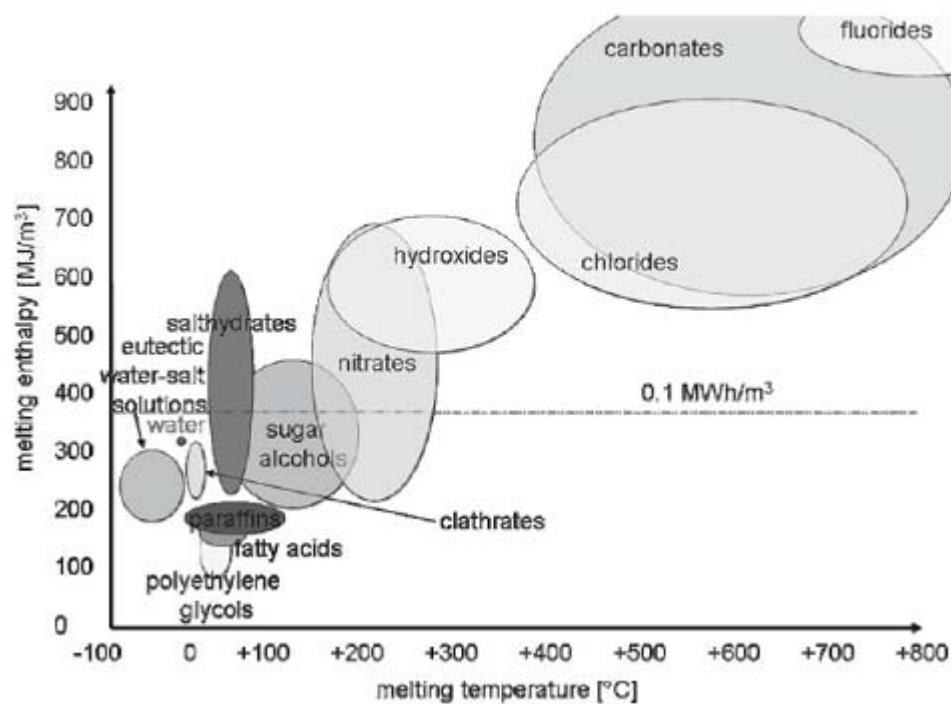


**Figure 2.1 :** Classes of PCMs and their range melting temperature and enthalpy (Mehling and Cabeza, 2008).

## **2.1 Classes of Materials**

PCMs are commonly categorized into three groups as organic, inorganic and eutectic materials.

Organic materials include congruent melting, self-nucleation and usually non-corrosiveness to the container material. Self-nucleation is an important property of organic materials, which means little or no supercooling takes place during freezing.

Compared to organic materials, inorganics usually have similar melting enthalpies per mass. However, they have greater melting enthalpies per volume due to high density and they occupy smaller volumes for the same amount of thermal load. The main disadvantage of these materials is their corrosive behavior. Inorganic materials begin to lose their chemical-water content after a period of thermal cycles and make the storage medium acidic and corrosive. Severe corrosion can be developed in some PCM-metal combinations (Farid, 2004).

An eutectic is a minimum melting composition of two or more components, each of which melts and freeze congruently forming a mixture of the component crystals during crystallization. Therefore, they solidify simultaneously without phase segregation. Eutectic water-salt solutions have melting temperatures below 0°C because the addition of salt reduces the melting temperature. The thermal conductivity of eutectic water-salt solutions is similar to that of water and they show similar volume changes like water during melting and solidification (Kenisarin, 2007).

### **2.1.1 Inorganic phase change materials**

Hydrated salts are attractive materials for use in thermal energy storage due to their high volumetric storage density and relatively high thermal conductivity. On the other hand, they have disadvantages due to their instability, following dehydration in the process of thermal cycling and high degree of supercooling. Their vapor pressure is lower than water, as the salt usually reduces the vapor pressure. They show volume change during melting and solidification up to 10 vol.% (Kenisarin, 2007).



Glauber salt ( $\text{NaSO}_4 \cdot 10\text{H}_2\text{O}$ ), which contains 44 %  $\text{Na}_2\text{SO}_4$  and 56 %  $\text{H}_2\text{O}$  by weight, is one of the oldest inorganic PCM studied by the researchers (Telkes, 1952). It has melting temperature of about  $32.4^\circ\text{C}$  and high latent heat of 254 kJ/kg and it is one of the cheapest materials that can be used for thermal energy storage. However, problems of phase segregation and supercooling limit its application (Biswar, 1977).

At this point, it is meaningful to analyse the phase segregation and supercooling problems of inorganic PCMs in more detail. The high storage density of salt hydrates is difficult to maintain and it usually decreases with cycling, because formation of lower hydrated salts makes the process irreversible and leading to decrease in their storage efficiency. Also, formation of lower hydrated salts increases the acidity of the medium with the released chemical water content. It may be severe for the encapsulation material due to its corrosive behavior.

In order to overcome these problems, a number of researchers have studied hydrated salts in direct contact heat transfer between an immiscible heat transfer fluid and a hydrated salt solution. The agitation caused by the fluid has minimized the supercooling and prevented phase segregation (Fouda, 1984; Farid, 1994).

In non-agitated thermal storage systems, development of nucleating agents and stabilizers gain importance for preventing phase segregation and supercooling. Ryu et al. (1992) have performed extensive study on suitable thickening and nucleating agents, which can be used for a number of hydrated salts.

Inorganic materials with improved properties or different melting temperatures can be developed with mixtures of different inorganics. Melting behavior of  $\text{CaCl}_2 \cdot 6\text{H}_2\text{O}$  has been improved with addition of NaCl and KCl without significant change in melting temperature (Lane, 1992). The combination of  $\text{Mg}(\text{NO})_3 \cdot 6\text{H}_2\text{O}$  and  $\text{MgCl}_2 \cdot 6\text{H}_2\text{O}$  results in an eutectic mixture with 58.7 (w/w) % and 41.3 (w/w) % composition, respectively, and it has much lower melting temperature than the inorganic components. The new formed inorganic eutectic mixture has melting point of  $58^\circ\text{C}$  and latent heat of 120-132 kJ/kg. The melting temperature of base material,  $\text{Mg}(\text{NO})_3 \cdot 6\text{H}_2\text{O}$ , decreases from  $89.5^\circ\text{C}$  to  $58^\circ\text{C}$  (Zhang, 1999). Thermal properties of several inorganic PCMs and mixtures are given in Table 2.1.

**Table 2.1** : Thermal properties of several inorganic PCMs and their mixtures.

Compound	Melting Temp. (°C)	Heat of Fusion (kJ/kg)	Reference
<b>MgCl<sub>2</sub>.6H<sub>2</sub>O</b>	117	168.6	(Lane, 1980)
<b>Mg(NO<sub>3</sub>).6H<sub>2</sub>O</b>	89	162.8	(Zhang, 1999)
<b>Ba(OH)<sub>2</sub>.8H<sub>2</sub>O</b>	78	265.7	(Lindner, 1996)
<b>CaCl<sub>2</sub>.6H<sub>2</sub>O</b>	29	190.8	(Lane, 1980)
<b>Na<sub>2</sub>S<sub>2</sub>O<sub>3</sub>.5H<sub>2</sub>O</b>	48	201-206	(Zhang, 1999)
<b>Na(CH<sub>3</sub>COO).3H<sub>2</sub>O</b>	58	245 ± 9	(Hong, 2004 )
<b>Na<sub>2</sub>HPO<sub>4</sub>.12H<sub>2</sub>O</b>	36	265	(Telkes, 1975)
<b>Na<sub>2</sub>P<sub>2</sub>O<sub>4</sub>.10H<sub>2</sub>O</b>	70	184	(Heckenkamp, 1997)
<b>Na<sub>2</sub>CO<sub>3</sub>.10H<sub>2</sub>O</b>	33	247	(Heckenkamp, 1997)
<b>Zn(NO<sub>3</sub>)<sub>2</sub>.6H<sub>2</sub>O</b>	36.4	147	(Hawes, 1993)
<b>CaBr<sub>2</sub>.6H<sub>2</sub>O</b>	34	115.5	(Dincer, 2002)
<b>(NH<sub>4</sub>)Al(SO<sub>4</sub>).6H<sub>2</sub>O</b>	95	269	(Heckenkamp, 1997)
<b>KF.4H<sub>2</sub>O</b>	18.5	231	(Hawes, 1993)
<b>60% Na(CH<sub>3</sub>COO).3H<sub>2</sub>O + 40% CO(NH<sub>2</sub>)<sub>2</sub></b>	30	200.5	(Li, 1991)
<b>61.5% Mg(NO<sub>3</sub>).6H<sub>2</sub>O + 38.5% NH<sub>4</sub>NO<sub>3</sub></b>	52	125.5	(Lane, 1980)
<b>47% Ca(NO<sub>3</sub>)<sub>2</sub>.4H<sub>2</sub>O + 33% Mg(NO<sub>3</sub>).6H<sub>2</sub>O</b>	30	136	(Abhat, 1983)
<b>53% Mg(NO<sub>3</sub>)<sub>2</sub>.6H<sub>2</sub>O + 47% Al(NO<sub>3</sub>)<sub>2</sub>.9H<sub>2</sub>O</b>	61	148	(Abhat, 1983)
<b>66.6% CaCl<sub>2</sub>.6H<sub>2</sub>O + 33.3% MgCl<sub>2</sub>.6H<sub>2</sub>O</b>	25	127	(Heckenkamp, 1997)

### 2.1.2 Organic phase change materials

Among organic materials, fatty acids and paraffins mostly attract the attention of researchers. The major advantages of these materials against inorganics are their chemical stability after extended thermal cycling and non-corrosiveness.

Fatty acids are preferred due to their high latent heat, the characteristic of constant temperature in the course of absorbing and releasing energy and low cost for energy storage. Fatty acids have superior properties over many PCMs such as melting congruency, good chemical stability and nontoxicity (Sarı, 2001). The melting temperatures and the latent heats of fatty acids vary from  $-5^{\circ}\text{C}$  to  $71^{\circ}\text{C}$  and from 45 kJ/kg to 210 kJ/kg, respectively (Kenisarin, 2007). Additionally, the compatibility of construction material to the PCM is a very important criterion for successful heat storage applications in long periods. Use of impregnated mixtures of fatty acids on walls can perform cooling functions that can sustain the room temperature within a comfortable range (Neeper, 2000).

Thermal properties of capric, lauric, palmitic and stearic acids and their binary mixtures have been analyzed by researchers. The results show that they are attractive materials for latent heat thermal energy storage in space heating applications. The melting temperatures and latent heats of these fatty acids vary from  $30^{\circ}\text{C}$  to  $65^{\circ}\text{C}$  and from 153 kJ/kg to 182 kJ/kg, respectively (Feldman, 1989).

Thermal properties of eutectic mixtures of fatty acids have been widely investigated by researchers. The eutectic mixture of capric and palmitic acids has 76.5 (w/w) % and 23.5 (w/w) % composition, respectively. The melting point of the eutectic mixture is  $21.85^{\circ}\text{C}$  and the latent heat is 171.22 kJ/kg (Sarı, 2008). Another eutectic mixture, which consists of capric and lauric acids, has 61.5 (w/w) % and 38.5 (w/w) % ratio, respectively. This composition melts simultaneously at a constant temperature of  $19.1^{\circ}\text{C}$  and it has latent heat of 132 kJ/kg (Kauranen, 1991). Figure 2.2 shows the heat flow curves of the eutectic mixture of capric and palmitic acids with respect to the acid components. Thermal properties of several fatty acids and eutectic mixtures are given in Table 2.2.

**Table 2.2 :** Thermal properties of several fatty acids and their mixtures.

<b>Compound</b>	<b>Melting Temp. (°C)</b>	<b>Heat of Fusion (kJ/kg)</b>	<b>Reference</b>
<b>n-Octanoic Acid (Caprylic Acid)</b>	16	149	(Abhat, 1983)
<b>n-Decanoic Acid (Capric Acid)</b>	21.5	153	(Lane, 1980)
<b>n-Dodecanoic Acid (Lauric Acid)</b>	42-44	178	(Abhat, 1983)
<b>n-Tetradecanoic Acid (Myristic Acid)</b>	58	187	(Lane, 1980)
<b>n-Hexanoic Acid (Palmitic Acid)</b>	64	185	(Lane, 1980)
<b>n-Octanoic Acid (Stearic Acid)</b>	69	202.5	(Lane, 1980)
<b>Oleic Acid (cis-2-Octadecenoic Acid)</b>	-5	75.5	(Cedeno, 2001)
<b>62.6 % Lauric Acid + 37.4 % Myristic Acid</b>	32.6	156	(Kauranen, 1991)
<b>34 % Myristic Acid + 66 % Capric Acid</b>	24	147.7	(Lane, 1980)
<b>64 % Myristic Acid + 36 % Stearic Acid</b>	44	182	(Sarı, 2005)
<b>58 % Myristic Acid + 42 % Palmitic Acid</b>	43	170	(Sarı, 2003)

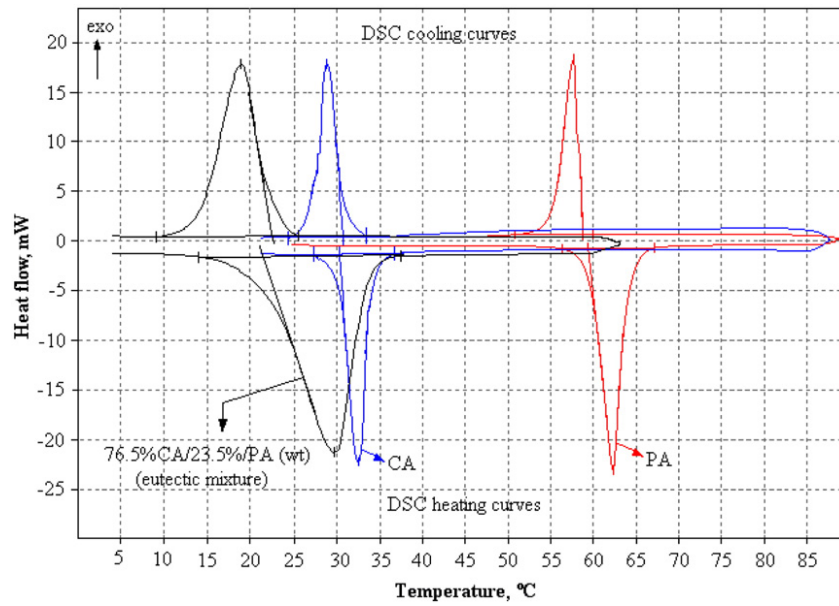


**Figure 2.2 :** Heat flow curves of eutectic mixture and its components (Sarı, 2008).

Paraffins show good storage density with respect to mass and they melt and solidify congruently with little supercooling. On the other hand, their thermal conductivity is very low, compared to inorganic materials. However, they are chemically very stable and they do not react with most common chemical reagents.

Pure paraffin is an expensive chemical. Therefore, paraffin waxes are being mostly used as latent heat storage media today. Paraffin wax consists of a mixture of mostly straight chain n-alkanes. Melting temperature and latent heat values rise with increased chain length. They are cheap with good thermal storage capacities, around 200 kJ/kg. Negligible supercooling, no phase segregation during phase transition and stability are their greatest advantage. However, paraffin waxes have similar low thermal conductivity as pure paraffins, around 0.2 W/m°C and they are moderately flammable. These undesirable effects can be partially eliminated by slight modification of the wax or the storage medium (Farid, 2004; Sharma 2009). Thermal properties of several paraffins are given in Table 2.3.

Polyethylene glycols are another group of materials, which is commercially produced and rather cheap. These materials are readily available for thermal energy storage, like paraffin waxes because they have already been investigated in detail. They are available in average molecular weight range from 200 g/mol to 35000 g/mol. Polyethylene glycols with average molecular weight between 200 g/mol and 400 g/mol are liquid at room temperature. The melting temperature of all polyethylene glycols with a molecular weight above 4000 g/mol is around 58 – 65°C (Mehling and Cabeza, 2008). Thermal properties of several polyethylene glycols are given in Table 2.3.

**Table 2.3 :** Thermal properties of several paraffins and polyethylene glycols.

<b>Compound</b>	<b>Melting Temp. (°C)</b>	<b>Heat of Fusion (kJ/kg)</b>	<b>Reference</b>
<b>Tetradecane</b>	5.8	227	(Himran, 1994)
<b>Hexadecane</b>	18	236	(Himran, 1994)
<b>Octadecane</b>	28	244	(Himran, 1994)
<b>Docosane</b>	44	252	(Himran, 1994)
<b>Paraffin C<sub>16</sub>-C<sub>28</sub></b>	42-44	189	(Abhat, 1983)
<b>Paraffin C<sub>20</sub>-C<sub>33</sub></b>	48-50	189	(Abhat, 1983)
<b>Paraffin C<sub>22</sub>-C<sub>45</sub></b>	58-60	189	(Abhat, 1983)
<b>Polyglycol E400</b>	8	99.6	(Dinçer, 2002)
<b>Polyglycol E600</b>	22	127.2	(Dinçer, 2002)
<b>Polyglycol E6000</b>	66	190	(Dinçer, 2002)

Fatty acid esters are a rather new material class and limited thermal data is available in literature. However, these materials can be accepted as possible alternatives of paraffins and salt hydrates according to the available thermal data in literature. Today, researches are mostly focused on low-chain fatty acid esters of stearic and palmitic acids. The melting temperature and latent heat of these new materials cover the range from 20°C to 40°C and from 180 kJ/kg to 200 kJ/kg, respectively (Suppes, 2003). These thermal properties decrease with increasing impurity concentration in commercial products (Feldman, 1986; Feldman, 1995). Low-chain di-esters are another branch of fatty acid derivatives, which have been investigated since the last few years (Li, 2007; Alkan, 2008). Thermal properties of several low-chain fatty acid esters are given in Table 2.4.

**Table 2.4 :** Thermal properties of several low-chain fatty acid esters.

<b>Compound</b>	<b>Melting Temp. (°C)</b>	<b>Heat of Fusion (kJ/kg)</b>	<b>Reference</b>
<b>Methyl Palmitate</b>	29	199	(Suppes, 2003)
<b>Methyl Stearate</b>	38	208	(Suppes, 2003)
<b>Ethyl Palmitate</b>	23	182	(Suppes, 2003)
<b>Ethyl Stearate</b>	33	188	(Suppes, 2003)
<b>Methyl Oleate</b>	-36	144	(Suppes, 2003)
<b>Ethylene Glycole Distearate</b>	65	215	(Alkan, 2008)
<b>Ethandiol Distearate</b>	56	189	(Li, 2007)
<b>Butandiol Distearate</b>	46.5	181	(Li, 2007)
<b>Hexandiol Distearate</b>	38.5	164	(Li, 2007)
<b>Octandiol Distearate</b>	41.4	156	(Li, 2007)
<b>Decanediol Distearate</b>	49.8	134	(Li, 2007)

## 2.2 Commercial PCMs

At present, the main suppliers in the market of phase change materials are Cristopia (France), TEAP Energy (Australia), Rubitherm GmbH (Germany), EPS Ltd. (UK), PCM Thermal Solutions (USA), Climator (Sweden) and Mitsubishi Chemical (Japan). Most commercial PCMs are based on salt hydrates, paraffins and eutectic water-salt solutions. However, they are not pure grade materials. Salt hydrates often have a nucleator added and the material is gelled or thickened with different base materials. On the other hand, a product based on paraffin is a mixture of different alkanes because pure alkanes are very expensive (Farid, 2004).

Commercial PCMs cover the temperature range from  $-40^{\circ}\text{C}$  to  $120^{\circ}\text{C}$ . The prices of commercial PCMs vary between 0.5 Euro/kg to 10 Euro/kg, which affect the cost and suitability of PCM applications. Today, electric energy price in İstanbul, Turkey is approximately 0.065 Euro/kWh for domestic usage. This means that 3600 kJ energy costs 0.065 Euro. If a PCM with 180 kJ/kg average storage density is taken into consideration, 20 kg of PCM is necessary store 3600 kJ or 1 kWh. This much of PCM costs  $20\text{ kg} \times 0.5\text{ Euro} = 10\text{ Euro}$ . To store heat with equivalent energy cost, 154 thermal cycles are necessary and additional investment costs have not been taken into consideration. This means that seasonal storage using PCM is far from being economic at current energy prices. However, if an application is not related to the energy grid, the economic situation is much better. For example, utilization of PCMs in solar energy applications, thermal storage containers or new fabrics for hot and cold climates are good areas where commercial PCMs can be very beneficial. Thermal properties of several commercial PCMs are given in Table 2.5.



**Table 2.5 :** Thermal properties of several commercial PCMs.

<b>Product Name / Manufacturer</b>	<b>Melting Temp. (°C)</b>	<b>Heat of Fusion (kJ/kg)</b>	<b>Reference</b>
<b>A 32 / EPS Ltd.</b>	32	215	Url-5
<b>A 39 / EPS Ltd.</b>	39	190	Url-5
<b>A 42 / EPS Ltd.</b>	42	195	Url-5
<b>S 7 / EPS Ltd.</b>	7	120	Url-5
<b>S 32 / EPS Ltd.</b>	32	186	Url-5
<b>S 46 / EPS Ltd.</b>	46	190	Url-5
<b>RT 21 / Rubitherm</b>	21	134	Url-1
<b>RT 27 / Rubitherm</b>	27	179	Url-1
<b>RT 42 / Rubitherm</b>	41	174	Url-1
<b>RT 52 / Rubitherm</b>	52	173	Url-1
<b>ClimSel C7 / Climator</b>	7	140	Url-6
<b>ClimSel C28 / Climator</b>	28	162	Url-6
<b>ClimSel C32 / Climator</b>	32	162	Url-6
<b>ClimSel C48 / Climator</b>	48	227	Url-6

### **2.3 Stability of PCMs under Extended Thermal Cycling**

Besides the features of an ideal PCM, given in Section 1.1.4, it must have long lasting thermal performance with regard to its thermal reliability depending on the number of thermal cycles. It is desirable to observe minimum changes in latent heat values and phase change temperatures after repeated melting and freezing processes. In this sense, accelerated thermal cycle tests should be conducted to study the changes in latent heat of fusion and melting temperature before utilization in an actual thermal energy system.

There are several studies on the thermal reliability of different PCMs. It has been found that addition of NaCl to improve the stability of  $\text{CaCl}_2 \cdot 6\text{H}_2\text{O}$  results in very stable material following more than 1000 thermal cycles (Kimura, 1984). Gibbs and Hasnain (1995) confirmed that paraffins have very good thermal stability. Sharma, et al. (2002) have conducted 1500 accelerated thermal cycle test to study the changes in latent heat of fusion and melting temperature of commercial acetamide, stearic acid and paraffin wax. They concluded that paraffin and acetamide have shown reasonably good thermal stability during the thermal cycle process.

Sarı (2003) studied the thermal reliability of stearic, palmitic, myristic and lauric acids. Fatty acids were subjected to 120, 560, 850 and 1200 thermal cycles and the changes in the thermal performance were determined. The melting temperatures decreased by  $7.87^\circ\text{C}$ ,  $5.84^\circ\text{C}$ ,  $6.78^\circ\text{C}$  and  $1.38^\circ\text{C}$ , after 1200 thermal cycles, for stearic, palmitic, myristic and lauric acids, respectively. The changes in latent heat values were -1.0%, -12.9%, -12.1% and -11.3%, after 1200 thermal cycles, for stearic, palmitic, myristic and lauric acids, respectively. It can be concluded that the latent heat of fatty acids decreased with the increased number of thermal cycles. However, the order of decrease was irregular. For example, the decrease in the latent of myristic acid was found to be -1.3%, -20.2% and -12.1% at 560, 850 and 1200 thermal cycles. The latent heat values after several thermal cycles are given in Table 2.6 for some fatty acids.

**Table 2.6 :** Latent heat values (kJ/kg) after repeated thermal cycles (Sarı, 2003).

No. of test cycles	Stearic Acid	Palmitic Acid	Myristic Acid	Lauric Acid
0	159.3	197.9	181.0	176.6
120	164.6	188.4	179.4	169.7
560	131.7	175.4	178.6	127.6
850	163.4	169.5	144.5	153.4
1200	157.7	172.4	159.1	156.6

Sarı (2004) studied the thermal reliability of eutectic mixtures of some fatty acids up to 360 thermal cycles. It has been found that the changes in the melting temperatures of the eutectic mixtures with increasing number of thermal cycling are not regular. However, no major changes in the melting temperatures have been observed. On the other hand, changes in the latent heat values range from -18 % to 2.9 % after 360 thermal cycles.

## **2.4 Encapsulation of PCMs**

In order to avoid loss of the liquid phase of the PCM and to keep the material isolated from the surrounding environment, PCMs need to be encapsulated for thermal applications. Therefore, the design of encapsulation and the materials being used are important for proper usage. The surface of the encapsulation acts as heat transfer surface and in some cases, it also serves as a construction element, i.e. it adds mechanical stability.

Depending on the application area, the requirements of PCM storage medium can be summarized as follows:

- meet the requirements of strength, flexibility, corrosion resistance and thermal stability;
- act as a barrier to protect the PCM from harmful interactions with the environment;
- provide sufficient surface for heat transfer;
- provide structural stability and easy handling.

Mainly two different techniques are used for encapsulation. These are “macroencapsulation” and “microencapsulation”.

### 2.4.1 Macroencapsulation

Macroencapsulation means filling the PCM in a macroscopic containment from several milliliters up to several liters. The shape of macrocapsules varies from rectangular panels to spheres or pouches without a defined shape. Macroencapsulation is very common because such bags and containers are available in many shapes and sizes. The key to successful macroencapsulation is to design the macrocapsule in such a way that it fits well the intended application. It is always preferred to minimize the loss of liquid PCM and to prevent changes in its composition due to contact with the surrounding.

Macroencapsulation is widely used in passive or air-cooled active systems and solar energy systems, where heat exchangers are involved. The PCM is usually contained in a number of thin flat containers with heat transfer fluid flowing through the gaps between the containers, similar to flat type heat exchangers (Farid, 1998; Vakilaltojjar, 2001). Alternatively, the PCM may be contained in small diameter tubes with the heat transfer fluid flowing along or across the tubes (Farid, 1989). It may also be contained in the shell of a shell and tube heat exchanger (Ismail, 1999). A large improvement in the heat transfer rate can be obtained by encapsulating the PCM in small plastic spheres to form a packed bed unit (Saitoh, 1986) because increase in the heat transfer surface area improves the heat transfer rate. It has been later modified by Farid et al. (1990) for a heat exchanger unit consisted of vertical tubes filled with three types of waxes having different melting temperatures. The heat exchanger unit filled with three different waxes is shown in Figure 2.3.

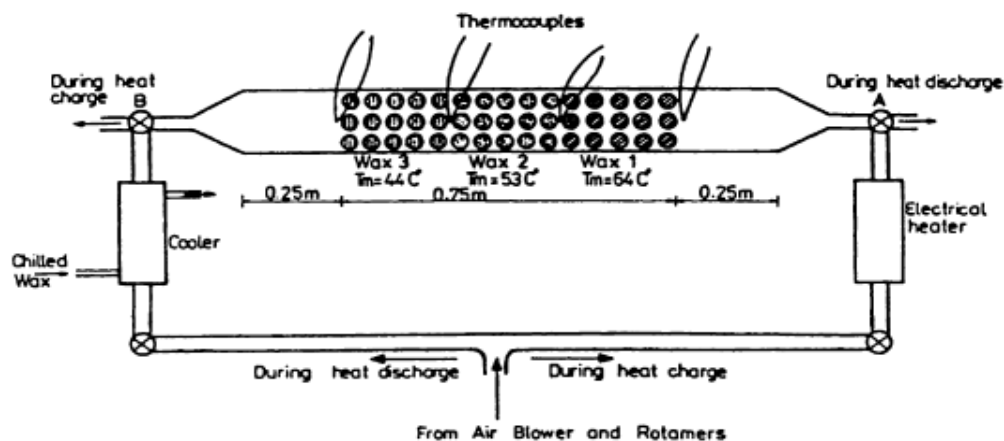


**Figure 2.3 :** Experimental PCM storage system using three waxes (Farid, 1990).

### **2.4.2 Microencapsulation**

Microencapsulation is the encapsulation of solid or liquid particles of 1  $\mu\text{m}$  to 1000  $\mu\text{m}$  diameter with a solid shell. Physical processes used in microencapsulation are spray drying, centrifugal and fluidized bed processes or coating processes. Chemical processes used are in-situ encapsulations like complex coacervation with gelatin, interfacial polycondensation to get a polyamide or polyurethane shell, precipitation due to polycondensation of amino resins and some others.

Advantages of microencapsulation are improvement of the heat transfer to the surrounding because of the high ratio of surface to volume of the capsules and better thermal reliability since phase segregation is restricted to micro scale. However, a potential drawback of microcapsules is the increased chance of supercooling behavior.

In coacervation, many products can be used as wall materials, like urea-formaldehyde resin or melamine formaldehyde resin. The first step is to disperse the core material in an aqueous gelatin solution at a temperature range between 40°C and 60°C, at which the solution of the wall material is liquid. The process is followed by adjusting the pH and concentration of polymer so that a liquid complex coacervate is formed. When it is formed, the liquid is cooled to room temperature. The final step is hardening and isolation of the microcapsules. Hardening can be done using formaldehyde, which crosslinks the wall material by reacting with amino groups located on the chain. After that, the pH should be raised to 9-11 by NaOH solution. Then the capsules are cooled down to 5-10°C and maintained at this temperature for 2 to 4 hours (Özonur, 2006).

The encapsulation of PCMs into the micropores of an ordered polymer film was investigated by Stark (1990). Paraffin wax and high density polyethylene wax were infiltrated successfully into extruded films of the ordered polymer by a solvent exchange technique to yield microcomposites with PCM levels of the order of 40 volume percent.

Royon et al. (1997) have developed a new material for low temperature storage. They contained the water as a PCM within a three dimensional network of polyacrylamide during the polymerization process. The final material remains well shaped, requiring no support or even coating, so it can be used directly.

Hong and Xin-shi (2000) have employed a compound phase change material, which consists of paraffin as a dispersed phase change material and a high density polyethylene (HDPE) as a supporting material. This new generation phase change material is very suitable for application in direct contact heat exchangers. The 75% paraffin and 25% HDPE mixture provides an eutectic phase change material that has latent heat of 157 kJ/kg compared to 199 kJ/kg of the paraffin and transition temperature around 57°C which is close to that of the paraffin.

### 3. FATTY ACID ESTERS

#### 3.1 Esterification and Fatty Acid Esters

Esterification is the general name for a chemical reaction in which two reactants, typically an alcohol and an acid, form an ester as the reaction product and the definition of organic esters arose from the assumption that these compounds were formed by reaction between the ionizable hydrogen of the acid,  $\text{RCOO}^-\text{H}^+$ , and hydroxyl of the alcohol,  $\text{R}'\text{OH}$ , to form water. This replacement was assumed to be in the same manner that the metal of an inorganic base replaced the ionizable hydrogen of an acid. However, subsequent experimental evidence obtained by use of oxygen isotope containing alcohol indicated that in the esterification reaction the alcohol yields the hydrogen and the acid the hydroxyl to form water. Esters may be broadly defined as any compound which on hydrolysis with water yields an acid and an alcohol or phenol (Markley, 1961).

The names for esters are derived from the names of the parent alcohol and the carboxylic acid. For esters derived from the simplest carboxylic acids, the traditional names are used, such as formate, acetate, propionate, and butyrate and for esters from more complex carboxylic acids; the systematic name for the acid is used, followed by the suffix -oate, like hexyl octanoate (Url-7).

Esters of several different types are found in nature and many of them are biologically and industrially important. Esters of aliphatic and aromatic alcohol and of aliphatic and aromatic acids are found in various fruit, floral, leaf, root essences or essential oils. For example, amyl acetate is found in various fruits, menthyl acetate is found in peppermint oil and benzyl acetate is found in jasmine and gardenia.

Esters of long-chain aliphatic alcohols and long-chain fatty acids occur predominantly in natural waxes of plants, insects, animals and bacteria. Esters, which are in the form of more complex combination of glycerol and fatty acids, are found in almost all living organisms.

Consequently, the occurrence of esters indicates that esterification is one of the fundamental reactions in the reproduction and development of living organisms in nature. Thereby, esterification reactions and the products of esterification are important in the chemistry and technology of fatty acids (Markley, 1961).

### **3.2 Esterification Reactions**

In the broadest sense of the term, esterification refers to any reaction by which an ester bond is produced as the primary end product and according to this broad definition the reactions can be classified into three main groups. The first group is the reaction between two compounds, which react to give an ester and a second compound. For example, reaction of an alcohol directly with an organic or inorganic acid, alcoholysis or displacement of an alcohol by another alcohol, acidolysis or displacement of an acid by another acid, exchange of alkyl groups between two esters and reaction between an amide and an alcohol are in Group 1. The second group consists of the reactions of ester formation by the addition of one compound to another. For example, anhydrides of a dibasic acid with an alcohol or sodium alcoholate, reaction between ketene or phenyl isocyanate and an alcohol and addition of acids to olefins are in Group 2. The third group consists of miscellaneous reactions, like reaction of ethylene oxide and an acid to form monoesters of glycol, condensation of aldehydes and dehydrogenation of alcohols.

#### **3.2.1 Esterification without catalyst**

The catalyst free esterification reaction can be carried out at high-temperatures and pressures and the reaction yield is strongly affected by the reaction conditions. For example, propanol can be treated with acetic acid acids in an autoclave at 150°C in poor to excellent yields. The reaction is strongly influenced by the reaction temperature and the yield of propyl acetate is only 18 % at 85°C (Magerramov, 1995).

The equilibrium in the reaction between ethanol and acetic acid can be shifted in favor of the ester by application of CO<sub>2</sub> pressure. The ester yield is increased from 63% to 72% in CO<sub>2</sub> at 60°C and 58.6 bars (Blanchard, 2001).



Although the esterification reactions under acid or base catalysis are conventional, the catalyst free reaction is ideal, but difficult to achieve. Some special conditions are necessary and rather limited reactants are available. Direct esterification of certain acids and alcohols are extremely difficult or impossible and indirect methods are used for the completion of the reaction.

### 3.2.1.1 Esterification without catalyst under vacuum

Esterification in the absence of catalyst and under vacuum was first introduced to the literature by Baykut and Aydın (1969). Such an esterification procedure is completely different than the other known esterification methods with and without catalyst. It is quite radical and contrary to the methods of Magerramov (1995) and Blanchard (2001).

According to the results of Baykut and Aydın (1969), the net yield of formation of fatty acid esters is higher than the esterification reactions in the presence of  $\text{TiOSO}_4$ ,  $\text{H}_2\text{SO}_4$ ,  $\text{Fe}_2(\text{SO}_4)_3$  and sulfosalicylic acid as catalyst.

The greatest yield that can be achieved with catalyst is 67.4 % in the presence of sulfosalicylic acid with 1:1.5 mole ratio of acid/alcohol. The yields of ester formation with different acid/alcohol mole ratios and in the presence of different catalyst are given in Table 3.1. It is seen that the increasing ratios of alcohol/acid mixture give better yields for each catalyst.

**Table 3.1 :** The yields of ester formation in the presence of catalyst (Baykut and Aydın, 1969).

Catalyst	Acid/Alcohol		
	1:1	1:1.2	1:1.5
$\text{TiOSO}_4$	57.6	57.9	61.2
$\text{H}_2\text{SO}_4$	57.0	57.5	64.8
$\text{Fe}_2(\text{SO}_4)_3$	54.4	56.4	64.2
Sulfosalicylic acid	52.4	53.2	67.4

On the other hand, esterification of homologous series of high-chain fatty acid esters, such as myristyl–myristate, –palmitate or –stearate, can be concluded with much greater yields under reduced pressure without catalyst, up to 94 %. In their work, they synthesized 84 high-chain fatty acid esters, 71 of which were unknown till 1969. High-chain fatty acid esters were synthesized by using pure saturated alcohols from  $C_{13}$  to  $C_{20}$  and pure saturated fatty acids from  $C_{10}$  to  $C_{20}$ .

The esterification apparatus is shown in Figure 3.1. According to the reaction procedure, an equimolar mixture of fatty acid and fatty alcohol is placed into (C) round bottomed flask. (C) flask contains a thermometer (A) immersed in the mixture, and the neck of the flask is also equipped with another thermometer (B) to show the temperature of the vapor phase to prevent distillation of acid or alcohol under vacuum. Dry calcium chloride is put into (D) bulb to remove the water which is formed during the course of esterification. The upper end of the side arm of the apparatus is connected to a vacuum pump. The fatty acid-alcohol mixture is kept at a temperature higher than the melting point of the acid at which no fatty acid or alcohol is distilled. The vacuum is removed half an hour later and cooled. The end product is purified by crystallization several times (Baykut and Aydın, 1969).

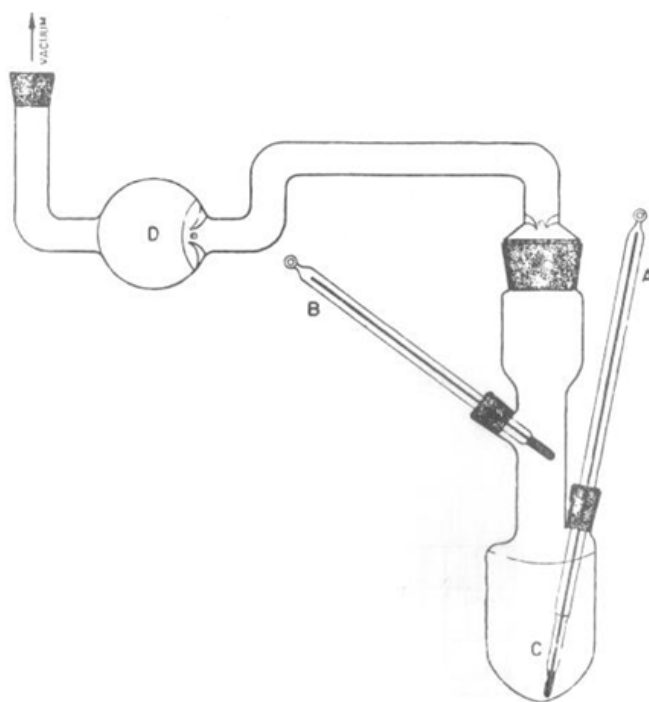


**Figure 3.1 :** Esterification apparatus; (A) thermometer, (B) thermometer, (C) reaction flask and (D) drying bulb (Baykut and Aydın, 1969).

### 3.2.2 Fischer esterification

Fischer esterification is acid catalyzed esterification by refluxing a carboxylic acid and an alcohol. Most carboxylic acids are suitable for the reaction, but the alcohol should generally be a primary or secondary alkyl (Fischer, 1895). Commonly used Bronsted acid catalysts include hydrochloric acid (Nudelman, 1998), sulfuric acid (Khurana, 1990), p-toluenesulfonic acid (Reid, 1953), and Lewis acids such as scandium(III) triflate or lanthanide(III) triflate (Barrett, 1997).

Fischer esterification is an example of nucleophilic acyl substitution based on the electrophilicity of the carbonyl carbon and the nucleophilicity of an alcohol. However, carboxylic acids tend to be less reactive than esters as electrophiles. Additionally, in dilute neutral solutions they tend to be deprotonated anions. Though very kinetically slow without any catalysts, pure esters will tend to spontaneously hydrolyse in the presence of water, so when carried out unaided, high yields for this reaction is quite unfavourable. On the other hand, the primary advantages of Fischer esterification compared to other esterification processes are based on its relative simplicity. Straightforward acidic conditions can be used if the substrates are acid resistant; otherwise milder Lewis acids should be used for acid sensitive substrates with longer reaction times.

Lewis acids are another important class of acid catalysts. Boron trifluoride etherate is the oldest Lewis acid which has been used as an esterification catalyst since  $\text{BF}_3\text{-CH}_3\text{OH}$  complex had been used for conversion of simple carboxylic acids to their methyl esters prior to gas-liquid chromatography (Sowa, 1936; Kadaba, 1971).  $\text{BCl}_3$  is also useful for esterification with primary alcohols, but yields are not so high with secondary and tertiary alcohols (Dyke, 2001).

3,4,5-Trifluorobenzeneboronic acid is the most effective acid among the boronic acids. Esterification proceeds smoothly if heavy alcohols such as 1-hexanol are employed (Ishihara, 1996).

In the presence of ZnO as catalyst, pentaerythritol and oleic acid form a triester (Chernova,1996). Paraben (p-hydroxybenzoic acid ester), which is a commercially important class of chemicals used widely as preservatives in the cosmetic and pharmaceutical industries, is produced from esterification of p-hydroxybenzylaldehyde and alcohol with  $\text{ZnCl}_2$  catalyst under microwave irradiation (Liao, 2002).

The reaction mechanism for this reaction can be explained in several steps. First, proton transfer from acid catalyst to carbonyl oxygen increases electrophilicity of carbonyl carbon. Then, the carbonyl carbon is attacked by the nucleophilic oxygen atom of the alcohol and proton transfer from the oxonium ion to a second molecule of the alcohol gives an activated complex. The protonation of one of the hydroxyl groups of the activated complex gives a new oxonium ion. Finally, loss of water from this oxonium ion and subsequent deprotonation gives the ester (Fischer, 1895). The mechanism is given in detail in Figure 3.2.

The natural esterification that takes place in wines and other alcoholic beverages during the aging process is an example of acid-catalysed esterification. Over time, the acidity of the acetic acid and tannins in an aging wine will catalytically protonate other organic acids, encouraging ethanol to react as a nucleophile. As a result, ethyl acetate is the most abundant ester in wines. Other combinations of organic alcohols and organic acids lead to a variety of different esters in wines, contributing to their different flavours, smells and tastes. When compared to Bronsted acid catalysed conditions, the acid conditions in a wine are mild, so yield is low and take years for ester to accumulate.

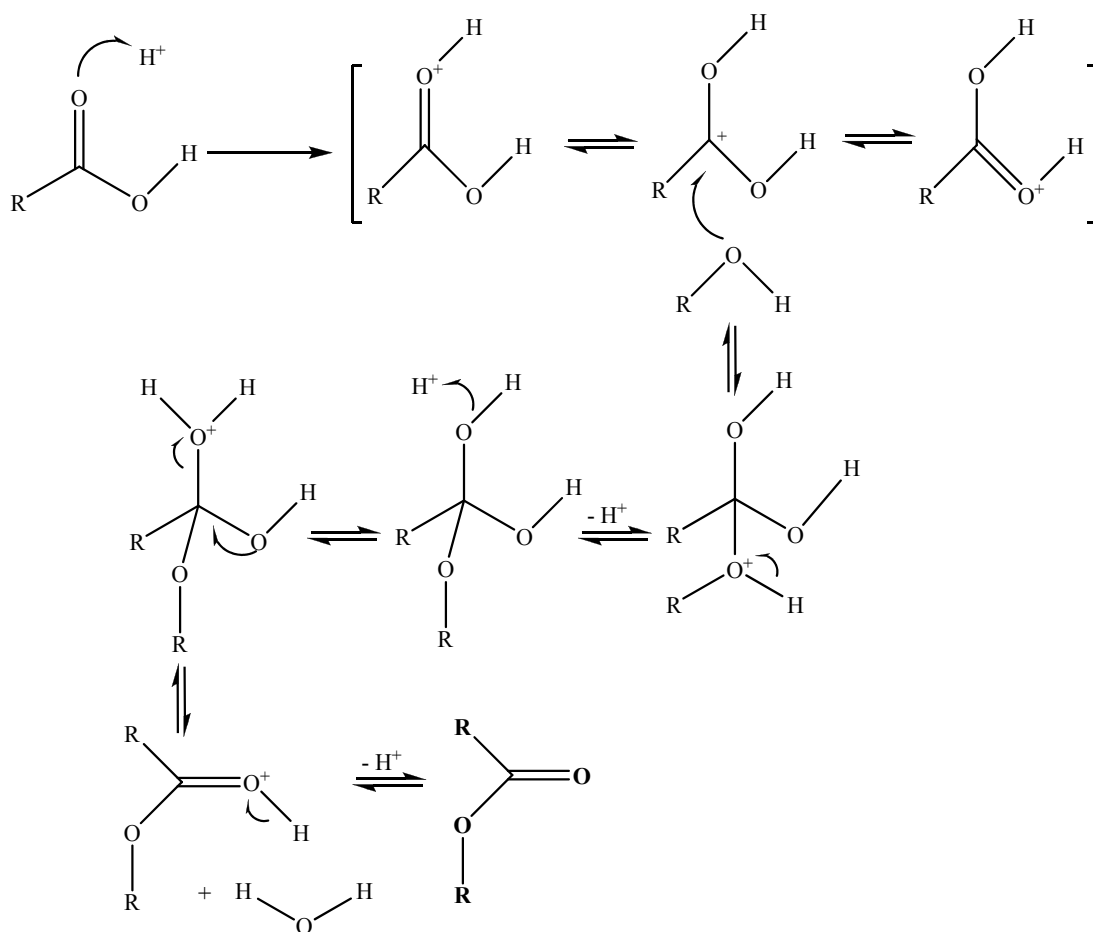


**Figure 3.2 :** The mechanism of Fischer esterification (Otera, 2003).

### 3.2.3 Mitsunobu reaction

The Mitsunobu reaction is an organic reaction that converts an alcohol into a variety of functional groups, such as an ester, using triphenylphosphine and diethyl azodicarboxylate (DEAD). Figure 3.3 shows the Mitsunobu reaction.

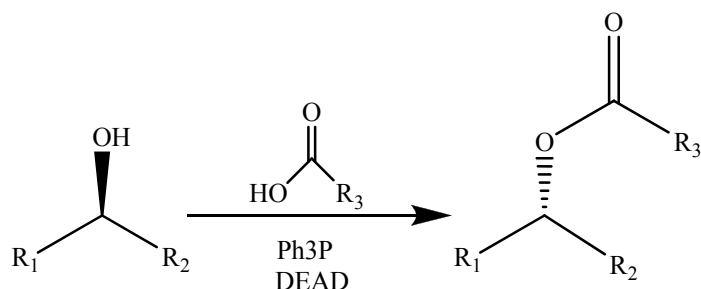


**Figure 3.3 :** Mitsunobu reaction (Mitsunobu, 1967).

The reaction mechanism of the Mitsunobu reaction is fairly complex. Initially, the triphenyl phosphine (2) makes a nucleophilic attack upon diethyl azodicarboxylate (1) producing a betaine intermediate (3), which deprotonates the carboxylic acid (4) to form the ion pair (5). The carboxylate ion deprotonates the alcohol (6) forming an alkoxide that can form the key oxyphosphonium ion (8). The ratio and interconversion of intermediates (8 – 11) depend on the carboxylic acid pKa and the solvent polarity. Although several phosphorus intermediates are present, the attack of the carboxylate anion upon intermediate (8) is the only productive pathway forming the desired product (12) and triphenylphosphine oxide (13) (Camp, 1989; Grochowski, 1989; Kumara, 2009). Figure 3.4 shows the overall mechanism of Mitsunobu reaction.

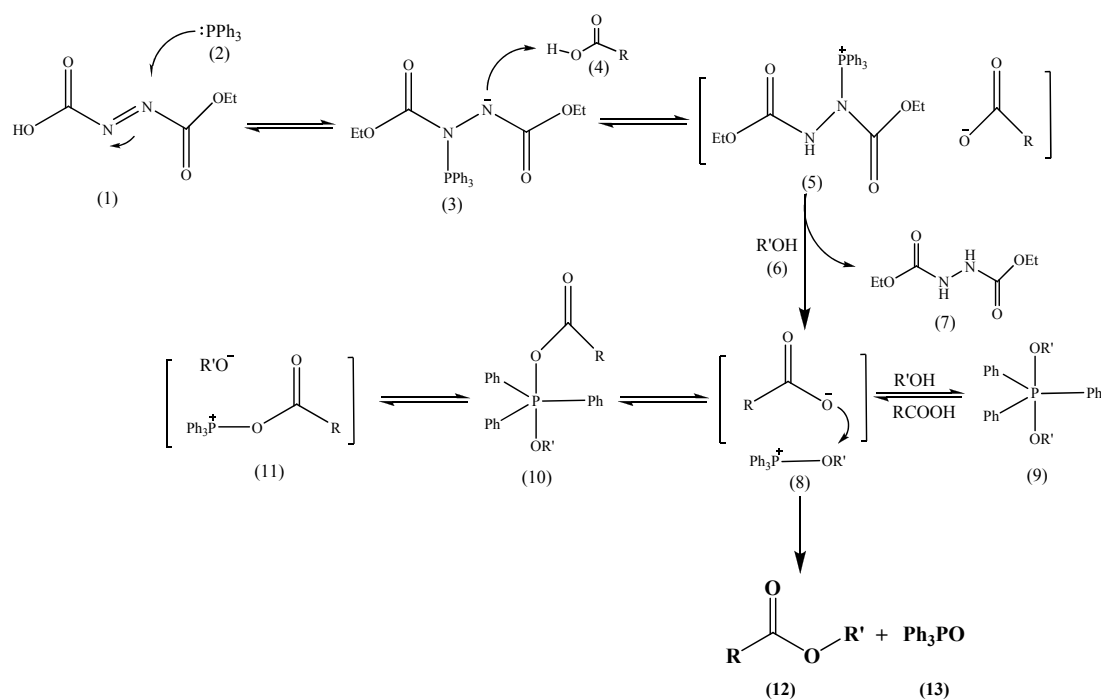


**Figure 3.4 :** The mechanism of Mitsunobu reaction (Otera, 2003).

### 3.2.4 Reaction with acyl halides

This is the reaction of a carboxylic acid halogenide, which is also called acyl halide, with an alcohol or phenol. This reaction is usually very rapid due to the high reactivity of the acyl halide and it is often performed at low temperatures. On the other hand, it tends to be difficult to control, often resulting in a mixture of low purity products and a high percentage of by-products. A non-nucleophilic weak base can be used to deprotonate the produced hydrogen halide to prevent side reactions caused by acidity (Markley, 1961). Figure 3.5 shows the ester formation with acid halides in general.

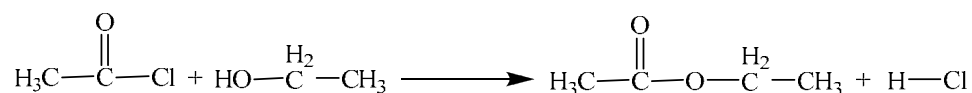


**Figure 3.5 :** Ester formation with acid halides (Markley, 1961).

### 3.2.5 Reaction with acid anhydrides

This method is favored for the synthesis of phenyl esters. The anhydride may be generated in situ, and catalysts are usually added, often in stoichiometric quantities of amines such as pyridine or triethylamine, which also serve to neutralize the acid formed. This method is very inefficient with respect to the acid because 2 moles of acid are required for each mole of alcohol. Therefore, it is mainly used either for low molecular weight acids or for very expensive alcohols (Markley, 1961). Figure 3.6 shows the ester formation with acid anhydrides in general.

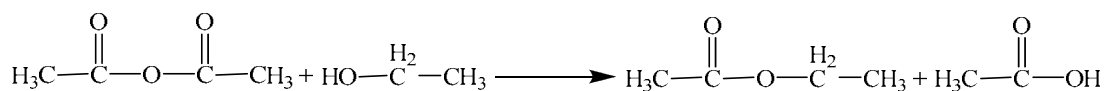


**Figure 3.6 :** Ester formation with acid anhydrides (Markley, 1961).

### 3.2.6 Reaction with carboxylate salts

This is not a reversible reaction and therefore can run to completion naturally. In the case that an alkyl chloride is used, an iodide salt may be added to catalyze the reaction. The carboxylate salt may be generated in situ or prior to the reaction. In difficult cases, the silver carboxylate may be used, since the silver ion coordinates to the halide aiding its departure and improving the reaction rate. This reaction can suffer from anion availability problems and therefore can benefit from the addition of phase transfer catalysts or highly polar aprotic solvents such as DMF (Markley, 1961). Figure 3.7 shows the ester formation with carboxylate salts in general.



**Figure 3.7 :** Ester formation with carboxylate salts (Markley, 1961).

### 3.2.7 Steglich esterification

The Steglich esterification is method of forming esters under mild conditions. The method is especially popular in peptide synthesis, where the substrates are sensitive to harsh conditions like high heat. It is an esterification reaction with dicyclohexylcarbodiimide as a coupling reagent and 4-(dimethylamino)-pyridine as a catalyst.

This reaction generally takes place at room temperature. A suitable solvent is dichloromethane. Because the reaction is mild, esters can be obtained that are inaccessible through other methods for instance esters of the sensitive 1,4-dihydroxybenzoic acid (Neises and Steglich, 1978). Figure 3.8 shows the Steglich esterification reaction.

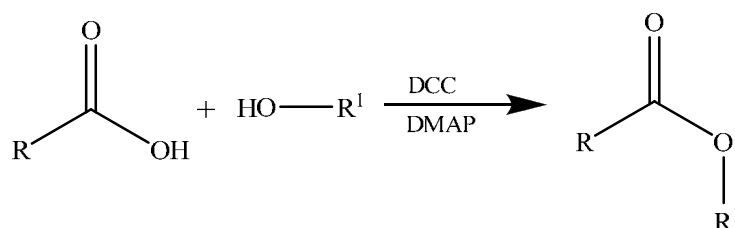


**Figure 3.8 :** Steglich esterification (Neises and Steglich, 1978).



#### 4. POLYURETHANE

A polyurethane, IUPAC abbreviation PUR, but commonly abbreviated PU, is any polymer consisting of a chain of organic units joined by urethane (carbamate) links. Polyurethane polymers are formed through step-growth polymerization by reacting a monomer containing at least two isocyanate functional groups with another monomer containing at least two hydroxyl groups in the presence of a catalyst.

The first essential component of a polyurethane polymer is the isocyanate. Molecules that contain two isocyanate groups are called diisocyanates. These molecules are also referred to as monomers or monomer units, since they themselves are used to produce polymeric isocyanates that contain three or more isocyanate functional groups. Isocyanates can be classed as aromatic, such as diphenylmethane diisocyanate (MDI) or toluene diisocyanate (TDI); or aliphatic, such as hexamethylene diisocyanate (HDI) or isophorone diisocyanate (IPDI). An example of a polymeric isocyanate is polymeric diphenylmethane diisocyanate, which is a blend of molecules with two-, three-, and four- or more isocyanate groups, with an average functionality of 2.7. Important characteristics of isocyanates are their molecular backbone, % NCO content, functionality, and viscosity (Szycher, 1999).

4,4'-MDI is produced from a reaction between aniline and formaldehyde, using hydrochloric acid as a catalyst. This reaction produces a complex mixture of polyamines which are phosgenated to obtain a polyisocyanate mixture. Afterwards, this mixture is split into polymeric MDI and pure MDI (Randal and Steven, 2002). Another catalytic synthesis of 4,4'-MDI consists of three steps. Starting from the catalytic reaction of aniline and dimethyl carbonate (DMC), methyl phenyl carbamate (MPC) is formed. Then MPC condenses with formaldehyde to produce dimethyl methylene diphenyl-4,4'-dicarbamate (MDC). Last, MDC is decomposed to MDI (Zhao, 2002).

In pure MDI, the main effect of the isocyanate groups (NCO) in the 2 and 4 positions is on reactivity. The isocyanate group in 2 (ortho) - position is three times less reactive than the isocyanate group in 4 (para) - position. Pure 4,4' - MDI is solid at room temperature, melts at 38°C and is a major raw material for adhesive and coating applications where high reactivity and linearity is required. The 2,4' - MDI isomer is not readily available in 100 per cent purity. Concentrations of up to 50 percent are commercially available. The so-called mixed isomer 50, with a melting point of 18°C, exhibits a good compromise between lower reactivity and liquidity. Above their melting point, both isomers and their mixtures have very low viscosities, typically below 10 mPa.s (Gurke, 2002). The isomeric chemical structures of pure MDI are given in Figure 4.1.

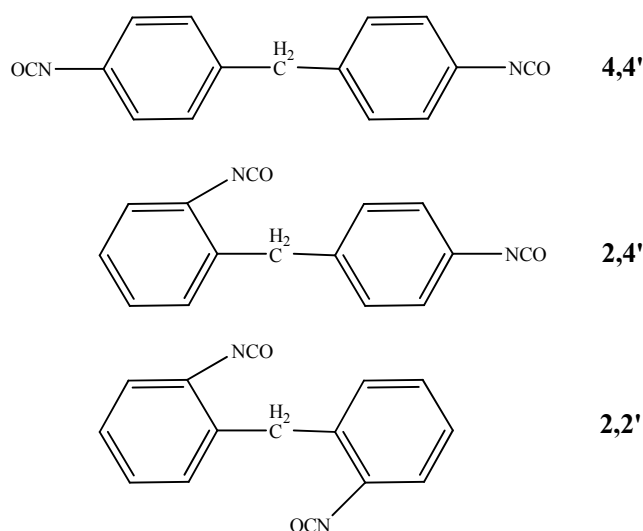


**Figure 4.1** : Chemical structures of pure MDI (Szycher, 1999).

The second essential component of a polyurethane polymer is the polyol. In practice, polyols are distinguished from short chain or low-molecular weight glycol chain extenders and cross linkers such as ethylene glycol (EG), 1,4-butanediol (BDO), diethylene glycol (DEG), glycerine, and trimethylol propane (TMP). Polyols are polymers in their own right. They are formed by base-catalyzed addition of propylene oxide (PO), ethylene oxide (EO) onto a hydroxyl or amine containing initiator, or by polyesterification of a di-acid, such as adipic acid, with glycols, such as ethylene glycol or dipropylene glycol (DPG). Polyols extended with PO or EO are polyether polyols. Polyols formed by polyesterification are polyester polyols. The choice of initiator, extender, and molecular weight of the polyol greatly affect its

physical state, and the physical properties of the polyurethane polymer. Important characteristics of polyols are their molecular backbone, initiator, molecular weight, % primary hydroxyl groups, functionality, and viscosity (Randal and Steven, 2002).

Relatively few basic isocyanates and a far broader range of polyols of different molecular weights and functionalities are used to produce the whole spectrum of polyurethane materials. Changes in the detailed chemical nature of the polyols, isocyanates or additives affect the properties of the final product, and minor changes in the mixing conditions and ratios allow for a fine tuning of the polymers produced (Demharter, 1998).

Polyurethanes are a family of step-growth polymers which produce the urethane linkage, NH-COO-, without any by-products. Polyurethanes can be produced in an extremely wide range of grades, in densities from 6 to 1220 kg/m<sup>3</sup> for different applications, like automotive, coatings, construction, footwear, furniture and thermal insulation (Raymond, 1992). The overall reaction is schematically given in Figure 4.2.

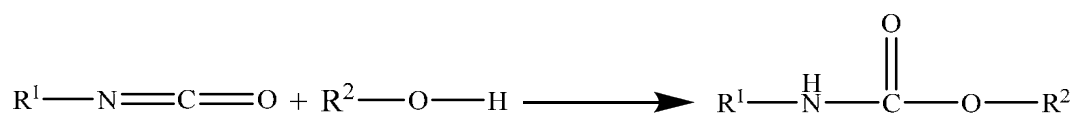


**Figure 4.2 :** Overall reaction of polyurethane formation (Randall, 2002).

In the automotive industry, polyurethane products are used to manufacture car parts, like car seats, headrests, liners, internal body parts, dashboards, bumpers and energy absorption parts. Flexible foams are used in car seats, carpet underlay and headrests. Semi-rigid foams are used to make liners, some internal body parts and energy absorbing structures.

The polyurethane coating industry consists of wide range of products that are used in many applications. Coatings for wood products have a major share in architectural coatings, used mainly for interior clear wood finishes. Anti-corrosion coatings are increasingly used instead of traditional coatings because their superior properties and longer life times decrease the cost of refurbishment. For example, in automotive industry high performance light-resistant coatings are dominated by products based on aliphatic diisocyanates.

The growth of the polyurethane construction market has mainly been driven by the penetration of polyurethanes in the wood binding area in the North American and European markets. The use of MDI based resins continue to replace pheolic resins as they can be more efficiently used with shorter production cycles. The use of polyurethane insulation panels in the constructions is to maintain higher energy efficiencies in the buildings with lower green house gas emissions, due to the lower energy consumption. Polyurethane panels offer the best insulation value per unit thickness with light weight (Randall, 2002).

#### **4.1 Polyurethane Rigid Foam**

Rigid polyurethane foams are prepared by mixing polymeric MDI, polyols, blowing agents and a variety of additives such as catalysts, surfactants, water and, optionally, fire retardants under controlled conditions. A wide range of polyols is used, normally in combination with polymeric MDI, and the additives are typically pre-blended into the polyol. The formation of highly cross-linked homogeneous network structure is crucial for the final properties of the rigid polyurethane foam.

According to the traditional reaction mechanism, the reaction is a three step process. The initial exothermic reaction is between isocyanate and water, forming carbamic acid. Carbamic acids are unstable, and decompose forming carbon dioxide and amine. The amine reacts with more isocyanate to give a substituted urea. Water has a very low molecular weight, so even though the weight percent of water may be small, the molar proportion of water may be high and considerable amounts of urea produced. The second exothermic reaction is between isocyanate and polyol, producing polyurethanes and isocyanate trimerisation. Afterwards, the blowing agents volatilize during the reaction process since the polymerization reaction is exothermic. The volatilized liquid fills and expands the cellular polymer matrix, creating foam structure at the third step (Demharter, 1998).

The centre temperature of the foam can reach up to 190°C, due to the exothermic reactions, but the reactions are not complete at the end of the foam rise and might continue for hours according to the used chemicals and stoichiometric ratios.

The low thermal conductivity of rigid polyurethane foam is one of the most important properties. It is determined from the rate of heat transfer through a material, which is proportional to the temperature difference divided by the thickness. It is important to note that the thermal conductivity related to the rate of heat transfer under steady-state conditions. At non-steady state conditions, the density and heat capacity of a material influence also the thermal behavior of the material. Low-density rigid foam equilibrates faster to the temperature change of the environment than high-density rigid foam, i.e. low-density material has much lower thermal conductivity (Randall, 2002). Figure 4.3 shows the required insulation thickness of polystyrene foam, mineral wool, cork, fibreboard and timber, equivalent to 25 mm polyurethane foam.

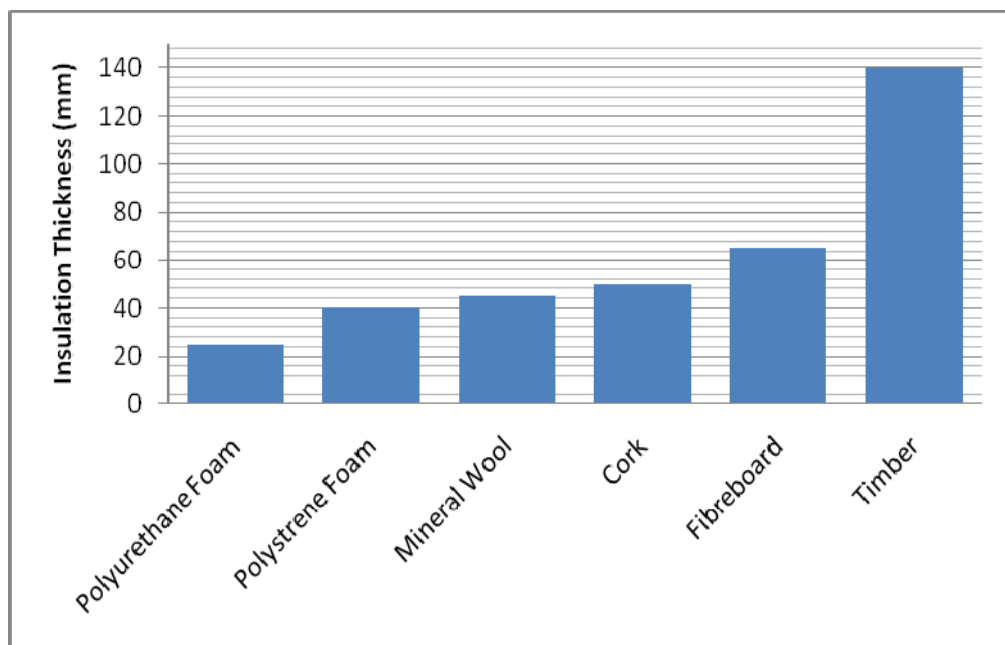


**Figure 4.3 :** Comparison of thermal insulation performance of several materials (Szycher, 1999).

In rigid foam production, polymeric isocyanates play an important role in forming homogeneous crosslinked networks. Polymeric MDI is a complex mixture of pure MDI and higher homologue. The letter “n” ranges from 1 to higher numbers, meaning that in polymeric MDI, polyisocyanates with functionalities of 3 and higher are present. A typical polymeric MDI consists of approximately 50 per cent pure MDI, 30 per cent triisocyanate, 10 per cent tetra-isocyanate, 5 per cent penta-isocyanate and 5 per cent higher homologue. The average functionality of a standard polymeric MDI is about 2.7 with a typical viscosity of approximately 200 mPa.s at 25°C. Standard polymeric MDI is storage stable as no crystallisation takes place down to temperatures of 0°C (Gurke, 2002). The general chemical structure of polymeric MDI is shown in Figure 4.4.

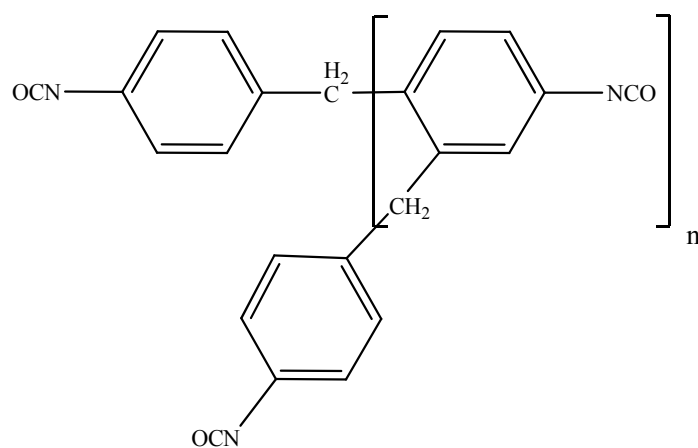


**Figure 4.4 :** General chemical structure of polymeric MDI (Randall, 2002).

The other essential component of rigid polyurethane foam is the polyol part. They are most easily classified as polyether polyols, which are made by the reaction of epoxides (oxiranes) with active hydrogen containing starter compounds, or polyester polyols, which are made by the polycondensation of multifunctional carboxylic acids and hydroxyl compounds. Polyether polyols come in a wide variety of grades based on their end use, but are all constructed in a similar manner. Polyols for flexible applications use low functionality initiators such as dipropylene glycol (f=2) or glycerine (f=3). Polyols for rigid applications use high functionality initiators such as sucrose (f=8), sorbitol (f=6), toluenediamine (f=4), and Mannich bases (f=4). Propylene oxide is then added to the initiators until the desired molecular weight is achieved.

Polyols extended with propylene oxide are terminated with secondary hydroxyl groups. In order to change the compatibility, rheological properties, and reactivity of a polyol, ethylene oxide is used as a co-reactant to create random or mixed block heteropolymers. Polyols capped with ethylene oxide contain a high percentage of primary hydroxyl groups, which are more reactive than secondary hydroxyl groups (Szycher, 1999).

Surfactants are used to emulsify the liquid components, regulate cell size, and stabilize the cell structure to prevent collapse and sub-surface voids. Polydimethylsiloxane-polyoxyalkylene block copolymers, silicone oils, nonylphenol ethoxylates are examples of surfactants (Oertel, 1985).





## 5. MATERIALS AND METHODS

### 5.1 Materials

In this research, 9 high-chain fatty acid esters of tetradecanol have been synthesized by using nine fatty acids with sequential carbon number. Starting with 12 carbon number dodecanoic acid, high-chain fatty acid esters have been synthesized according to the esterification procedure of Baykut and Aydın (1969) under reduced pressure without catalyst, up to 20 carbon number eicosanoic acid.

High-chain ester of myristyl alcohol with myristic acid (tetradecyl tetradecanoate) has been widely used in cosmetic formulations and it has been commercially sold by Cognis Türk A.Ş., Şekerpinarı-İstanbul with the product name of “Cetiol MM”. This commercial product is the 10<sup>th</sup> high-chain fatty acid ester which has been investigated in this research. Except the impurities of the bulk product, the chemical composition is the same with the synthesized tetradecyl tetradecanoate.

Tetradecanol (myristyl alcohol, 97%, Aldrich), dodecanoic acid (>99%, Sigma), tridecanoic acid (>98%, Sigma), tetradecanoic acid (myristic acid, 99-100%, Sigma), pentadecanoic acid (>99%, Aldrich), hexadecanoic acid (palmitic acid, >99%, Sigma), heptadecanoic acid (98%, Sigma), octadecanoic acid (stearic acid, >98.5%, Sigma), nonadecanoic acid (>99%, Sigma), eicosanoic acid (arachidic acid, >99%, Aldrich), n-hexacosane (99%, Aldrich) and n-triacontane (99%, Aldrich) were used without further purification.

Polyurethane rigid foam – PCM composites have been synthesized by using industrial raw materials. The raw materials were kindly provided by the Flokser Group, Hadımköy-İstanbul.

Polymeric diphenylmethane diisocyanate (PMDI), Suprasec 5025, is the product of Hunstman with isocyanate value (NCO) of 31 % and density of  $1.23 \text{ g/cm}^3$  at  $25^\circ\text{C}$ . It consists of approximately 50 percent pure MDI, 30 percent tri-isocyanate, 10 percent tetra-isocyanate, 5 percent penta-isocyanate and 5 per cent higher homologue. The average functionality of this standard polymeric MDI is about 2.7 with a typical viscosity of 200 mPa.s at  $25^\circ\text{C}$ , approximately.

Polyether polyol, Petol PZ 400-5G, is the product of Olctchim with hydroxyl value of  $425 \pm 25 \text{ mg KOH/g}$ . The average functionality of the polyether polyol is 5 and molecular weight is 700 a.u. Its density is  $1.05 - 1.15 \text{ g/cm}^3$  at  $25^\circ\text{C}$ .

Catalyst, Dabco EG, is the product of Air Products which is mainly composed of 33% triethylenediamine and 67% monoethylene glycol. It is used as a standard catalyst in microcellular applications.

Silicon additive, Tegostab B 8950, is the product of Degussa. It is a polysiloxane polyether block copolymer which serves as an auxiliary agent in the process of manufacturing.

## **5.2 Instrumentation**

### **5.2.1 Differential scanning calorimeter (DSC)**

Perkin Elmer Jade DSC was used for thermal analysis of the PCMs. The measurements were carried out under inert nitrogen atmosphere at 20 ml/min flow rate. All the DSC thermal analyses of enthalpy were conducted at  $2^\circ\text{C/min}$  heating and cooling rate and the rate was rised to  $5^\circ\text{C/min}$  for the thermal analyses of polyurethane rigid foam – PCM composites due to the broader scanned temperature interval.

The heat flow calibration of the instrument was performed by indium reference and the temperature calibration was performed by indium and zinc references. Sapphire was used as an internal reference following the heat and temperature calibrations for the specific heat analyses. Calibration was performed systematically prior to the first analyses of each workday.

Melting and freezing temperatures, latent heat of melting and freezing, the changes in thermal performance after 1000 extended cycling and solid and liquid phase specific heat values were determined with the help of DSC analyses at Marmara University, Chemistry Department.

DSC analyses were conducted according to the ASTM standard test methods with designation numbers E 792–06 and D 2766–95, explaining the determination of enthalpies of fusion and freezing and specific heat of liquids and solids, respectively. Every presented DSC result in this research is calculated according to the results of at least 4 individual analyses in order to minimize the uncertainty of the balance with four decimal digits.

### **5.2.2 Thermogravimetric analysis (TGA)**

Perkin Elmer STA 6000 was used for the thermogravimetric decomposition analysis of the PCMs. The analyses were carried out under inert nitrogen atmosphere at 20 ml/min flow and 10°C/min heating rates.

The weight calibration was performed by using the reference weight with known standard mass and the temperature calibration was performed by starting the automatic sensor calibration of the instrument. Calibration was performed systematically prior to the first analyses of each workday.

The decomposition characteristics, decomposition onset and 5 (w/w) % decomposition temperatures of the high-chain esters and PCM-rigid polyurethane composites were determined with the help of TGA at Marmara University, Chemistry Department.

Analyses were conducted according to the general principles given in BS EN ISO 11358:1997. Every presented TGA result in this research is calculated according to the results of 2 individual analyses. The instrument has built-in balance with six decimal digits.

### **5.2.3 DNA thermal cyclers**

In this research, Bio-Rad MJ Mini DNA thermal cycler has been used to provide automated 1000 heating and cooling cycles in order to observe the thermal performance change of each PCM at Istanbul Technical University, Molecular Biology and Genetics Department and Marmara University, Biology Department.

### **5.2.4 Fourier transform infrared spectroscopy (FT-IR) analysis**

FT-IR spectra were recorded on a Perkin Elmer FT-IR Spectrum 100 spectrometer with universal ATR accessory between 4000 – 380  $\text{cm}^{-1}$  at Marmara University, Chemistry Department.

### **5.2.5 Optical microscope imaging**

At Marmara University, Biology Department, Olympus BX51 optical microscope was used to take images of PCM – Polyurethane rigid composites at x400 magnification in order to clarify the homogeneous distribution of PCM particles throughout the polyurethane matrix. The optical microscope has Evolution LC color camera equipment and Image Proexpress software.

### **5.2.6 Scanning electron microscope (SEM) imaging**

At Istanbul Technical University, Chemical Engineering Department, JEOL JSM-6390LV scanning electron microscope was used to take images of PCM – Polyurethane rigid composites at x2000 magnification in order to clarify the main particule size distribution of the PCM particles throughout the polymer matrix.

### **5.2.7 X-ray diffraction (XRD)**

At Istanbul Technical University, Prof. Adnan Tekin Applied Research Centre of Materials Science and Production Technologies, Philips X'Pert Pro Panalytical XRD instrument with monochromated  $\text{CuK}\alpha_1$  radiation (40 mA, 45 kV) and X'Pert High Score Plus software was used to analyse the crystal structure of Cetiol MM between 5° and 120°.

### 5.3 Synthesis

#### 5.3.1 Synthesis of high-chain fatty acid esters

Esterification of series of myristyl alcohol high-chain fatty acid esters was conducted according to the synthesis method of Baykut and Aydın (1969) at Marmara University, Chemistry Department. Throughout this research, 9 high-chain fatty acid esters with high purity were synthesized and investigated. The list of synthesized esters is given in Table 4.1.

**Table 5.1 :** High-chain fatty acid esters of myristyl alcohol.

Nomenclature	Representation
Tetradecyl dodecanoate (Myristyl laurate)	14 – 12
Tetradecyl tridecanoate	14 – 13
Tetradecyl tetradecanoate (Myristyl myristate)	14 – 14
Tetradecyl pentadecanoate	14 – 15
Tetradecyl hexadecanoate (Myristyl palmitate)	14 – 16
Tetradecyl heptadecanoate	14 – 17
Tetradecyl octadecanoate (Myristyl stearate)	14 – 18
Tetradecyl nonadecanoate	14 – 19
Tetradecyl eicosonate	14 – 20

An equimolar mixture of fatty acid and alcohol was placed into the reaction bulb and two thermometers were mounted to show the temperature of the mixture and the vapor phase. Dry calcium chloride was used to remove the water which is produced as by-product during esterification. The temperature of the alcohol – acid mixture was kept above the melting point of each component, at which no fatty acid or alcohol distilled. The open end of the apparatus was connected to vacuum pump.

After 60 minutes, the vacuum was removed and the new formed mass in the reaction bulb was taken out by means of a convenient solvent. The ester was obtained by crystallization of this solution 8 times with acetone and ether. The esterification apparatus is shown in Figure 3.1 of Chapter 3.

### **5.3.2 Synthesis of polyurethane rigid foam and composite**

Synthesis of polyurethane rigid foam and PCM–rigid foam composite was conducted at Marmara University, Chemistry Department by using industrial raw materials in order to show the promising production possibility of such modified insulators.

The polymeric MDI, polyether polyol, silicon and catalyst, used in this research, are industrial raw materials of different companies around the world and they are excessively used for the production of polyurethane rigid foam.

Cetiol MM, which is a commercial product of Cognis Türk A.Ş., was used as the PCM part of the rigid foam. It is the industrial scale corresponding product of laboratory scale synthesized myristyl myristate.

According to the conventional rigid foam production, basic formulation consists of two main components. One of them is the polymeric isocyanate part and the other is the polyol mixture. The polyol mixture is consisted of polyester or polyether polyol, water, silicon, catalyst and secondary blowing agent. When these two components are mixed, exothermic polymerization takes place and foam expands with formed carbon dioxide and blowing agent, which evaporates due to temperature increase. However, the formulation, used in this research, has been modified because of the PCM added into the polyol mixture. The modified polyurethane rigid foam formulation is given in Table 4.2. This modification is discussed in Chapter 6 in detail.

**Table 5.2 :** Modified polyurethane rigid foam formulation with/without PCM.

Polyether polyol (Petol PZ 400-5G)	50 g
Silicon (Tegostab B 8950)	0.5 g
Catalyst (Dabco EG)	0.5 g
Tetrahydrofuran	20 ml
PCM (Cetiol MM)	appropriate amount
Polymeric MDI (Suprasec 5025)	55 g

### **5.3.3 Characterization of high-chain fatty acid esters and polyurethane rigid foam with/without PCM**

High-chain fatty acid esters were synthesized from high purity alcohol and fatty acid reagents with 97 % or better purity grade and the synthesized products were crystallized at least 8 times with acetone and ether to obtain the final product at very high purity. FT-IR was used to determine the absence of unreacted fatty acid and alcohol impurities.

Polyurethane rigid foam with and without PCM were analyzed by FT-IR to show the formed polyurethane matrix and the PCM entrapped inside it. Optical microscope and SEM imaging were used to show the homogeneous distribution and the dominant particle size of the entrapped PCM.

DSC and TGA instruments have been intensively used for the thermal characterization throughout the research in every step. Melting and freezing temperatures, latent heat of melting and freezing (ASTM E793-06), the changes in thermal performance after 1000 extended thermal cycling, solid and liquid specific heat values and total enthalpy changes were determined by DSC analyses. The decomposition characteristics, decomposition onset, 5 (w/w) % decomposition temperatures and ash content were determined by thermogravimetric analyses.

DSC analyses of high-chain esters were conducted at 2°C/min and 5°C/min heating and cooling rates under 20 ml/min nitrogen flow for determination of the latent heat values and the specific heat capacity, respectively. The polyurethane foam samples were analyzed at 5°C/min heating and cooling rate under 20 ml/min nitrogen flow. TGA analyses of both ester and polyurethane samples were conducted at 10°C/min heating rate under 20 ml/min nitrogen flow.



## **6. RESULTS AND DISCUSSION**

### **6.1 Synthesis of High-Chain Fatty Acid Esters**

In this research, esterification method of Baykut and Aydın (1969), based on the synthesis under reduced pressure and in the absence of catalyst, was chosen instead of other common methods because of its simplicity and high reaction yield.

The very best known and the most common synthesis method of esterification is the Fischer esterification, which takes place in the presence of acid catalyst. However, the net reaction yield of this method is low and the synthesis procedure is harsh. The primary disadvantages of the Fischer esterification are its thermodynamic reversibility and relatively slow reaction rates, depending on the reaction conditions. Workarounds to this can be inconvenient if there are other functional groups sensitive to strong acid, in which case other catalytic acids may be chosen. If the product ester has a lower boiling point than either water or the reagents, the product may be distilled rather than water. It is common as esters with no protic functional groups tend to have lower boiling points than their protic parent reagents. Purification and extraction are easier if the ester product can be distilled away from the reagents and byproducts, but reaction rate can be slowed because overall reaction temperature can be limited in this scenario. A more inconvenient scenario is if the reagents have a lower boiling point than either the ester product or water, the reaction mixture must be capped and refluxed and excess of starting material must be added.

Esterification of an alcohol and a fatty acid involves a reversible equilibrium and therefore the reaction does not go to completion. The maximum yield that can be achieved by simultaneous removal of water and presence of excess of one reagent is less than 70 % (Baykut and Aydın, 1969). Higher yields are unlikely to be maintained by the Fischer esterification due to slow reaction rates and the necessity of heating up the reaction medium in order to remove the formed water content. The slow reaction rate increases the interaction time of the reagents with the heated reaction medium, resulting in distillation of low boiling point reagents or end-

product rather than water.

The main advantages of the present synthesis method for production of fatty acid higher esters are its fast reaction rate and the high reaction yield, up to 94 %. The applied vacuum maintains the removal of water in a much easier manner at lower temperatures, above the melting temperature of the alcohol and the fatty acid. With higher reaction rate, the formation of water is faster and the total reaction time is limited to 60 minutes. Hence, the end-product is formed rapidly and the possibility of distillation of reagents is minimized with short reaction time. As the reagents are liquid at the applied temperature in the reaction bulb without any inconvenient effect of the reaction medium, it is possible to get 85 % or greater yields of ester formation by the method of Baykut and Aydın (1969).

In this research, dry calcium chloride was used to absorb the water vapor under vacuum and the temperature was kept around maximum 60°C above the melting point of the fatty acid at which no fatty acid or alcohol is distilled. High purity fatty alcohol and fatty acids were used in the synthesis of high-chain fatty acid esters. The reagent grade solvents were used in order to obtain the end product with the highest purity. An equimolar mixture of fatty acid and alcohol was the starting composition of each esterification reaction and the end-product, high-chain fatty acid ester, formed in the reaction bulb was taken out by means of a convenient solvent. The process vacuum pressure was around 5 – 10 mmHg and the equimolar fatty acid – alcohol mixtures were prepared according to the stoichiometric calculations to obtain around 2 g of end product. The pure ester was obtained by crystallization of the end product 8 times with acetone and ether.

## **6.2. Chemical and Thermal Characterization of High-Chain Fatty Acid Esters**

### **6.2.1 FT-IR analysis**

A FT-IR spectrum of an ester shows distinct peaks at specific wavenumbers. The characteristic peaks can easily be recognized and comments on composition of the final product can be made in terms of the presence of the peaks of alcohol and fatty acid at different wavenumbers.

Fatty acid esters show characteristic bands of carbonyl stretching vibrations of acyclic saturated ester around  $1735 - 1750\text{ cm}^{-1}$  and the sharp peaks of carbon–hydrogen stretching vibrations are seen just below  $3000\text{ cm}^{-1}$  wavenumber.

The reagents, which are fatty acid and alcohol, contain hydroxyl groups which give significant absorptions. Fatty acids show a very broad trough of bonded oxygen–hydrogen stretching vibrations between  $2500 - 2700\text{ cm}^{-1}$  and alcohols show a similar broad trough at higher wavenumbers, in the range of  $3230 - 3550\text{ cm}^{-1}$ . The carbonyl stretching vibrations of saturated fatty acids absorb in the range of  $1700 - 1725\text{ cm}^{-1}$  (Dyer, 1965).

FT-IR spectra were taken in  $4000 - 380\text{ cm}^{-1}$  wavenumber interval with universal ATR accessory. In the following, the FT-IR spectra of tetradecanol, hexadecanoic acid and the selected high-chain fatty acid esters are given in Figure 6.1 – 6.3. The FT-IR spectra of the other high-chain fatty acid esters are given in Appendix A.1.

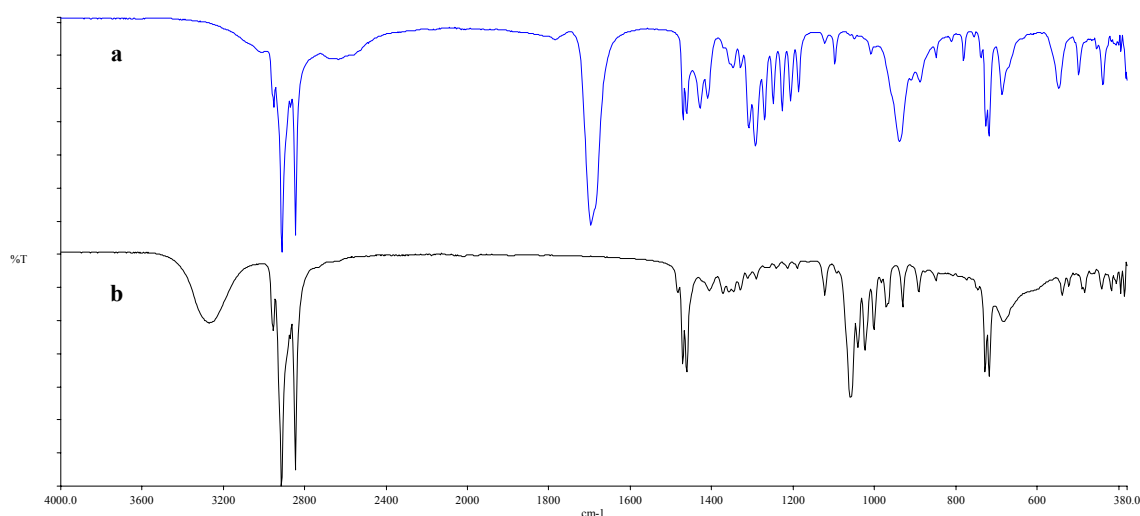


**Figure 6.1 :** FT-IR spectra of (a) hexadecanoic acid and (b) tetradecanol.

It can be concluded that the synthesized high-chain fatty acid esters are obtained at high purity after 8 crystallizations with acetone and ether. The carbonyl stretching vibrations of acyclic saturated esters can easily be seen on the spectra. The absence of hydroxyl stretching bands of alcohol and the bonded oxygen–hydrogen stretching vibrations of fatty acids show that the final crystallized pure products do not contain any unreacted alcohol and fatty acid impurities. The carbonyl stretching vibrations of saturated fatty acids are shifted to  $1735 - 1750\text{ cm}^{-1}$  wavenumbers of carbonyl stretching vibrations of acyclic saturated esters as a result of the ester formation.

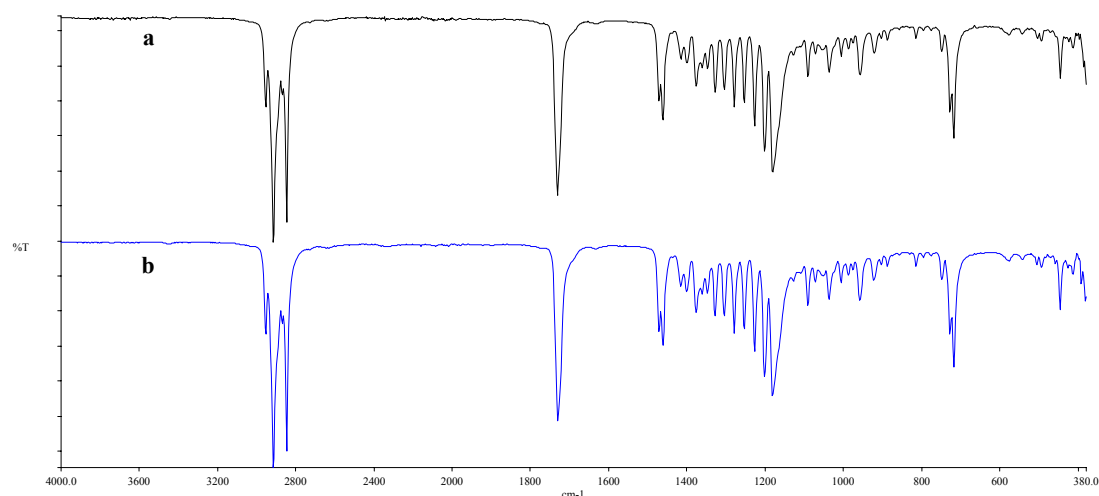


**Figure 6.2 :** FT-IR spectra of (a) Cetiol MM and (b) 14 – 14.

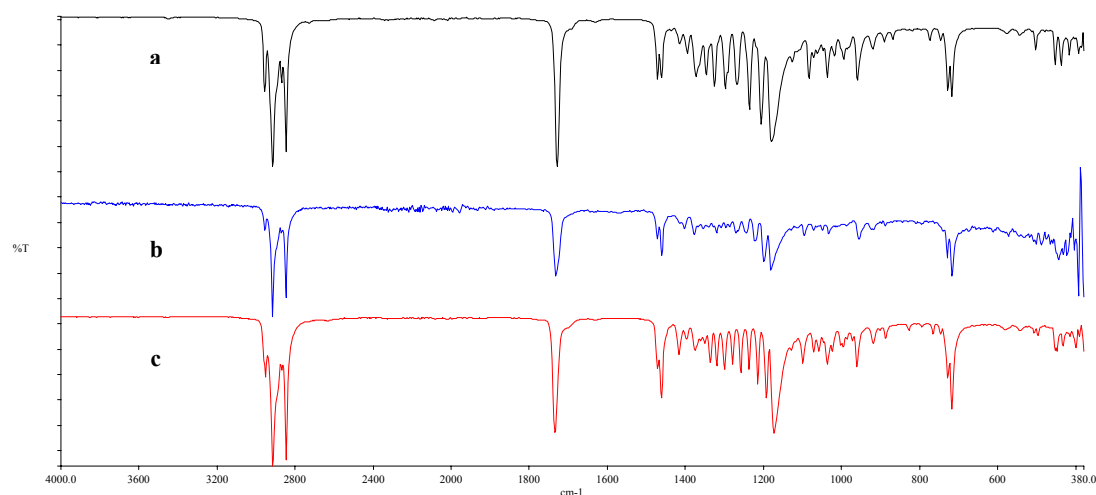


**Figure 6.3 :** FT-IR spectra of (a) 14 – 12, (b) 14 – 16 and (c) 14 – 17.

## 6.2.2 DSC analysis

### 6.2.2.1 Determination of phase change enthalpies and temperatures

Analyses of determination of phase change enthalpy and temperature were conducted according to the ASTM standard test method with designation number E 793–06. The measurements were carried out under inert nitrogen atmosphere at 20 ml/min flow rate and at 2°C/min heating and cooling rate.

The temperatures and enthalpies are determined with the help of the derivative of the heat flow curve. At first, the starting and end points are determined on the derivative and these points are marked on the original graph. Then, the area under the curve between the marked points is calculated by the software and divided by the mass of the sample to give the phase change enthalpy per mass of the sample. The phase change temperatures are actually the onset temperatures showing intersection point of the characteristic line and the tangent with the greatest slope at the beginning of the phase change.

The melting and freezing temperatures and the phase change enthalpies of each novel organic PCM are given in Table 6.1 and 6.2, respectively.

**Table 6.1 :** Phase change temperatures of the novel organic PCMs.

PCM	Melting Temperature (°C)	Freezing Temperature (°C)
14 – 12	38.05	36.10
14 – 14	41.60	40.03
Cetiol MM	39.92	39.34
14 – 16	48.08	47.37
14 – 18	49.58	48.30
14 – 20	52.84	51.84
14 – 13	40.03	38.71
14 – 15	45.43	44.66
14 – 17	46.69	46.02
14 – 19	50.19	49.56

According to the measured temperatures of melting and freezing, it can be concluded that these organic PCMs do not show significant supercooling. It has been stated in the literature that a suitable PCM should have small supercooling degree (Kenisarin and Mahmadoy, 2007). Sharma, et al. (2009) indicates that supercooling of more than a few degrees effects the heat extraction from the store, and 5–10°C supercooling can prevent it entirely.

The temperature differences between melting and freezing change in the range of 0.6°C to 1.95°C and this little temperature difference indicates that the phase change process occurs homogeneously with proper crystal growth during freezing at 2°C/min heating and cooling rate. This means that these materials will show less temperature difference in applications, where the heat flow causes slower temperature change in practice. Such kind of thermal behavior of the synthesized high-chain fatty acid esters is an important advantage for engineering approaches and applications.

Besides the low supercooling degree and melting temperature range of 38°C and 53°C, the investigated novel organic PCMs have very promising phase change enthalpy values. The phase change enthalpy of each organic PCM is more than 200 kJ/kg and it is higher than most of the inorganic and organic PCMs in literature, which are given in Table 2.1, Table 2.2, Table 2.3 and Table 2.4 of Chapter 2. It is interesting to point out that the phase change enthalpy increases with the increased carbon number of fatty acid. The order of increase is smooth and continuous up to reaching the climax of approximately 219 kJ/kg enthalpy of 14 – 18. The esters of nonadecanoic acid and eicosanoic acid reverse the increasing drift till reaching the lowest enthalpy of approximately 201 kJ/kg of 14 – 20.

Another interesting effect of chemical structure on the phase change enthalpy is that the methyl and ethyl esters of palmitic and stearic acids given in Table 2.4 have less enthalpy values than the myristyl esters of palmitic and stearic acids. That might be because of increase in carbon number of alcohol which enhances the thermal properties in terms of phase change enthalpy and increases the melting temperature of the material.

**Table 6.2 :** The phase change enthalpies of the novel organic PCMs.

PCM	Enthalpy of Fusion (kJ/kg)	± 95 % Conf. Interval	Enthalpy of Freezing (kJ/kg)	± 95 % Conf. Interval
14 – 12	208.03	± 3.21	- 207.82	± 3.20
<b>Relative SD</b>	0.62 %		0.62 %	
14 – 14	210.00	± 6.02	- 210.68	± 5.57
<b>Relative SD</b>	1.80 %		1.66 %	
Cetiol MM	201.54	± 5.46	- 202.03	± 5.86
<b>Relative SD</b>	3.52 %		3.77 %	
14 – 16	216.71	± 2.87	- 217.14	± 2.24
<b>Relative SD</b>	0.53 %		0.42 %	
14 – 18	219.17	± 6.86	- 219.45	± 6.66
<b>Relative SD</b>	1.97 %		1.91 %	
14 – 20	201.18	± 6.76	- 200.16	± 6.90
<b>Relative SD</b>	2.11 %		2.17 %	
14 – 13	205.71	± 2.73	- 205.26	± 3.14
<b>Relative SD</b>	1.07 %		1.23 %	
14 – 15	212.82	± 7.10	- 213.35	± 7.73
<b>Relative SD</b>	2.10 %		2.27 %	
14 – 17	216.16	± 2.61	- 217.06	± 2.57
<b>Relative SD</b>	1.00 %		0.97 %	
14 – 19	204.97	± 2.09	- 205.01	± 2.95
<b>Relative SD</b>	1.10 %		1.55 %	

The phase change thermal properties of the novel organic PCMs vary between 201 kJ/kg and 220 kJ/kg in the temperature range of 38°C and 53°C. Thermal values above 200 kJ/kg make them very valuable because there are not many organic substances in literature which have similar heat absorption capacity of melting at temperatures lower than 60°C. A brief comparison of the results of this work with the selected organic and inorganic PCMs is given in Table 6.3.

Among the organics, these materials are at the top rank between 38°C and 53°C according to the modified graph of Mehling and Cabeza (2008), given in Figure 6.3. The clathrates and sugar alcohols are the only two organic groups, which have more heat absorption capacity. However, these two groups work at temperatures lower than 20°C and above 70°C, respectively.

**Table 6.3 :** Brief comparison of the selected PCMs with the results of the presented work.

Compound	Melting Temp. (°C)	Enthalpy of Fusion (kJ/kg)	Melting Temp. & Enthalpy of Fusion Ranges of the Novel Organic PCMs	
Na <sub>2</sub> S <sub>2</sub> O <sub>3</sub> .5H <sub>2</sub> O (Zhang, 1999)	48	201 – 206	38 – 53°C	201 – 220 kJ/kg
CaCl <sub>2</sub> .6H <sub>2</sub> O (Lane, 1980)	29	190.8		
Zn(NO <sub>3</sub> ) <sub>2</sub> .6H <sub>2</sub> O (Hawes, 1993)	36.4	147		
Polyglycol E6000 (Dincer, 2002)	66	190		
Paraffin C <sub>20</sub> -C <sub>33</sub> (Abhat, 1983)	48 – 50	189		
Methyl Stearate (Suppes, 2003)	38	208		
Ethyl Stearate (Suppes, 2003)	33	188		

Among the organic and inorganic PCMs, the inorganics are the largest group, including materials with high latent heat values in a very broad temperature interval, starting from subzero degrees up to 800°C. However, supercooling and corrosion are their two important drawbacks. Therefore, it is advantageous today to introduce new organic materials with proper thermal properties above 200 kJ/kg as alternatives to those inorganic materials like salt hydrates.



It is not possible to find any alternatives which work above 250°C because most of the organic materials tend to degrade after 200°C. However, new organics can meet the requirements at lower temperatures. The results of this work are valuable to introduce new organic materials with high latent heat of fusion at temperatures lower than 60°C as new alternatives of inorganic salt hydrates. If it is assumed that the density of the new high-chain fatty acid esters is close to 1 g/mL, the roughly estimated place of the novel organic PCMs submitted in this work is clearly seen in Figure 6.4.

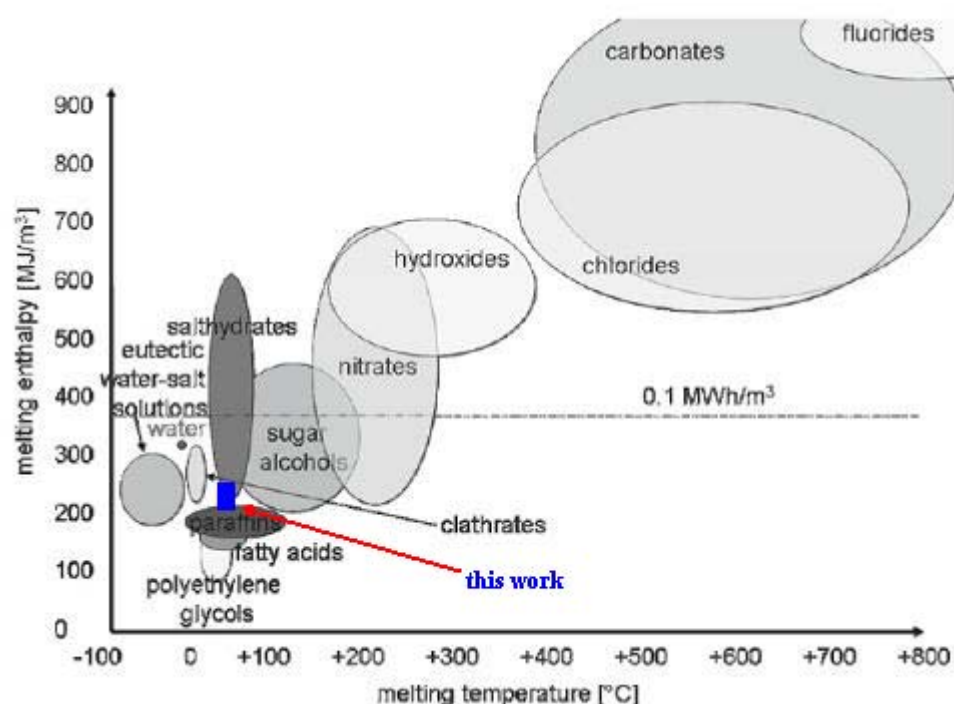


**Figure 6.4 :** Modified graph of Mehling and Cabeza (2008).

The synthesized organic PCMs show single sharp phase change peak throughout the scanned temperature interval, which is a great advantage to be used in applications. Single sharp peak implies that these materials are pure and they do not show any secondary solid – solid phase change before reaching the melting temperature in terms of reconfiguration of the crystal structure, so that, the excess heat is absorbed from the surrounding in one single step at a defined temperature. The heat flow graphs of the selected novel organic PCMs are given in Figure 6.5. The heat flow graphs of the other high-chain fatty acid esters are given in Appendix A.1.

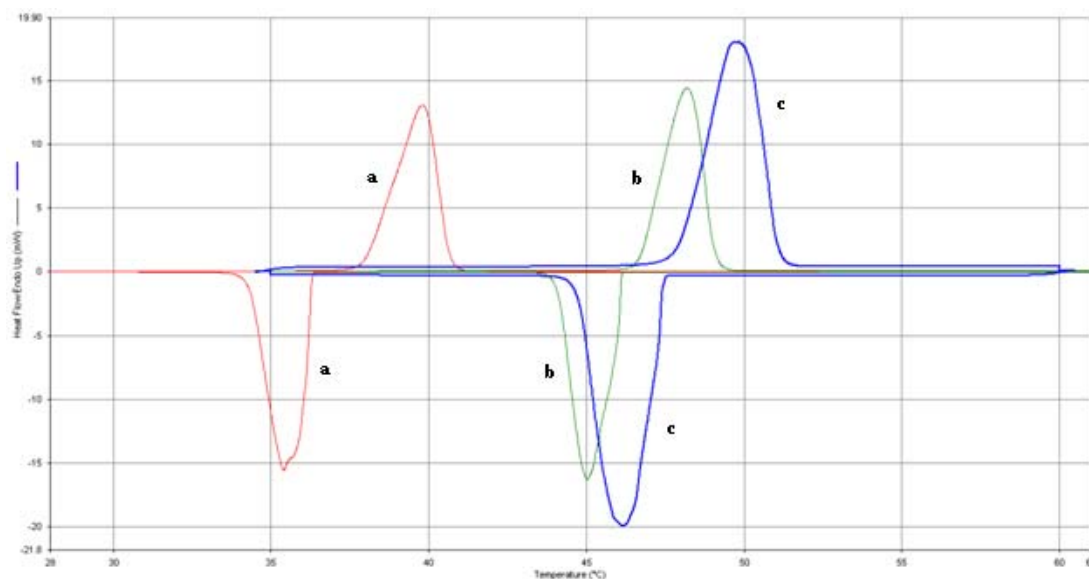


**Figure 6.5 :** Heat flow graphs of (a) 14 – 12, (b) 14 – 17 and (c) 14 – 16.

The DSC data of Cetiol MM is very similar to 14 – 14 with single peak but it has lower onset temperatures and phase change enthalpies. In addition to that the single phase change peak of Cetiol MM is not as sharp as the one of 14 – 14 ester. The difference between the onset and enthalpy values and the characteristics of the peaks imply that the commercial product is mainly composed of myristyl myristate, but also some impurities are present in the product, as expected. The heat flow graphs of both of the PCMs are given in Figure 6.6.

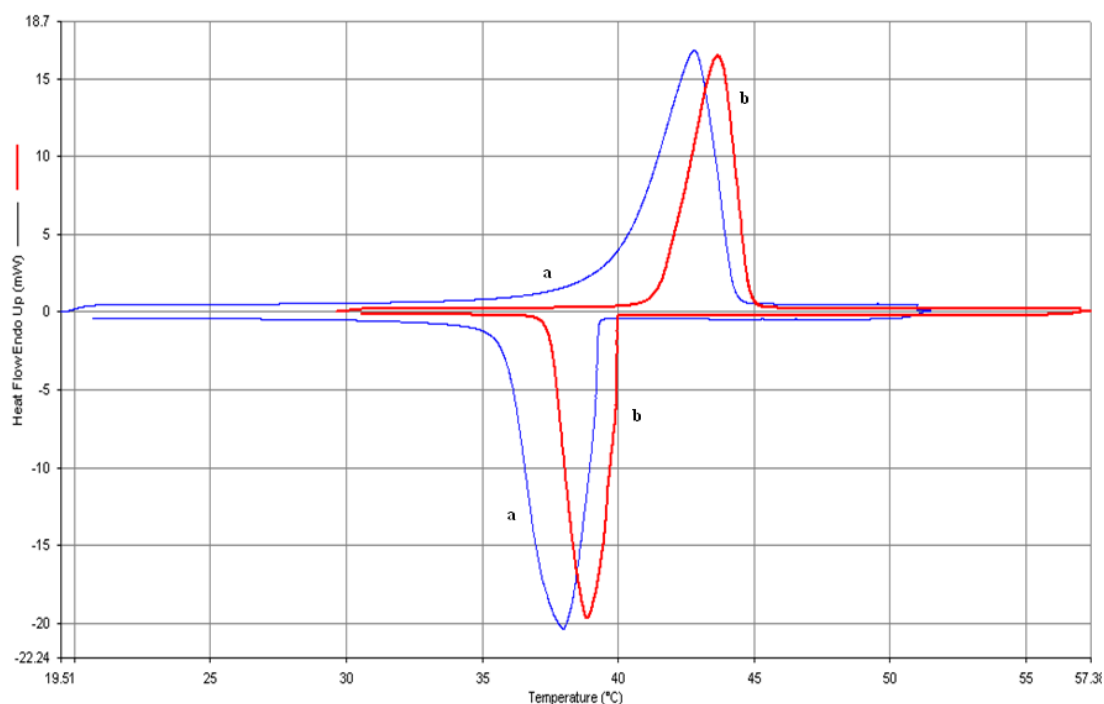


**Figure 6.6 :** Heat flow graphs of (a) Cetiol MM and (b) 14 – 14.

#### 6.2.2.2 The effect of ester bond on the thermal properties of the organics

The effect of ester bond has also been investigated in this research to determine its contribution to the thermal properties. For this purpose, two linear alkanes with carbon numbers equivalent to two of the high-chain fatty acid esters have been chosen and DSC analyses have been conducted in order to observe the differences between the thermal properties of the materials.

N-hexacosane and n-triacontane have the same number of carbon atoms with 14 – 12 and 14 – 16 esters, respectively. The only difference between the n-alkanes and the corresponding fatty acid esters is the ester bond, which is present in the esters between the hydrocarbon tails of fatty acid and alcohol. However, this difference entirely affects the thermal properties of the chemicals. The chemical structures of n-hexacosane, n-triacontane and the corresponding high-chain esters are given in Figure 6.7.

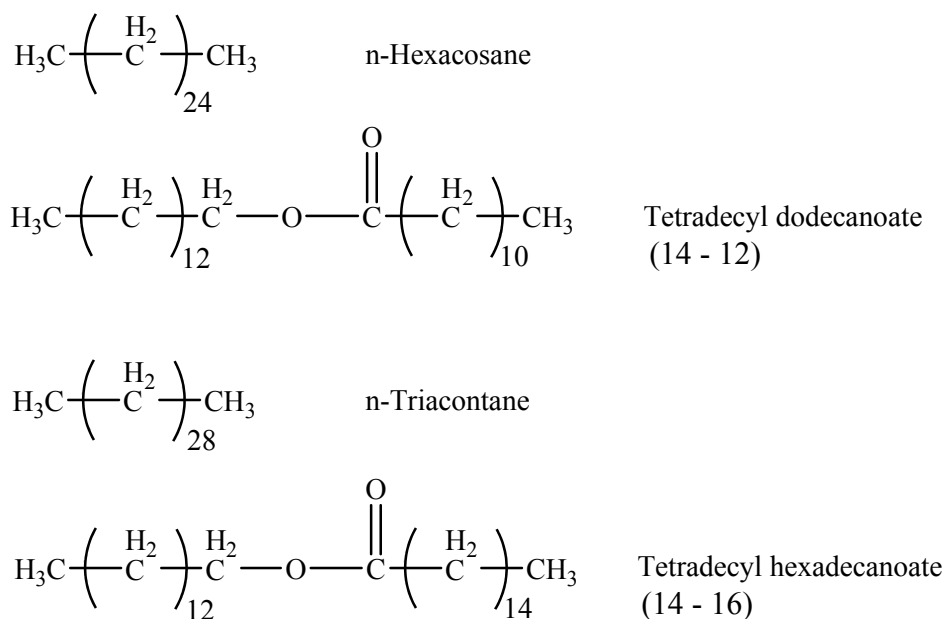


**Figure 6.7 :** The chemical structures of n-alkanes and fatty acid esters.

The DSC analyses show that both of the alkanes undergo two distinguishable phase changes. The first sharp peak represents solid – solid phase change of crystal structure re-conformation and the second one is the solid – liquid phase change in the heating step, and vice versa during cooling. According to Briard, et al. (2003), n-hexacosane and n-triacontane undergo order-disorder transitions at solid state close to the melting point. They stated that the order-disorder solid – solid transition is characterized by the higher thermal effect observed at the solid state close to the melting point. This behavior is clearly seen in Figure 6.8 and Figure 6.9. On the other hand, esters undergo just solid – liquid phase change with single sharp phase change peak.

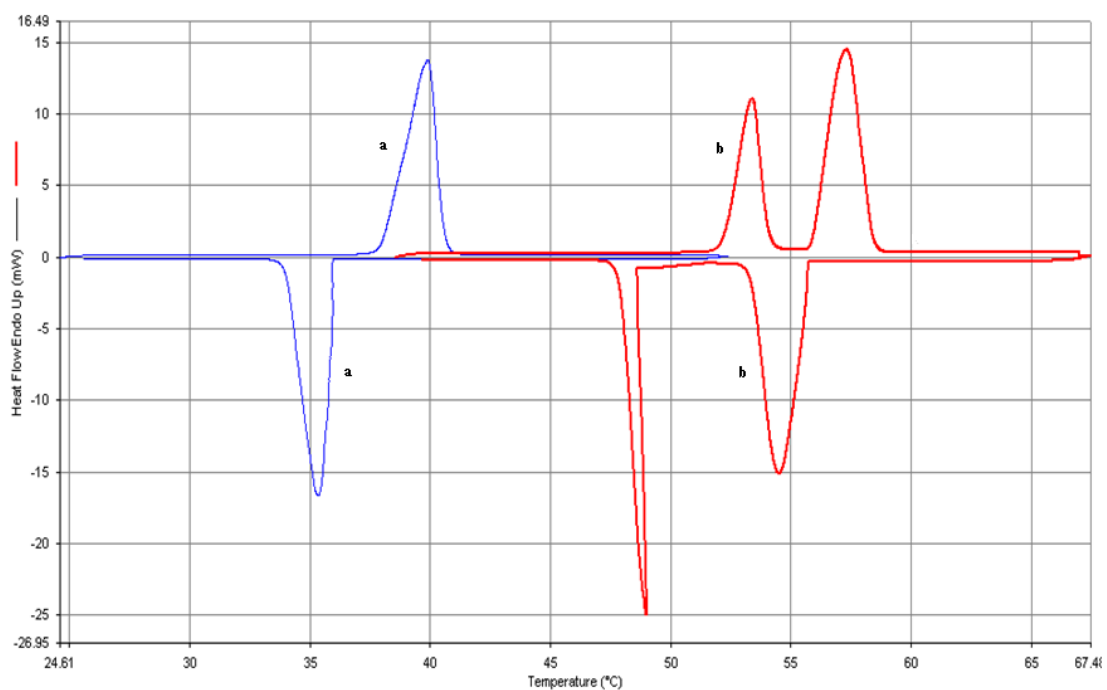


**Figure 6.8 :** Heat flow graphs of (a) 14 – 12 and (b) n-hexacosane.

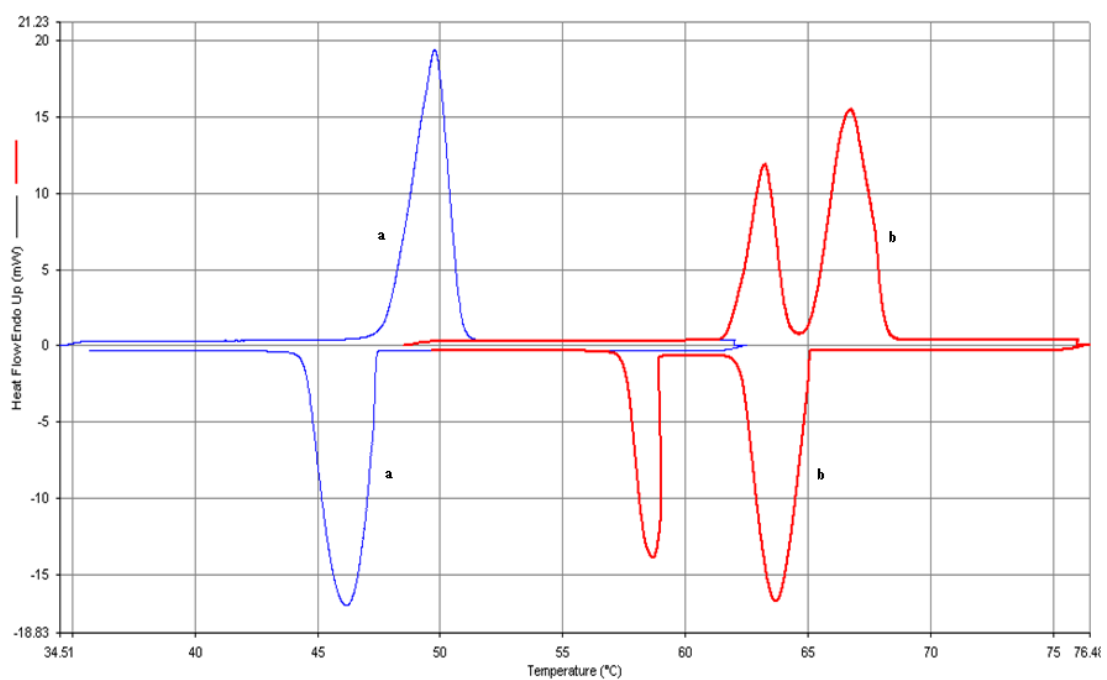


**Figure 6.9 :** Heat flow graphs of (a) 14 – 16 and (b) n-triacontane.

The total phase change enthalpies and phase change temperatures of n-hexacosane and n-triacontane are higher than the corresponding esters. The comparison is tabulated in Table 6.4 and Table 6.5. It is important to point out that the decrease in phase change temperature and enthalpy given below is particular for 14 – 12 and 14 – 16 esters. The degree and sign of change might be different for other high-chain fatty acid esters with the same number of carbon atoms, but with different fatty acid and alcohol combinations.

Another significant effect of the ester bond is the important modification on the thermal behavior of the organic materials. It provides one step heat transfer during phase changes, i.e. the heat is stored or released at one particular temperature in great extent and this property makes the esters useful for utilization. A chemical with thermal behavior similar to the alkanes is not suitable for thermal applications because the response of the chemical to the ambient temperature change is interrupted by sequential phase changes and the total amount of transferable heat is divided into sub-groups in a broader temperature interval.

**Table 6.4 :** Phase change temperatures of the n-alkanes and PCMs.

<b>Alkane/PCM</b>	<b>Melting Temperature (°C)</b>	<b>Freezing Temperature (°C)</b>
n-Hexacosane	54.10	48.69
14 – 12	38.05	36.10
n-Triacontane	64.19	65.09
14 – 16	48.08	47.37

**Table 6.5** : Phase change enthalpies of the n-alkanes and PCMs.

Alkane/PCM	Enthalpy of Fusion (kJ/kg)	± 95 % Conf. Interval	Enthalpy of Freezing (kJ/kg)	± 95 % Conf. Interval
n-Hexacosane	251.09	± 6.22	- 250.39	± 6.83
<b>Relative SD</b>	1.56 %		1.71 %	
14 – 12	208.03	± 3.21	- 207.82	± 3.20
<b>Relative SD</b>	0.62 %		0.62 %	
n-Triacontane	257.82	± 9.96	- 256.44	± 9.69
<b>Relative SD</b>	1.56 %		1.52 %	
14 – 16	216.71	± 2.87	- 217.14	± 2.24
<b>Relative SD</b>	0.53 %		0.42 %	

The effect of the ester bond on the thermal properties can also be observed by the comparison of those properties of fatty acids and their constituent high-chain fatty acid esters. A fatty acid consists of a polar carboxylic acid head with a hydrocarbon tail and an ester is almost a non-polar compound with the formed ester bond in the chemical structure.

The fatty acids of myristyl laurate, myristyl myristate, myristyl stearate and myristyl palmitate, solely, have less enthalpy than the esters formed with myristyl alcohol. The ester bond formed between the fatty acid and alcohol parts enhances the enthalpy of phase change and decreases the melting temperature to a point lower than the myristic, palmitic and stearic acids. At this point, it is interesting to state that even if the length of the molecule increases, the melting point decreases with the formed ester linkage and decreased polarity. The comparison is tabulated in Table 6.6.

**Table 6.6 :** Comparison of the thermal properties of the selected fatty acids and the related fatty esters.

<b>Fatty Acid</b>	<b>Melting Temp. (°C)</b>	<b>Enthalpy of Fusion (kJ/kg)</b>	<b>High-Chain Fatty Acid Ester</b>	<b>Melting Temp. (°C)</b>	<b>Enthalpy of Fusion (kJ/kg)</b>
Lauric Acid (Abhat, 1983)	42 – 44	178	14 – 12	38.05	208.03
Myristic Acid (Lane, 1980)	58	187	14 – 14	41.60	210.00
Palmitic Acid (Lane, 1980)	64	185	14 – 16	48.08	216.71
Stearic Acid (Lane, 1980)	69	202.5	14 – 18	49.58	219.17

### 6.2.2.3 Determination of change in thermal properties with extended cycling

A suitable PCM must have good thermal reliability depending on the number of thermal cycles. Minimum changes in phase change enthalpy and temperature after several thermal cycles are required for a useful PCM. Therefore, thermal reliability of the new chemicals should be determined before introducing them to the literature as novel PCMs.

In this research, the thermal reliability of the novel organic PCMs has been determined with the help of a DNA thermal cycler by conducting 1000 heating and cooling cycles, i.e. the sample melts 1000 times, and the thermal properties are re-analyzed by DSC afterwards in order to clarify the differences between the original and the aged samples. The DSC calibration and analysis were conducted according to the same ASTM procedure and under the same conditions of the previous analyses.

Number of phase changes of a PCM in one year period depends on the type of application, in which it is being used. If it is assumed that a suitable PCM changes phase according to the temperature difference between day and night, then 1000 thermal cycles are equivalent to approximately 3 years of shift. However, this shift might be longer if the ambient temperature does not oscillate around the phase change temperature everyday.



According to the DSC analyses of the aged samples, it has been found that the high-chain fatty acid esters do not show any significant changes in thermal properties after 1000 thermal cycles. The changes in the phase change enthalpies and temperatures are lower than 1 % and there are not any phase segregation or decomposition peaks in the heat flow graphs of the novel PCMs. The percentage changes in the phase change temperatures and enthalpies after thermal cycling are tabulated in Table 6.7 and Table 6.8.

**Table 6.7 :** The percentage changes in the phase change temperatures after thermal cycling.

PCM	Melting Temperature Difference	Freezing Temperature Difference
14 – 12	0.01 %	0.71 %
14 – 14	- 0.34 %	0.14 %
Cetiol MM	- 0.64 %	- 0.14 %
14 – 16	- 0.18 %	- 0.27 %
14 – 18	- 0.10 %	- 0.07%
14 – 20	0.42 %	0.54 %
14 – 13	0.09 %	- 0.21 %
14 – 15	0.26 %	- 0.12 %
14 – 17	0.60 %	- 0.38 %
14 – 19	- 0.16 %	- 0.02 %

**Table 6.8 :** The percentage changes in the phase change enthalpies after thermal cycling.

PCM	Enthalpy of Fusion Difference	Enthalpy of Freezing Difference
14 – 12	- 0.78 %	- 0.90 %
14 – 14	0.12 %	0.18 %
Cetiol MM	- 0.08 %	- 0.39 %
14 – 16	- 0.66 %	- 0.86 %
14 – 18	0.54 %	0.52 %
14 – 20	0.68 %	0.87 %
14 – 13	0.03 %	0.51 %
14 – 15	0.24 %	0.33 %
14 – 17	0.43 %	0.64 %
14 – 19	- 0.86 %	- 0.94 %

The overlapped heat flow graphs clarify that the aged samples show the same thermal behavior as the originals do during heating and cooling according to the measured enthalpy values. The slope of the peaks and the onset temperatures are significantly similar and there are no any secondary peaks on the graphs of the aged samples, i.e. the novel PCMs are stable after 1000 thermal cycles in terms of chemical and thermal properties. Any chemical decomposition would be determined with the help of the heat flow graphs if there were any chemical structure disorders. The offset temperature and the height of the peaks are dependent on the amount of sample and that is why, they are not taken into consideration for comparison. The onset temperature and the characteristic of the peaks are the two distinct properties of DSC graphs. Overlapped heat flow graphs of selected PCMs are given in Figure 6.10 and Figure 6.11.

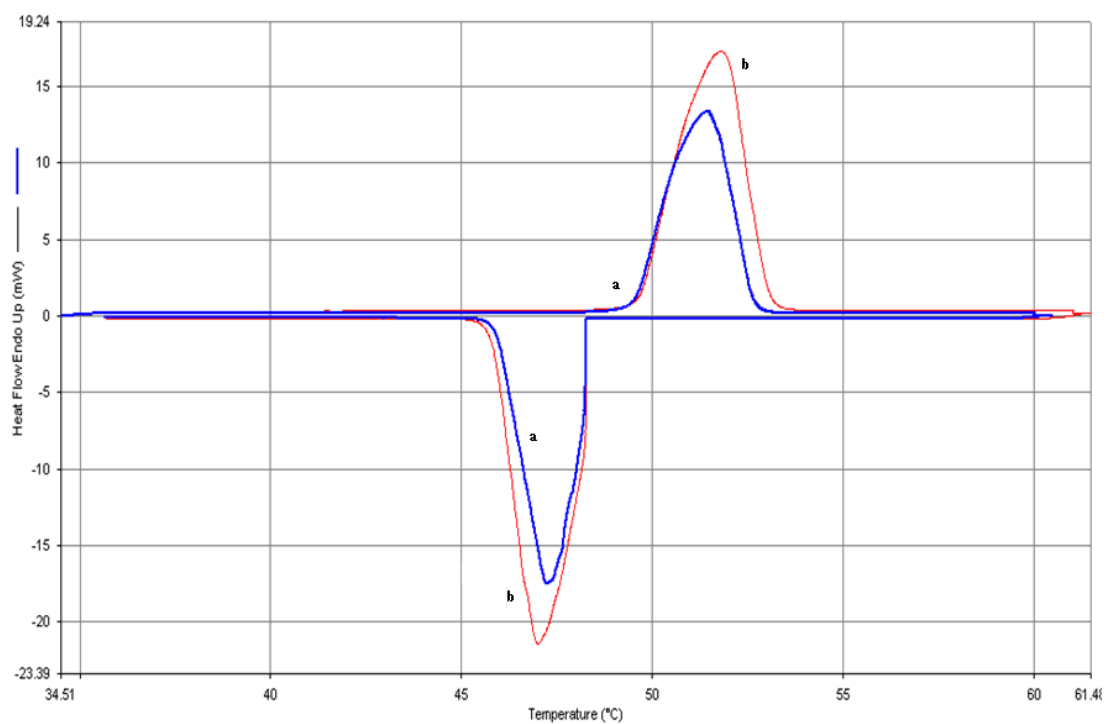


**Figure 6.10 :** Heat flow graphs of (a) 14 – 18 aged and (b) 14 – 18.

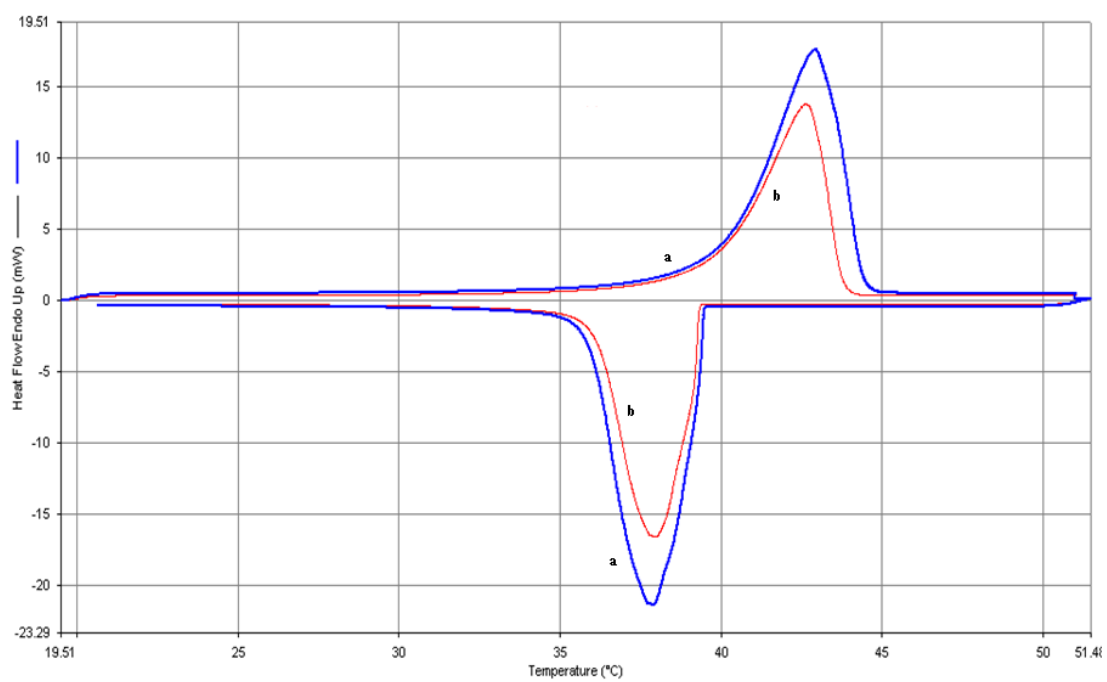


**Figure 6.11 :** Heat flow graphs of (a) Cetiol MM and (b) Cetiol MM aged.

#### **6.2.2.4 Determination of specific heat capacity ( $C_p$ ) of the novel organic PCMs**

Analyses of determination of specific heat capacity of solid and liquid phases were conducted according to the ASTM standard test method with designation number E 1269–05.

The measurements were carried out under inert nitrogen atmosphere at 20 ml/min flow rate and at 5°C/min heating rate. In addition to zinc and indium standards, sapphire standard was used for internal calibration. The sample data, obtained after each analysis, were corrected according to the data of the sapphire standard. The analyses were performed between 5°C and 85°C and the temperature interval of the calculated data was between 10°C and 80°C.

The procedure of specific heat capacity determination is similar to enthalpy analysis with some differences. The blank analysis, which is made with empty crucibles in order to eliminate the internal error of the instrument, is not automatically subtracted from the analysis of the sample. Therefore, the curves of blank analysis and the sample analysis are given on the final graph and the specific heat is directly proportional to the difference between the two curves. An illustrative example is given in Figure 6.12. Another important point is that the specific heat data is calculated between points, at which no phase change occurs. Preferably, 5 – 10°C difference between the phase change interval and the nearest specific heat point should be taken into account. Also, duration of the isothermal stage, which is determined in the program of each analysis, should be long enough to let the instrument reach its heat flow balance at the beginning and at the end of the analysis.

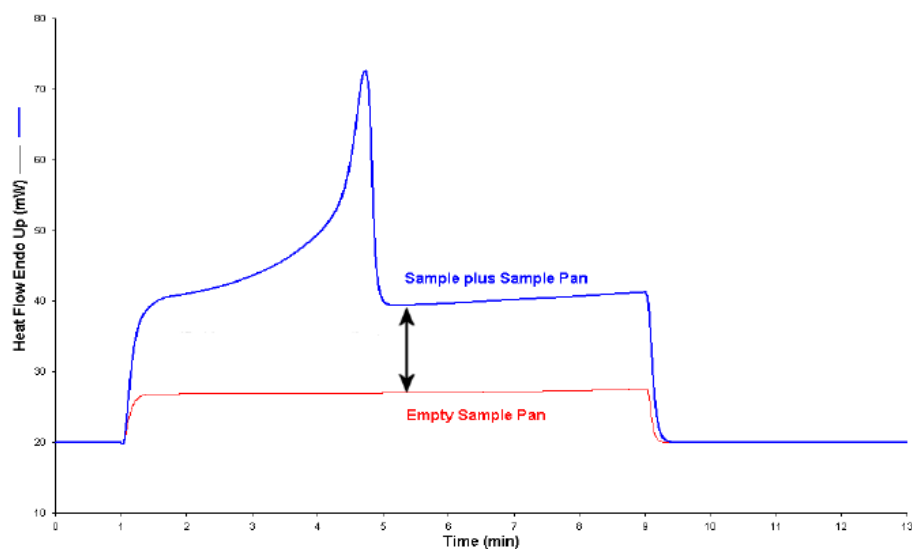


**Figure 6.12 :** An example of specific heat analysis (Robinson, 2003).

The DSC graphs of specific heat capacity analyses of 14 – 16 and 14 – 13 are given in Figure 6.13 and Figure 6.14, respectively. The red striped line represents the DSC heat flow data of sample and the blue striped line denotes the data of empty crucibles. The heat flow difference between these two lines gives the heat absorbed by the sample inside the crucible and the black line indicates the calculated specific heat capacity values in the scanned temperature interval.

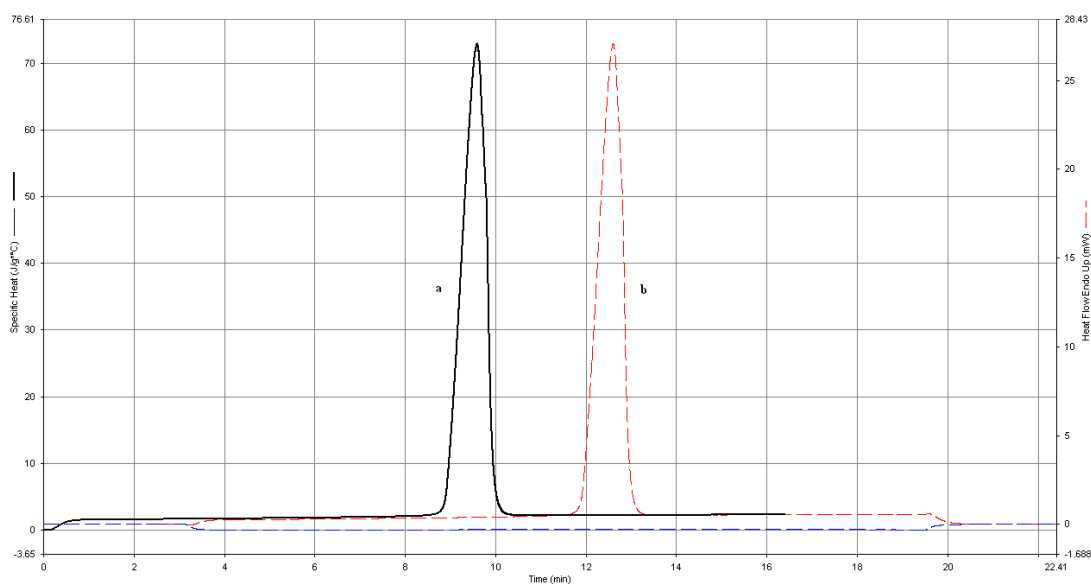


**Figure 6.13 :** The specific heat capacity analysis of 14 – 16:  
(a) specific heat change and (b) heat flow.

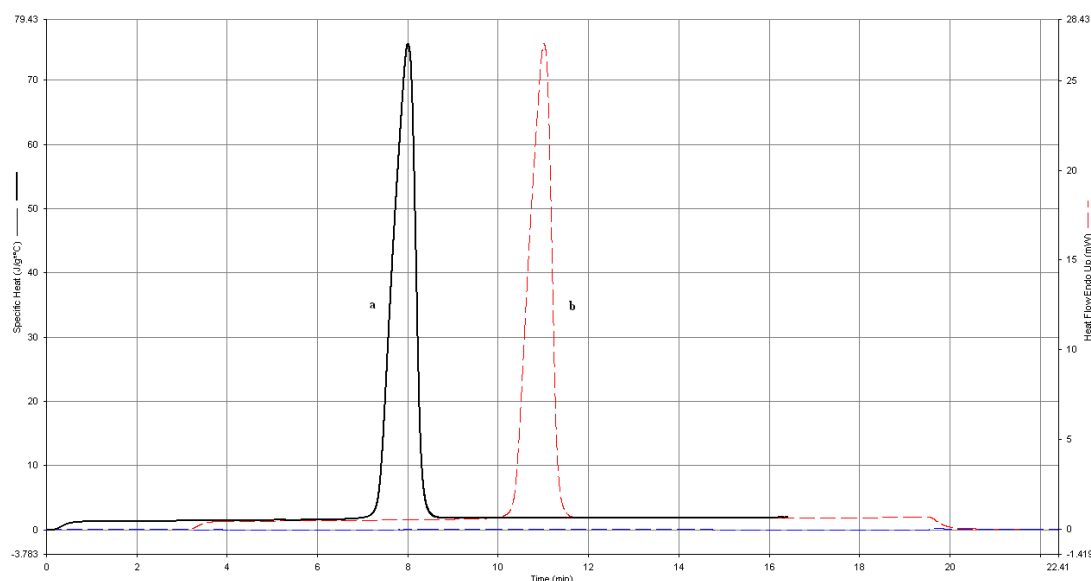


**Figure 6.14 :** The specific heat capacity analysis of 14 – 13:  
(a) specific heat change and (b) heat flow.

The specific heat capacity values at different temperatures can be reported as discrete average values or in terms of a polynomial equation, representing heat capacity values as a function of temperature. Scientists generally prefer using polynomial equations if the specific heat capacity values at the given temperatures are needed for accuracy instead of using the average. Therefore, the specific heat capacity of the novel organic PCMs are given as a function of temperature. The specific heat capacity in (kJ/kg.°C) unit can be calculated by using the the second order polynomials as a function of temperature. The second order polynomial can be written in general form as  $C_p(T) = A.T^2 + B.T + C$  for all novel organic PCMs and the coefficients of A, B and C are given for solid and liquid phases in Table 6.9 and Table 6.10 with the coefficient of determination ( $R^2$ ), respectively. The polynomials are calculated according to the measured data between 10°C and 80°C. The reliability of the presented data is between  $\pm 2 - 3 \%$ .

The coefficients were calculated with the help of curve fitting by using the mean values of the calculated specific heat data with respect to temperature. The specific heat values of each analysis were determined by the software of the instrument.

**Table 6.9 :** Coefficients of the second order polynomials in solid state.

PCM	A	B	C	R <sup>2</sup>
14 – 12	- 0.0001	0.0143	1.6865	0.99
14 – 14	0.0001	0.0071	1.5795	0.99
Cetiol MM	0.0002	0.0121	1.4607	0.99
14 – 16	$6.10^{-5}$	0.0092	1.6365	0.99
14 – 18	$6.10^{-5}$	0.0076	1.6030	0.99
14 – 20	0.0002	0.0026	1.1073	0.99
14 – 13	0.0002	0.0062	1.1332	0.99
14 – 15	0.0002	0.0060	1.3123	0.99
14 – 17	$2.10^{-5}$	0.0091	1.5203	0.98
14 – 19	0.0007	- 0.0040	1.5637	0.99

**Table 6.10 :** Coefficients of the second order polynomials in liquid state.

PCM	A	B	C	R <sup>2</sup>
14 – 12	$2.10^{-5}$	$9.10^{-5}$	2.2705	0.96
14 – 14	$-6.10^{-5}$	0.0095	1.8289	0.89
Cetiol MM	$-1.10^{-6}$	0.0026	1.9389	0.98
14 – 16	$-5.10^{-6}$	0.0042	2.0960	0.99
14 – 18	$-2.10^{-5}$	0.0067	1.9982	0.99
14 – 20	$9.10^{-5}$	-0.0112	2.0836	0.84
14 – 13	$-3.10^{-6}$	0.0079	1.3821	0.99
14 – 15	$1.10^{-4}$	-0.0111	2.3441	0.96
14 – 17	$7.10^{-5}$	-0.0026	2.0424	0.99
14 – 19	$-2.10^{-5}$	0.0041	1.9306	0.93

The average heat capacity values of solid and liquid phases were calculated with the help of the given polynomials, and they are tabulated in Table 6.11. The order of the magnitude of the specific heat capacity values is different than the order of enthalpy. The average values are calculated according to the measured data between 10°C and 80°C.

**Table 6.11 :** Average specific heat capacity ( $C_p$ ) of solid and liquid phases.

PCM	Solid Phase (kJ/kg.°C)	Liquid Phase (kJ/kg.°C)
14 – 12	1.919	2.349
14 – 14	1.814	2.192
Cetiol MM	1.810	2.110
14 – 16	1.909	2.363
14 – 18	1.832	2.390
14 – 20	1.292	1.718
14 – 13	1.323	1.900
14 – 15	1.549	2.094
14 – 17	1.710	2.190
14 – 19	1.690	2.130

### 6.2.3 Thermogravimetric analysis of the novel organic PCMs

Thermogravimetric analysis (TGA) determines changes in weight as a function of change in temperature. The results can be given as onset decomposition temperature to show the temperature at which decomposition has already started and cannot be stopped. Presenting onset temperature is more preferable instead of giving the temperature at which decomposition starts because the starting temperature varies and can be determined inaccurately according to the judgements of different people looking at the same graph.



Onset temperature is determined with the help of the derivative of the graph. The starting and maximum points can easily be determined on the derivative and these points are marked on the original graph. The point, which is at the position of the derivative maximum, is positioned to make the longest tangent and the point, which is at the position of the start of the derivative, is directed to show the characteristic of the graph before weight loss. The intersection point is the onset decomposition temperature, which is more accurately determined than the starting temperature of decomposition.

TGA data is important to determine the temperature at which the material can withstand without chemical decomposition. The onset decomposition temperatures should be taken into consideration in choosing the encapsulation type and application area for utilization of PCMs.

Thermogravimetric analyses were conducted according to the general principles given in BS EN ISO 11358:1997. They were carried out at 10°C/min heating rate and under 20 ml/min nitrogen flow. The results are presented in Table 6.12.

**Table 6.12 :** Thermal decomposition temperatures of high-chain fatty acid esters.

PCM	Onset Decomposition Temperature (°C)	5 % Weight Loss Temperature (°C)
14 – 12	278.86	244.01
14 – 14	302.49	259.53
Cetiol MM	292.18	249.78
14 – 16	304.22	264.77
14 – 18	321.43	279.50
14 – 20	309.32	260.57
14 – 13	296.34	253.94
14 – 15	308.90	264.23
14 – 17	307.85	267.01
14 – 19	307.32	265.01

The onset decomposition and 5 % weight loss temperatures are above 270°C and 240°C, respectively, for all high-chain esters. This means that these materials can easily withstand an encapsulation procedure around 160°C without any thermal decomposition.

Esters with even carbon number show significant increase in thermal stability with increasing carbon number up to 14 – 20. The increase in fatty acid chain length promotes the durability of the material. On the other hand, esters with odd carbon number do not show any significant difference with increasing carbon length. The durability of the commercial product is 10°C lower than the high purity myristyl myristate synthesized in the laboratory, as expected.

The TGA data of the selected high-chain fatty acid esters are given in Figure 6.15 and Figure 6.16. The thermal decomposition graphs of the other high-chain fatty acid esters are given in Appendix A.1.

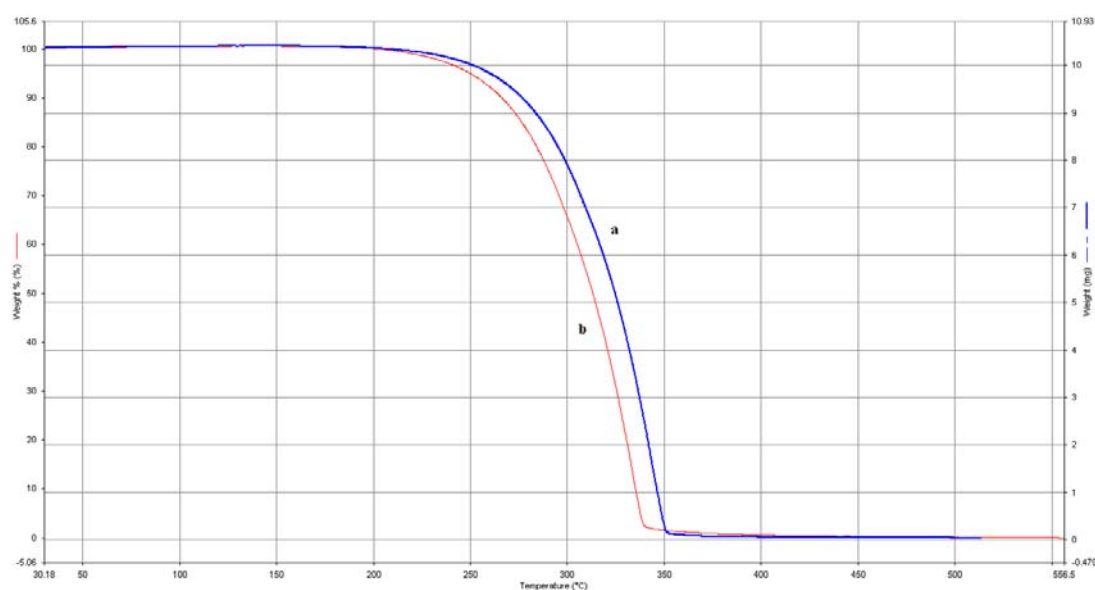


**Figure 6.15 :** Thermal decomposition graphs of (a) 14 – 14 and (b) Cetiol MM.

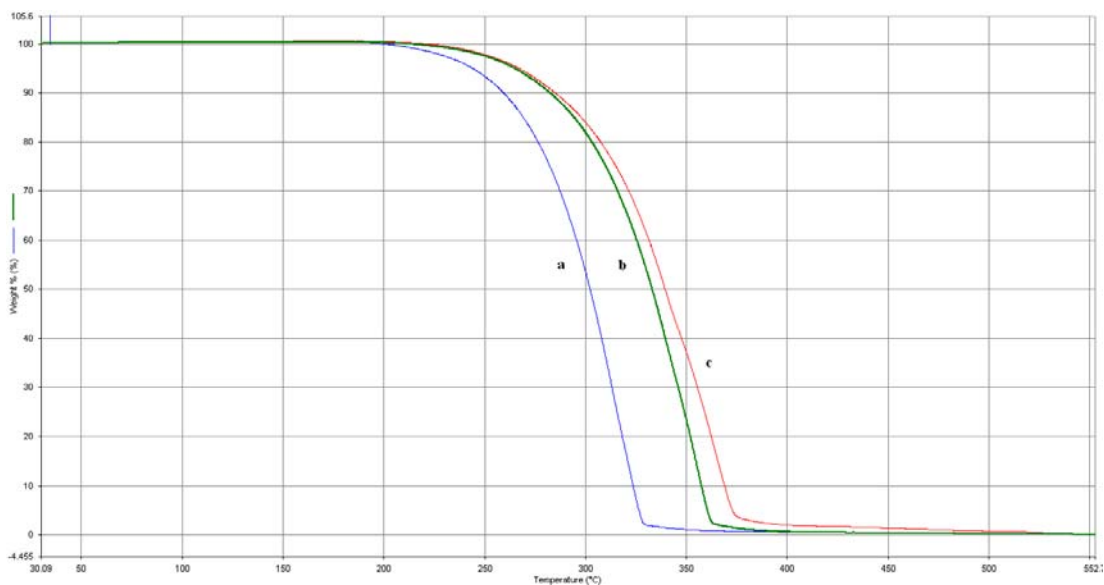


**Figure 6.16 :** Thermal decomposition graphs of (a) 14 – 12, (b) 14 – 16 and (c) 14 – 17.

### 6.2.3.1 The effect of the ester bond on gravimetric analyses of the organics

In addition to determination of the differences between the thermal properties of the organics, the thermogravimetric decomposition behavior has also been investigated. N-hexacosane and n-triacontane were analyzed at 10°C/min heating rate and under 20 ml/min nitrogen flow.

Unlike the DSC analyses, the results show that the effect of the ester bond is not so significant on the decomposition behavior of the organics. The characteristics of the overlapped graphs are very similar and the calculated onset temperatures are very close to each other with a slight difference of 1 %. The overlapped graphs are given in Figure 6.17 and Figure 6.18 and the onset temperatures are tabulated in Table 6.13.

At first glance, it is difficult to claim that the ester bond has a distinct effect on the thermal decomposition of the esters. However, even if no significant difference can be seen on the overlapped graphs, the onset temperature of 14 – 12 ester is lower than the corresponding alkane by 1 % and vice versa for the 14 – 16 ester. At this point, it is possible to mention that the effect of the ester bond can be more intense on high chain esters with the same number of carbon atoms, but with different fatty acid and alcohol combinations. The effect cannot be clearly seen between the 14 – 12 and 14 – 16 esters and the corresponding alkanes.

**Table 6.13** : Onset decomposition temperatures of the materials.

Material	Onset Decomposition Temperature (°C)
14 - 12	278.86
n-Hexacosane	281.54
14 – 16	304.22
n-Triacontane	301.15

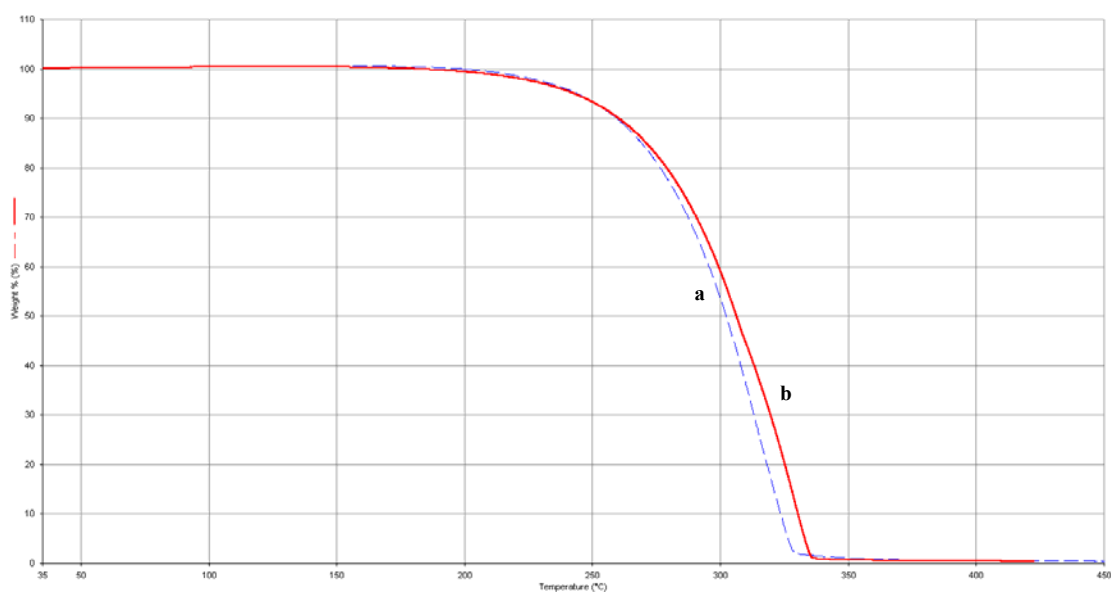


**Figure 6.17** : Thermal decomposition graphs of (a) 14 – 12 and (b) n-hexacosane.

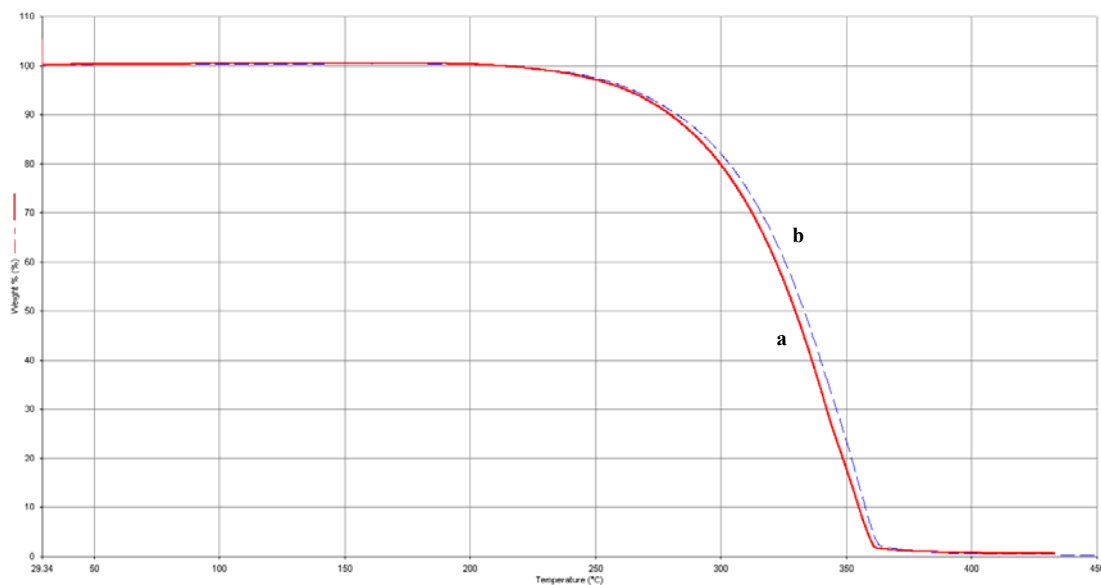


**Figure 6.18 :** Thermal decomposition graphs of (a) n-triacontane and (b) 14 – 16.

### 6.3 Synthesis of Polyurethane Rigid Foam – PCM (PU – PCM) Composite

In general, the synthesis of polyurethane rigid foam is a simple exothermic process, which takes place spontaneously in the presence of catalyst and blowing agents. There are many different formulations and several raw materials in the market to assure specifications of several products which are used in different areas.

A basic polyurethane rigid foam formulation consists of two parts. The first part is the polymeric isocyanate and the second part is the mixture of polyol, silicon, water, catalyst and blowing agent. When these two parts are mixed and stirred vigorously for a short time, the reaction between the polymeric isocyanate and polyol takes place and foam rises. However, the foaming process is easily interrupted when a chemically inert, but thermally active chemical is introduced into the reaction medium. Therefore, the synthesis formulation must be modified in such a way that the reaction thermodynamics are not interfered.

At the beginning of the PU – PCM composite synthesis research, the formulation given in Table 6.14 was used to observe foaming. Even though the foaming improves smoothly and ends with formation of a thick final product with trim surface, the presence of PCM in powder form terminates the rise of foam and a useless thin product with many large holes on its surface is formed. Such a counter result can be explained with the heat storage effect of the solid PCM granulates during melting.

During foaming, the temperature of the reaction medium increases and blowing agent evaporates, forming the closed-cell structure inside the foam with the help of the diffusion of carbon dioxide which is produced as a result of the reaction between water and isocyanate. However, this procedure is interrupted by phase change of the PCM which is present inside the reaction medium in solid form. The heat produced during the exothermic reaction is absorbed as it melts. This physical change prevents the rise of temperature, which in turn effects the evaporation of the blowing agent and formation of closed-cells.

**Table 6.14 :** Basic polyurethane rigid foam formulation.

<b>Part 1</b>	<b>Amount (g)</b>	<b>Part 2</b>	<b>Amount (g)</b>
Polyether Polyol	100.0	Polymeric MDI	130.0
Water	1.0		
Catalyst	0.5		
Blowing Agent	15.0		
Silicon	1.0		

After several blank foaming experiments in the presence of PCM, it has been concluded that the problem can be overcome by dissolving the PCM in an organic solvent and removing the water and blowing agent from the formulation. When PCM granulates are dissolved in an organic solvent and introduced into the reaction medium as the third part, they cannot strongly interfere the rise of reaction temperature, which results in formation of useful final products. According to the new mechanism, the organic solvent works as blowing agent and PCM crystals settle gradually as it evaporates. Thus, the heat absorption effect during the exothermic reaction is minimized and fine and homogeneous distribution of the PCM particles throughout the polymer matrix is provided by settlement of crystals from the organic solvent. The modified formulation is given in Table 5.2 of Chapter 5.

At this stage of the research, PU – PCM composites have been synthesized according to the modified method at different weight percentages to examine the contribution of PCM in thermal behavior of the insulation material with respect to the reference foam sample. 9.2 (w/w) %, 13.9 (w/w) % and 22.6 (w/w) % PCM containing foam blocks have been successfully synthesized in this research. Square foam blocks with 1 cm thickness were obtained by using wooden molds with dimensions of 8 cm x 8 cm x 1 cm. The bottom and top plates of each mold have randomly spaced 21 and 9 holes, respectively, to open gateways for evaporation of the blowing agent. The photograph of the foam blocks is given in Figure 6.19.

22.6 (w/w) % PCM content is the maximum value that can be reached according to the modified formulation due to the restrictive condition of PCM solubility in the solvent. The determined value of solubility of Cetiol MM in grams in tetrahydrofuran is 1.54 – 1.55 times the volume of the solvent at room temperature, i.e. 20 ml of tetrahydrofuran can dissolve approximately maximum 30.8 – 31.0 g of Cetiol MM at room temperature.

Further investigations on increasing the PCM content resulted in unsuccessful attempts with increased solvent volume. Even though the synthesis of the reference foam was with 30 ml of solvent without PCM, the increased PCM content inhibited proper formation of foam and solvent was trapped inside the polymer matrix due to lack of evaporation with decreased reaction temperature. In addition to that, 40 ml of solvent decreased the viscosity of the mixture during vigorous stirring and the polymerization reactions could not even reach completion properly in the absence of PCM.



**Figure 6.19 :** The PU – PCM composites: **(a)** reference, **(b)** 9.2 (w/w) %, **(c)** 13.9 (w/w) % and **(d)** 22.6 (w/w) % blocks.



## 6.4 Chemical and Thermal Analyses of PU – PCM Composites

### 6.4.1 FT-IR analysis

Several particular bonds in the chemical structure of polyurethane rigid foam show distinct peaks at specific wavenumbers. Stretching vibrations of (N–H), residual isocyanate, (C=O) urethane bonded can easily be noticed on the spectrum.

The FT-IR spectra of polymeric MDI, polyether polyol and reference foam are given in Figure 6.20. The strong bands of stretching vibrations of the isocyanate group and the (C–C) aromatic ring are clearly seen in the spectrum (a) with strong sharp peaks at  $2241\text{ cm}^{-1}$  and  $1520\text{ cm}^{-1}$  wavenumbers. Non-bonded isocyanate stretching vibration of (C=O) is seen at  $1721\text{ cm}^{-1}$  as a small trough.

The polyether polyol (b) shows a characteristic trough of the oxygen–hydrogen bond of the polyol part at  $3422\text{ cm}^{-1}$  and the polyether part of the chemical is clearly seen with the broad trough of stretching vibration of (C–O–C) aliphatic ether at  $1090\text{ cm}^{-1}$ . The absence of (C=O) band at around  $1680 - 1750\text{ cm}^{-1}$  shows that the sample is an ether with a single broad trough at  $1080\text{ cm}^{-1}$  instead of being ester.

The spectrum (c) of the reference foam is a combination of (a) and (b) as a result of the foaming reaction. The broad trough of stretching vibration of (N–H) is seen above  $3200\text{ cm}^{-1}$  and the stretching vibration of the bonded (C=O) urethane has another broad trough at  $1702\text{ cm}^{-1}$ . The weak absorbance at  $2280\text{ cm}^{-1}$  shows that residual isocyanate is present in the reference foam. The (C–O–C) stretching of the aliphatic polyether part of the polyurethane foam has a broad trough at around  $1090\text{ cm}^{-1}$  wavenumber (Dillon, 1969).

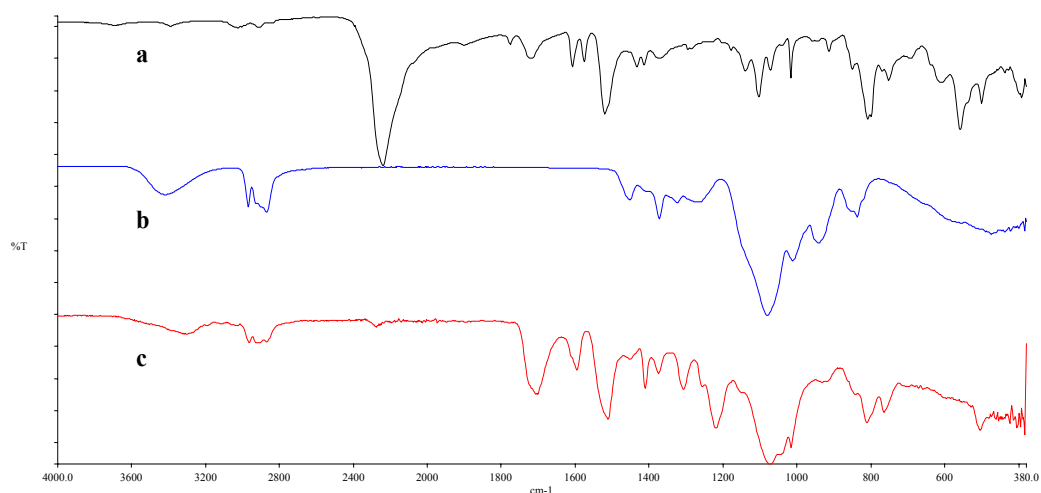


**Figure 6.20 :** FT-IR spectra of (a) polymeric MDI, (b) polyether polyol and (c) reference.

The FT-IR spectra of the reference foam, PU – PCM composites and Cetiol MM are given in Figure 6.21. The stretching vibrations of (N–H) and bonded (C=O) urethane show characteristic troughs of polyurethane rigid foam on the first four spectra. However, the shape of the absorbance of the bonded (C=O) changes with the increased PCM content and it shifts from  $1702\text{ cm}^{-1}$  to  $1731\text{ cm}^{-1}$  in the reference foam and 22.6 (w/w) % PU – PCM composite, respectively, with increased PCM content. The presence of weak absorbance around  $2280\text{ cm}^{-1}$  shows that residual isocyanate is present in the samples.

The (C=O) double bond is common in the chemical structures of esters and urethanes. However, the shapes and wavenumbers of the bands differ because of the nature of the bond in urethane and ester structures with its surrounding. Therefore, the change in shapes and places of the peaks should be taken into consideration in order to observe the increase in PCM content of the composites. It can be concluded that the trough like absorbance of (C=O) stretching of the urethane of the reference sample is transformed with the increased PCM content and shifted to  $1731\text{ cm}^{-1}$  wavenumber. The stretching vibration of (C=O) of Cetiol MM is seen at  $1733\text{ cm}^{-1}$  wavenumber with a sharp peak in spectrum (d).

The broad trough of (C=O) stretching of the reference sample is first modified with change in shapes of the end points and then formation of secondary minor absorbance in spectra (b) and (c) with increased PCM content. In spectrum (d), the end point of the absorbance is transformed into pin point and the sharp end is shifted to  $1731\text{ cm}^{-1}$  wavenumber. The spectrum of the sample with the highest PCM content is more similar to the spectrum of Cetiol MM than any others.

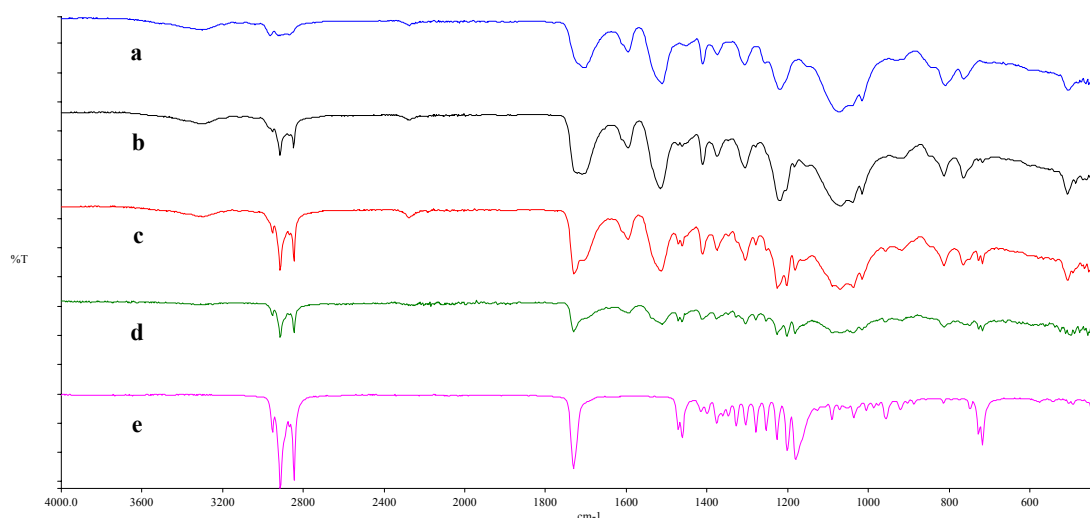


**Figure 6.21 :** FT-IR spectra of (a) reference, (b) 9.2 (w/w) %, (c) 13.9 (w/w) %, (d) 22.6 (w/w) % PU – PCM composites and (e) Cetiol MM.

#### 6.4.2 DSC analysis

Analyses of phase change enthalpy, temperature and total enthalpy change were conducted using Perkin Elmer Jade DSC at  $5^{\circ}\text{C}/\text{min}$  heating and cooling rate, under 20 ml/min nitrogen flow. DSC analyses were performed according to the ASTM standard test methods with designation numbers E 793–06 and E 1269–05.

The DSC analyses help to understand the thermal behavior of the PCM inside the polymer matrix and its contribution to the insulation property of the polyurethane rigid foam with changing percentages with respect to the reference foam. The net enthalpy of fusion and freezing is measured and compared with the calculated stoichiometric ratio of the PCM content in order to clarify that the PCM part inside polymer matrix responses to the thermal changes without any hinderances.

According to the DSC analyses of Cetiol MM, the PCM melts and crystallizes around 40°C and it has  $201.54 \pm 5.46$  kJ/kg and  $-202.03 \pm 5.57$  kJ/kg enthalpy of fusion and freezing, respectively. The samples, containing 9.2 (w/w) %, 13.9 (w/w) % and 22.6 (w/w) % PCM, are supposed to have  $18.54 \pm 0.5$  kJ/kg,  $28.01 \pm 0.76$  kJ/kg and  $45.55 \pm 1.23$  kJ/kg of heat of fusion, respectively, if there are no chemical or physical hinderances, which are affecting the thermal performance of the PCM.

The measured and calculated stoichiometric enthalpy values are tabulated in Table 6.15 with the measured phase change temperatures. It is clearly seen from Table 6.15 that the calculated and measured thermal values are very close to each other, i.e. the material does not involve in the polymerization reaction and acts like an inert material during the chemical reactions and the whole content added in tetrahydrofuran as the third part into reaction medium stays uninterrupted. Another important point is that the phase change temperatures of the entrapped PCM samples are almost equal to the results of the single analyses of the PCM. The slight difference is due to the changes in penetration of heat into the material inside the polymer matrix.

**Table 6.15 :** The thermal properties of the PU – PCM composites.

Percentage (w/w)	Heat of Fusion (kJ/kg)	Melting Temperature (°C)	Heat of Freezing (kJ/kg)	Freezing Temperature (°C)
9.2 %	$18.52 \pm 1.01$	36.56	$-17.91 \pm 0.33$	36.95
<b>Calculated</b>	$18.54 \pm 0.50$		$-18.59 \pm 0.54$	
13.9 %	$28.46 \pm 1.12$	37.62	$-28.59 \pm 2.81$	37.08
<b>Calculated</b>	$28.01 \pm 0.76$		$-28.08 \pm 0.81$	
22.6 %	$45.69 \pm 1.90$	39.25	$-45.55 \pm 1.92$	38.36
<b>Calculated</b>	$45.55 \pm 1.23$		$-45.66 \pm 1.32$	

The DSC graphs show that the reference polyurethane rigid foam does not show any latent thermal activity between  $-1^{\circ}\text{C}$  and  $67^{\circ}\text{C}$ . The additional latent heat absorption capacity comes from the PCM content embedded into the polymer matrix and it is easily observed in Figure 6.22 with respect to the reference foam.

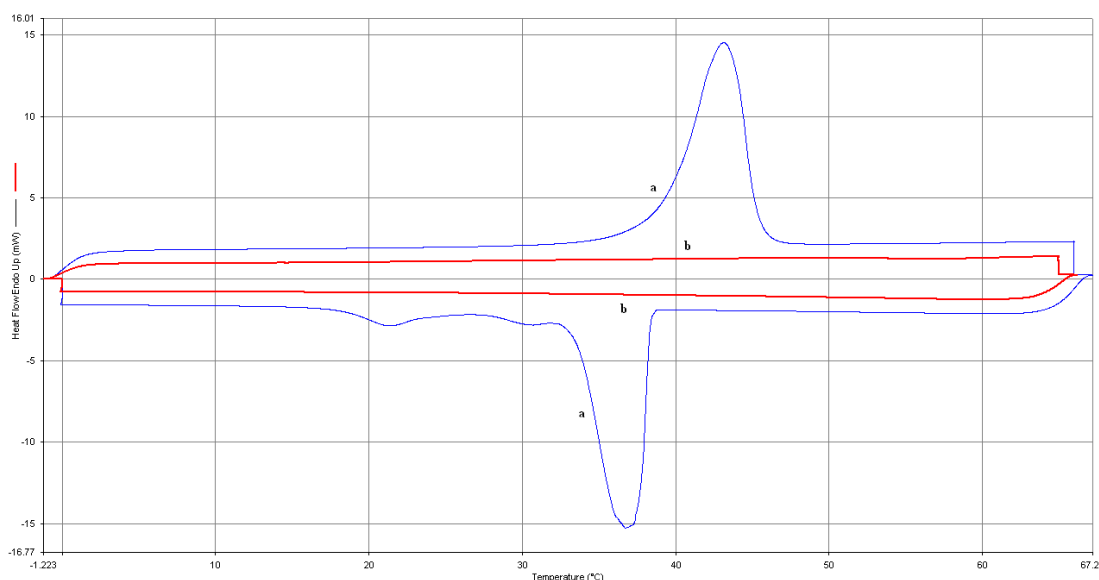


**Figure 6.22 :** Heat flow graphs of (a) 22.6 (w/w) % PU – PCM composite and (b) reference.

The thermal response of the new composites during melting is quite similar to the melting behavior of single Cetiol MM, which takes place in one single step. On the other hand, freezing is divided into regions and concluded after subsequent steps. By looking at Figure 6.22, it is possible to think that the PCM does not act like a chemically inert material and some side reactions take place during polymerization. However, such an opinion would be inconvenient because of the given calculated and measured heat of fusion and freezing results. Then, there must be another explanation to throw light on the different thermal behavior during cooling.

Freezing and melting are actually two different physical processes which are assumed to be opposite of just one another. Therefore, the difference is observed on one run instead of both. During cooling, desorption of heat is thermally hindered by freezing of PCM particles and the freezing is initiated by decrease in temperature of the surrounding boundary of a PCM particle. If the concentration of PCM particles is low, the thermal initiation is ceased and thermal response is lagged, i.e. broader DSC response is seen on the graphs instead of one sharp peak. In Figure 6.23, such a thermal response is observed with changing PCM contents. As the concentration of PCM increases, the first sharp peak of freezing gets more distinctive than the further lagged thermal response region.

The thermal response is mostly delayed according to the graph of 9.2 (w/w) % PCM containing sample and it is partially improved with the increase of concentration to 13.9 (w/w) %. It is clearly seen that the first sharp peak is more prominent even though there is still great proportion of lagged thermal response. However, this proportion is minimized with the increase of concentration to 22.6 (w/w) % PCM and most of the heat desorption is observed in the first step with ongoing phase change initiation of adjacent PCM particles.

Similar effect is also observed during melting in a different manner. Eventhough the thermal response of heat absorption is observed in one single step in every PCM concentration, the sharpness of the climax changes. The climax is transformed into cutting edge from gentle peak with changing concentration, i.e. the response of the material is more strongly transmitted throughout the polymer matrix as the PCM content increases.

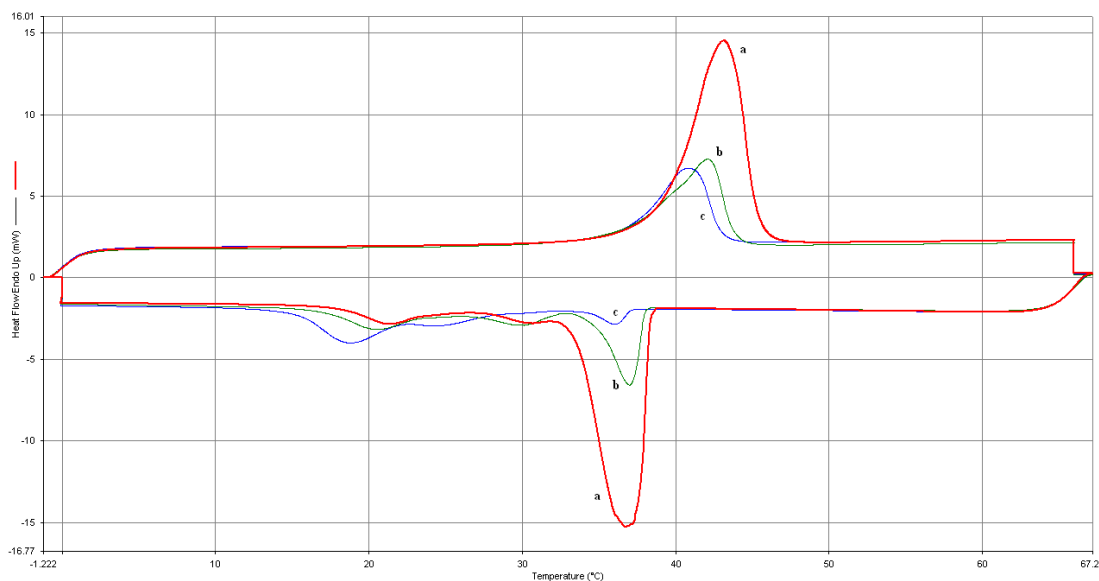


**Figure 6.23 :** Heat flow graphs of (a) 22.6 (w/w) %, (b) 13.9 (w/w) % and (c) 9.2 (w/w) % PU – PCM composites.

#### 6.4.2.1 Total enthalpy change of composites in a specific temperature interval

Improvement of the heat absorption capacity of the polyurethane rigid foam samples, provided by PCM, can also be expressed in terms of the total enthalpy change in a broader temperature interval. In the previous section, the net effect of PCM on the thermal behavior was given with respect to the additional latent heat, which is limited to the phase change interval.

In order to find out how much heat is totally absorbed by the composites with different PCM contents in terms of latent and specific heat, DSC analyses were carried out in broader temperature interval of 4 – 87°C. The analyses were conducted at 5°C/min heating rate, under 20 ml/min nitrogen flow and with using sapphire as internal reference.

The calculated results of the total enthalpy analyses are given in Table 6.16. The results show that the net amount of total heat absorbed by PU – PCM composites reach up to 34 % more than the total heat absorbed by the reference foam between 4°C and 87°C with respect to the mean values.

**Table 6.16 :** The total heat absorbed by reference foam and PU – PCM composites.

Composite	Total Enthalpy Change $\pm 95 \% \text{ Conf. Int.}$	Heat Absorption Enhancement
Reference	$156.82 \pm 14.69 \text{ kJ/kg}$	—
9.2 (w/w) %	$190.63 \pm 19.82 \text{ kJ/kg}$	$\sim 21 \%$
13.9 (w/w) %	$197.40 \pm 13.50 \text{ kJ/kg}$	$\sim 26 \%$
22.6 (w/w) %	$210.08 \pm 12.25 \text{ kJ/kg}$	$\sim 34 \%$

According to the DSC results given in Table 6.16, it is possible to maintain same amount of insulation property with approximately 34 % thinner polyurethane rigid foam block with 22.6 (w/w) % PCM content. The DSC graph of total enthalpy change of 22.6 (w/w) % PU – PCM composite is given in Figure 6.24. The total heat absorption capacity is directly proportional to the PCM content of the composites.

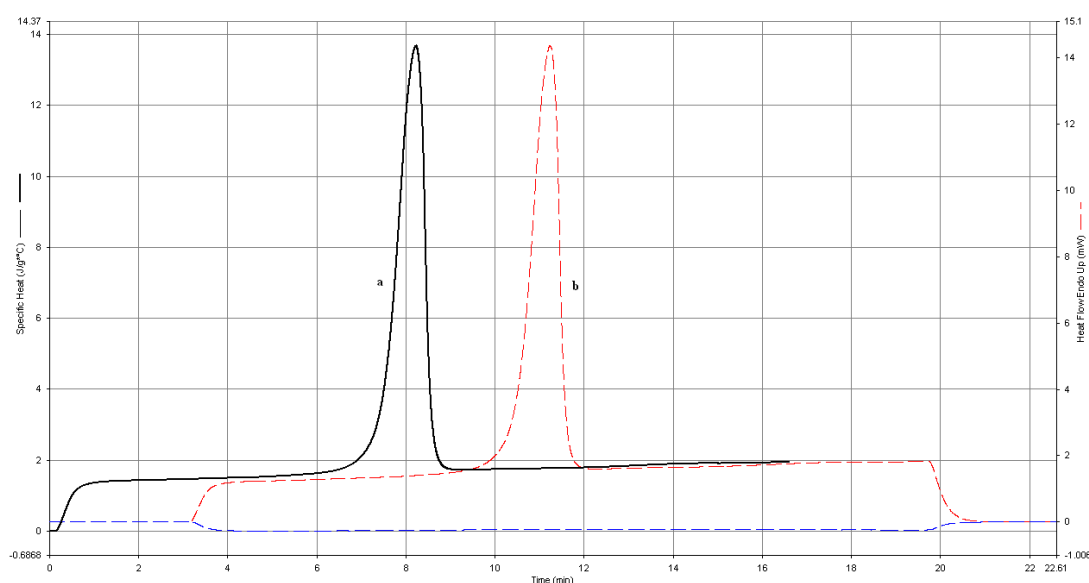


**Figure 6.24 :** Total enthalpy change of 22.6 (w/w) % PU – PCM composite:  
(a) specific heat change and (b) heat flow.



### 6.4.3 Thermogravimetric analysis

Thermogravimetric analyses of the PU – PCM composites were conducted using Perkin Elmer STA 6000 TGA at 10°C/min heating rate and under 20 ml/min nitrogen flow. TGA analyses were performed according to the general principles given in BS EN ISO 11358:1997.

Thermogravimetric analyses help to determine the maximum temperature that the material can withstand without decomposition. However, polyurethane is not a very resistant material to heat in its own chemical nature. It can catch fire if fire preservative additives are not used in its formulation.

The formulation of the synthesized foams does not contain any fire preservative additive and therefore the material is more sensitive to heat. Even though the thermogravimetric analyses were performed under inert nitrogen atmosphere, the absence of such preservatives affects the decomposition results. It can be concluded that the samples can withstand up to 110°C and further on decomposition is initiated slightly as the temperature increases.

It is clearly seen in Figure 6.25 that the increase in the PCM content of the composites decreases the resistance of the material and among the samples, including the reference, the reference is the most durable material. Also, the final ash content which is the remained pyrolyzed mass at 845°C shows that with the increased PCM content most of the material decomposes at the main decomposition stage and less polyurethane part is left for pyrolysis. The decomposition onset temperatures and ash content of the samples are given in Table 6.17.

**Table 6.17 :** TGA results of the PU – PCM composites.

<b>Composite</b>	<b>Decomposition Onset Temp. (°C)</b>	<b>Ash Content (%)</b>
Reference	307.01	~ 20.1
9.2 (w/w) %	303.39	~ 16.8
13.9 (w/w) %	300.08	~ 16.5
22.6 (w/w) %	279.96	~ 15.8

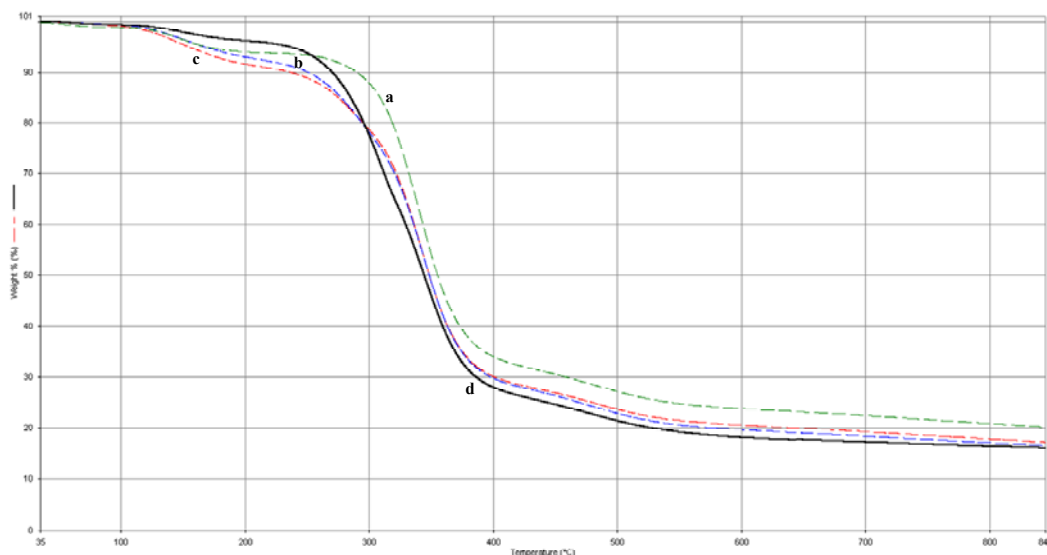


**Figure 6.25 :** Thermal decomposition graphs of (a) reference, (b) 9.2 (w/w) %, (c) 13.9 (w/w) % and (d) 22.6 (w/w) % PU – PCM composites.

### 6.5 Optical Microscope and SEM Images of PU – PCM Composites

The homogeneity and particle size distribution are two important factors which are affecting the uniform thermal response of the composites in larger scale. Therefore, the distribution of the PCM particles should be examined in order to support the results of the thermal analyses to prove that the given data would also be valid if the PU – PCM composite foam was produced in pilot scale. In this research, the distribution of PCM throughout the polymer matrix has been examined with the help of the optical microscope and SEM images.

The low magnification images of optical microscope (x400) show that the distribution of the PCM particles is homogeneous in every composite sample and the main detectable size distribution is around 7 – 8  $\mu\text{m}$ . The smooth polymer matrix is clearly seen in Figure 6.26 and the entrapped spherical PCM particles are spread along the matrix in Figure 6.27 – 6.29.

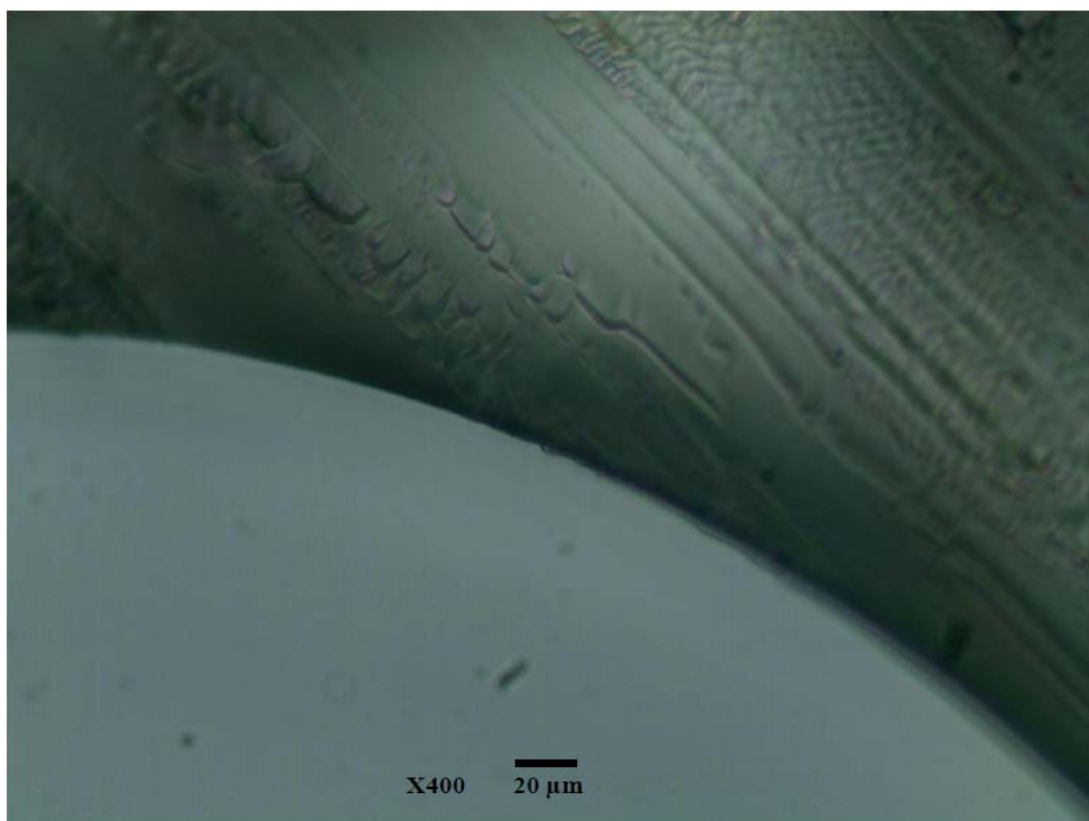


**Figure 6.26 :** The optical microscope image of reference foam.

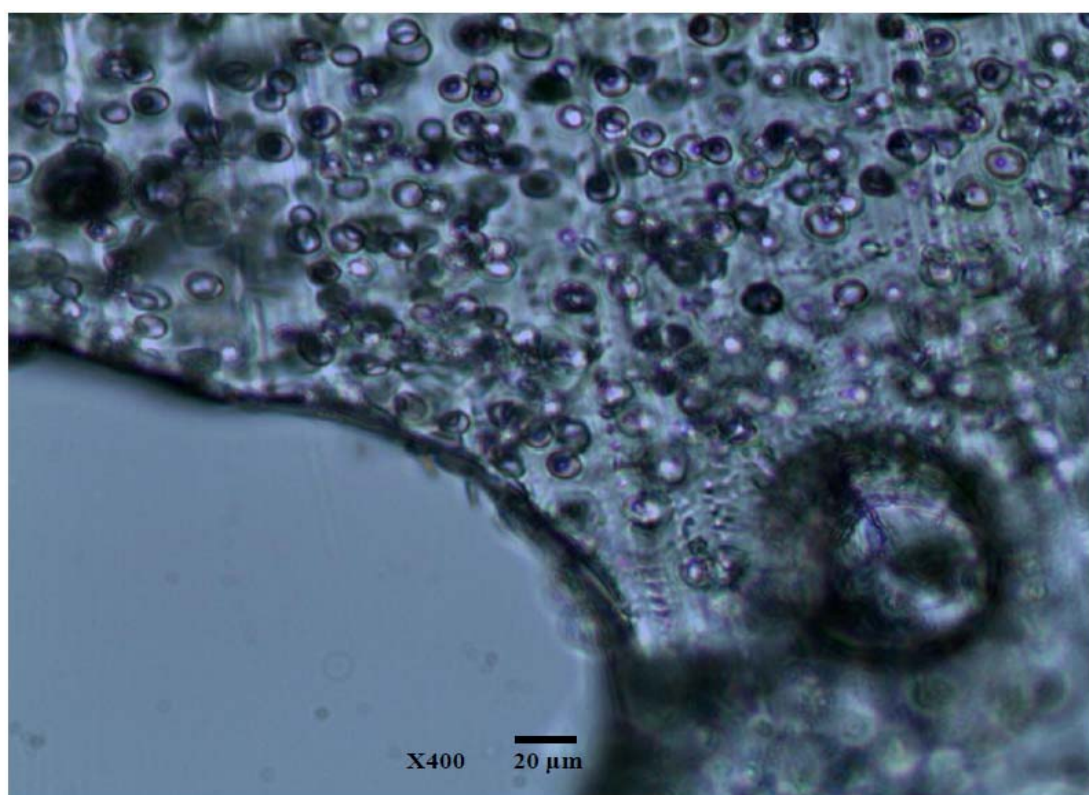


**Figure 6.27 :** The optical microscope image of 9.2 (w/w) % PU – PCM composite.

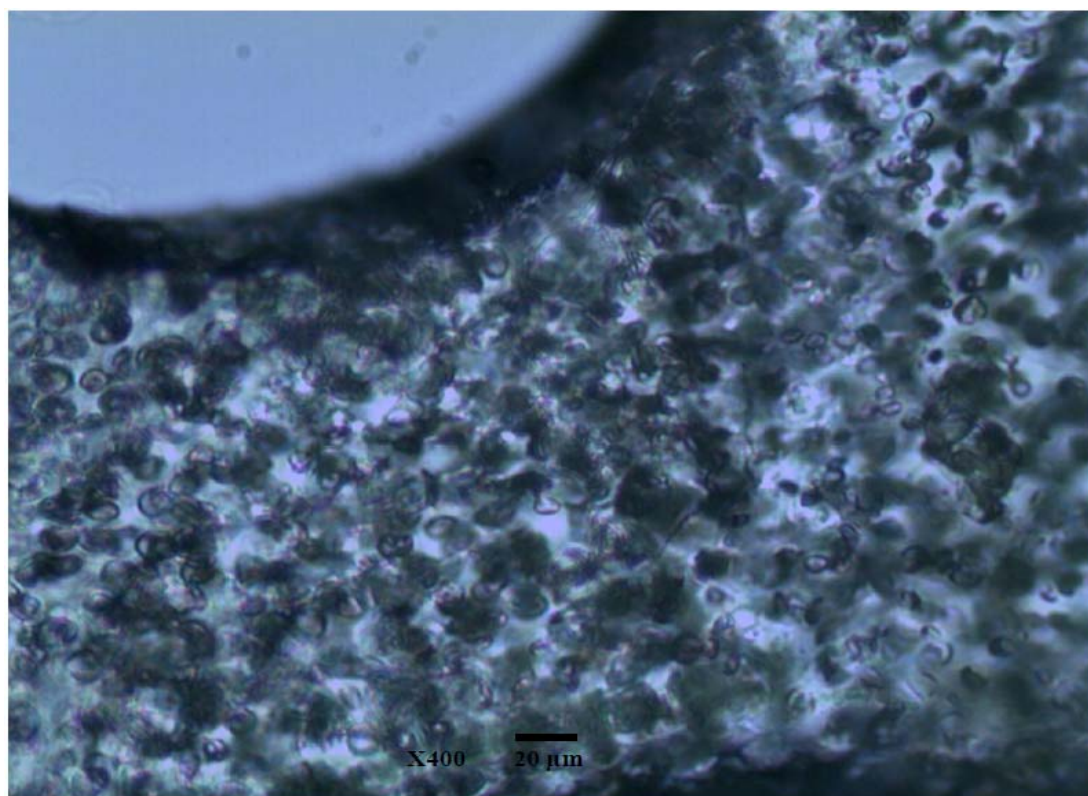


**Figure 6.28 :** The optical microscope image of 13.9 (w/w) % PU – PCM composite.

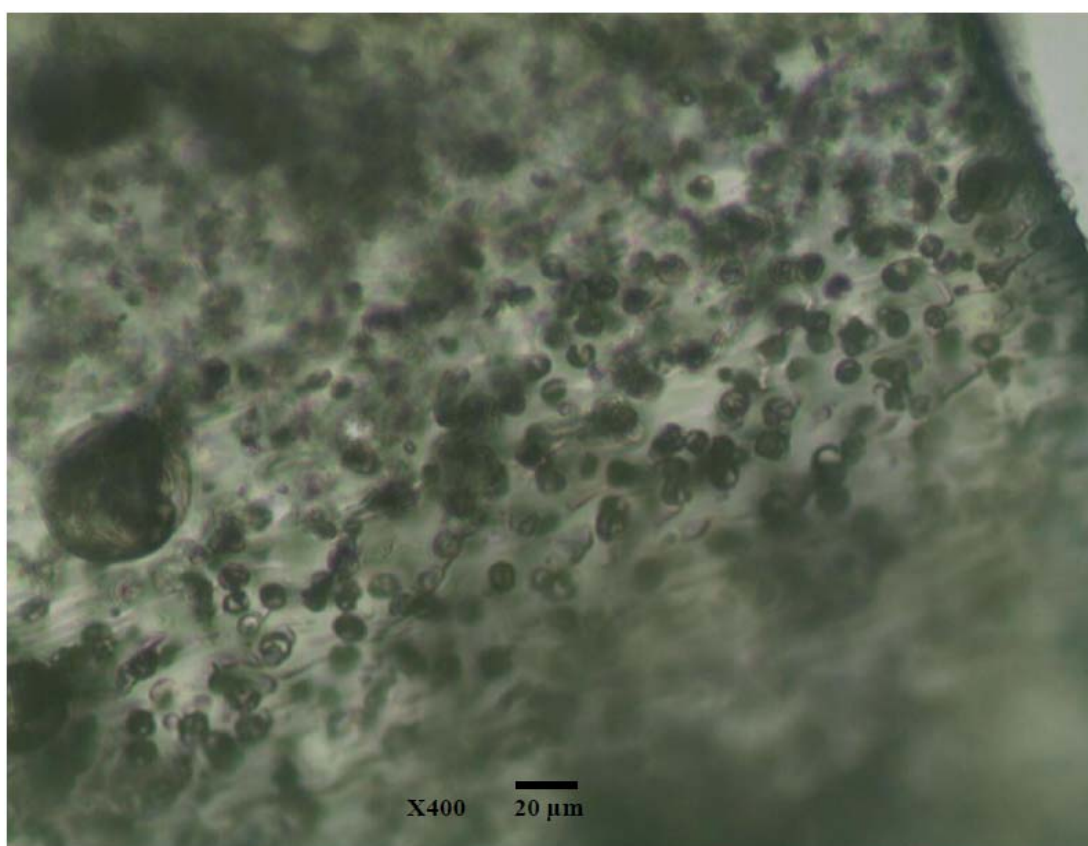


**Figure 6.29 :** The optical microscope image of 22.6 (w/w) % PU – PCM composite.



According to the SEM images (x2000) of the PU – PCM composites, particles around 1  $\mu\text{m}$  are present inside the polymer matrix. However, the main particle size distribution is between 2 – 4  $\mu\text{m}$  which is independent of PCM mass percentage. The small size distribution of the composites is an advantage for providing effective thermal response against the changes in the ambient temperature because the total heat transfer area of the PCM particles increases with smaller size distribution and the heat is absorbed in a finely distributed homogeneous medium which works like a buffer. The SEM images of the PU – PCM composites are given in Figure 6.30 – 6.32.

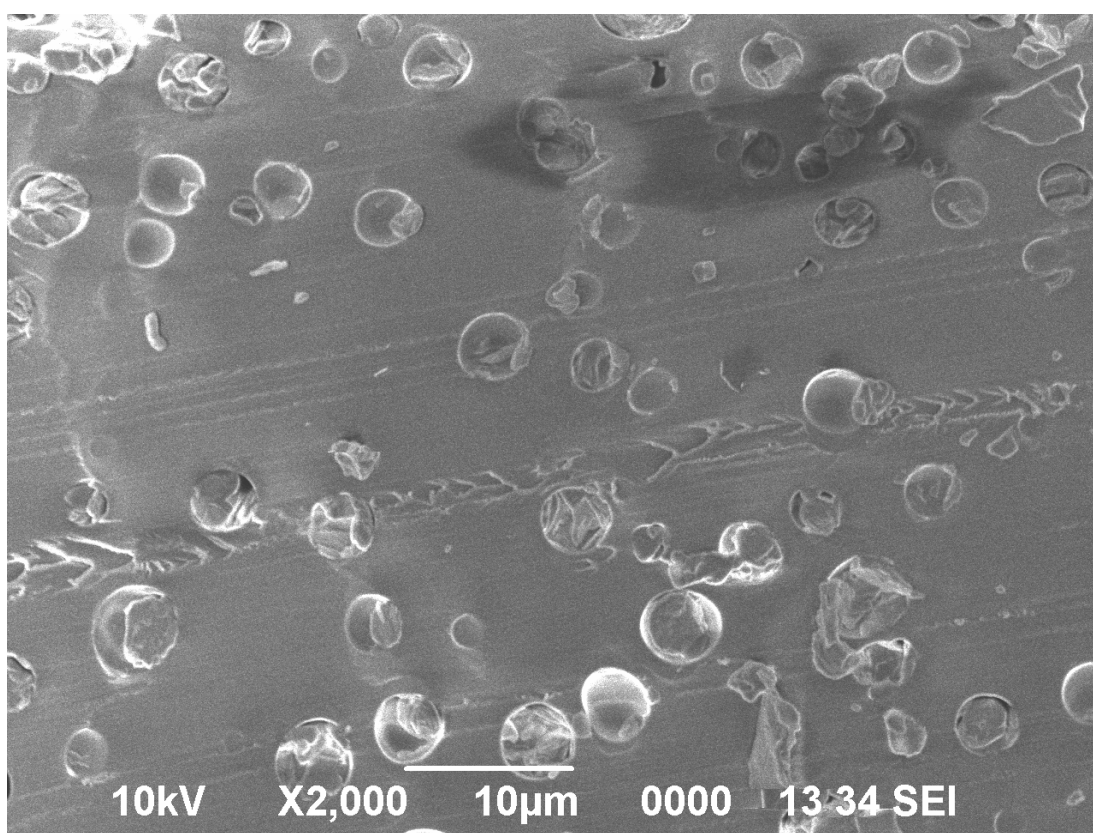


**Figure 6.30 :** SEM image of 9.2 (w/w) % PU – PCM composite.

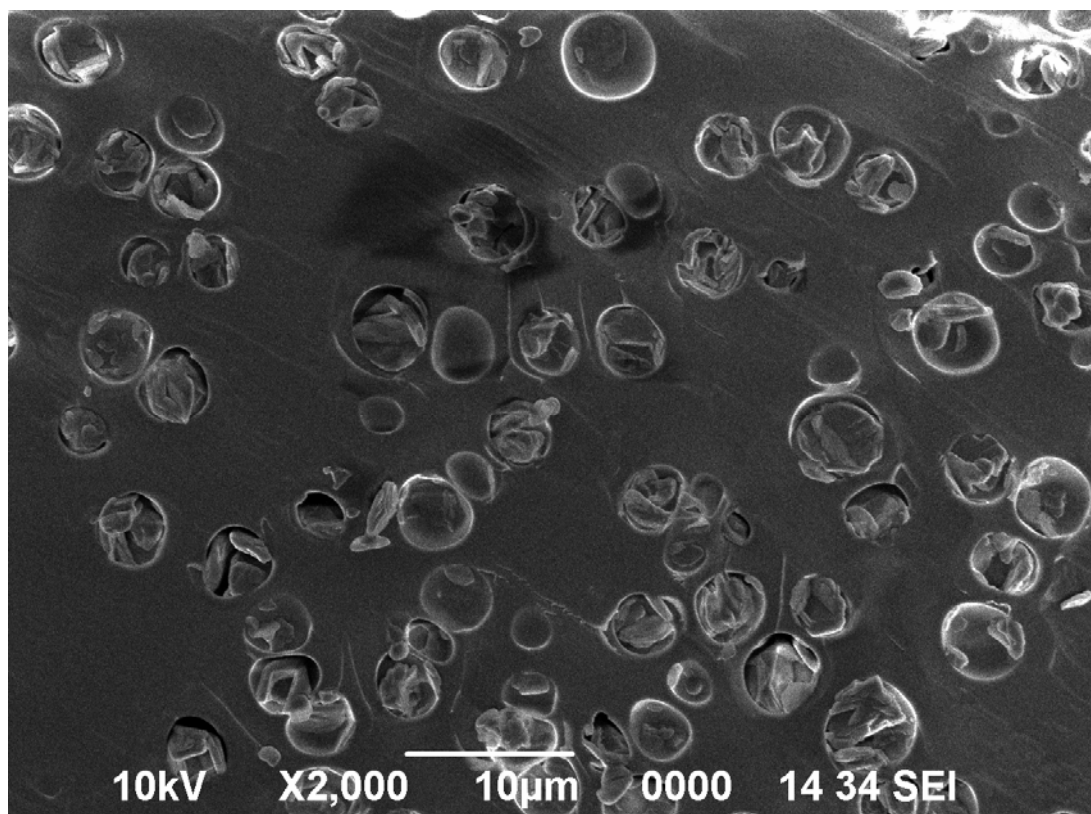


**Figure 6.31 :** SEM image of 13.9 (w/w) % PU – PCM composite.

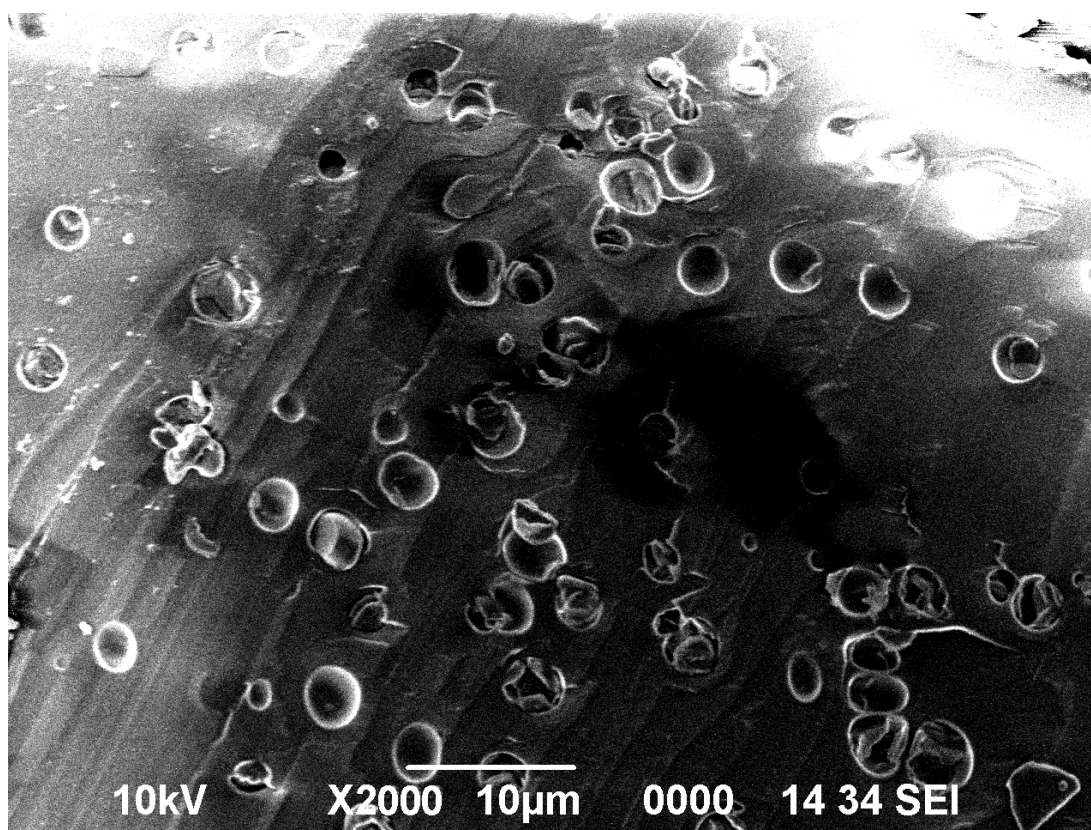


**Figure 6.32 :** SEM image of 22.6 (w/w) % PU – PCM composite.

## 6.6 X-Ray Diffraction of Cetiol MM

The XRD spectra of Cetiol MM show that the material is in crystalline form and the crystallinity of the material is not affected after several thermal cycles. However, the size of the crystal structure increases after repeated thermal cycles. The XRD spectra are given in Figure 6.33.

The XRD data support the DSC analyses of Cetiol MM and PU – PCM composites. The data show that these materials have equal melting and freezing enthalpies and Cetiol MM has insignificant changes in the thermal properties after 1000 thermal cycles due to stable crystallinity.

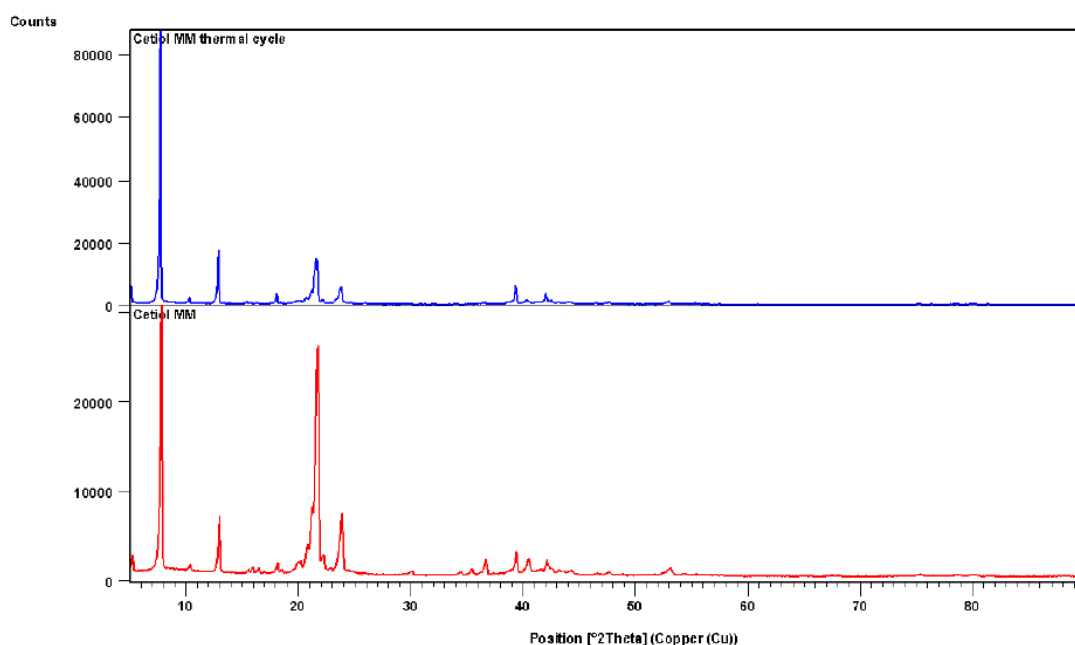


**Figure 6.33 :** XRD spectra of Cetiol MM.





## 7. CONCLUSION

The energy consumption of the world's population increased drastically during the last decades with increased fossil fuel consumption and carbon dioxide emissions. However, world's limited crude oil reserves and rise in barrel prices triggered the researches on utilization of renewable energy sources and energy efficiency. Concerning the energy efficiency issue, "thermal energy storage" plays an important role in energy conservation and reducing the costs with less fuel consumption.

As being conscious of the energy problems and related environmental issues, this PhD research is consisted of the synthesis and thermal analyses of novel "organic phase change materials" and enhancement of the thermal properties of "polyurethane rigid foam" with PCM to improve its insulation property.

- A new group of materials, which is high-chain fatty acid esters of myristyl alcohol, has been successfully introduced for thermal energy storage between 38°C and 53°C. 9 high-chain esters of myristyl alcohol with fatty acids, starting from dodecanoic acid to eicosanoic acid, have been synthesized according to the esterification method of Baykut and Aydın (1969) and analyzed to determine their thermal properties. In addition to the synthesized materials, a commercial product of Cognis Türk Kimya A.Ş. has also been analyzed and compared with the corresponding synthesized ester.

The high-chain fatty acid esters have never been investigated by researchers to determine their thermal properties before. Apart from the investigated low-chain fatty acid esters of methyl, ethyl and butyl alcohols in literature, the presented work is completely novel to introduce a new group of organic phase change materials to the literature. Besides, the submitted materials have superior thermal properties compared to the other organic and inorganic phase change materials.

Reagent grade, high purity products of Sigma – Aldrich were used for the synthesis of the high-chain fatty acid esters and the final products have been crystallized several times to remove the unreacted impurities. The FT-IR spectra show that the final pure products do not contain any unreacted fatty acid or alcohol impurities.

The melting temperatures of the introduced materials are spread between 38°C and 53°C and the phase change enthalpy values vary between 201 kJ/kg and 220 kJ/kg which are quite high among the known organic phase change materials. Additionally, the materials show one distinct sharp phase change peak and they absorb or release heat in one step which helps to use their capacity completely at once. These properties make them very promising materials to be used in thermal energy storage applications like solar units and devices or thermal insulation.

Another superior property of the submitted materials is that they do not show supercooling tendency between the temperatures of melting and freezing. It is indicated by Sharma, et al. (2009) that supercooling of 5–10°C effects proper transfer of heat. However, the temperature differences between melting and freezing process are in the range of 0.6°C and 1.95°C at 2°C/min heating and cooling rate. Such kind of behavior of high-chain fatty acid esters of myristyl alcohol make them suitable for engineering approaches together with the high latent heat values and proper phase change behaviors.

These introduced novel organic phase change materials work at similar temperatures with salt hydrates and they suppress the disadvantages of most of the inorganic materials. The main drawbacks of inorganic phase change materials are phase segregation and supercooling problems. Phase segregation results in formation of lower hydrated salts and increase in acidity of the medium, which in turn affects the endurance of the encapsulation material. Also, phase segregation causes decrease in phase change enthalpy and the material loses its thermal capacity after several thermal cycles.

Extended thermal cycling of 1000 thermal cycles has been applied to the new organic PCMs to examine their thermal reliability. The results show that the phase change temperatures and the latent heat enthalpies are not affected significantly after repeated cycles. The changes in temperature and enthalpy are less than 1 % and the heat flow curves are very similar to the ones of the original materials with one sharp phase change peak. It is also possible to indicate that the stability of the thermal values means that these materials are also chemically stable for 1000 thermal cycles. The stability of the thermal capacity of the materials after several phase change cycles is very important for the sustainability of the designed systems in practice. For example, being stable for 1000 thermal cycles can be considered as a shift period of 3 years if one phase change cycle takes place everyday. However, the time period might change depending on the type of application.

The specific heat capacity of the materials is another property that has been given in this research. Eventhough the specific heat capacity has minor effect on thermal energy storage; it has been analyzed in this research to determine the property of the solid and liquid states. The values are presented as second degree polynomials as a function of temperature and average values of solid and liquid states are given in the temperature range of 10°C and 80°C.

The decomposition behavior of the materials is another important property for the determination of the thermal stability limits. The thermal stability limits are important to choose a proper application area, in which the material is stable at the maximum temperature of the process, and to decide the type of encapsulation to be performed if an exothermic process is under consideration. It is found that the materials show similar decomposition curves with different onset temperatures. According to the analyses, the thermal decomposition onset temperatures of the materials vary between 275°C and 321°C. It is possible to indicate that the materials are stable up to 180°C in general.

Besides the synthesis and determination of the thermal properties of the high-chain fatty acid esters, the effect of the ester bond on the thermal properties of the materials has also been investigated in this research to find out the contribution of the chemical structure. Therefore, aliphatic n-alkanes with the same number of carbon atoms with 14–12 and 14–16 esters were chosen to study the effect of the ester bond in the chemical structure on the superior thermal properties of the high-chain fatty acid esters. It is found that n-hexacosane and n-triacontane show two sharp peaks during melting and freezing, which are related to solid – solid and solid – liquid phase changes and the phase change temperature and enthalpy values are higher than the corresponding esters. However, the presence of ester bond provides one step heat transfer which makes the introduced materials suitable for applications at lower temperatures. Even if the decrease in the enthalpy values is around 40 kJ/kg, the two step heat transfer mechanisms of the alkanes make them improper for utilization.

The effect of the ester bond on the thermal stability of the materials cannot be clearly seen as the effect on the phase change properties. The characteristics of the overlapped graphs are very similar and the difference between the onset decomposition temperatures is around 1 %.

It is important to state that the observed differences between the 14 – 12 and 14 – 16 esters and the corresponding n-alkanes are particular for the fatty acid – alcohol combinations of 14 – 12 and 14 – 16. The effect of the ester bond can be more intense with different fatty acid and alcohol combinations.

- In addition to the investigation of a new group of organic phase change materials, utilization of the introduced commercial product of Cognis Türk Kimya A.Ş in enhancement of the thermal properties of one of the most common insulation materials has also been studied in this PhD research. The purpose of such a research is to find out if it is possible to combine the heat absorption property of a PCM and polyurethane rigid foam to use thinner insulation panels of PU – PCM composites instead of the conventional ones.

Unlike the first part of the PhD research, industrial grade raw materials have been used in this part to define the conditions that PU – PCM composites can be synthesized with industrial grade materials. The reagents of the polyurethane rigid foam and the PCM part were kindly supplied by the Flokser Group and Cognis Türk Kimya A.Ş., respectively.

One of the first problems encountered during this part of the research was to succeed in the proper formation foam in the presence of solid PCM content. The basic formulation of polyurethane rigid foam had to be modified because the solid PCM granules inside the reaction medium interrupted the chemical thermodynamics. The reason of such a counter effect is that the PCM in solid form melts during the exothermic reaction conditions and the absorbed heat affects the proper formation of foam. After several blank experiments, it is decided to modify the basic formulation to overcome the phase change heat absorption problem of the solid PCM. Afterwards, the PU – PCM composites have been successfully synthesized with the compositions of 9.2 (w/w) %, 13.9 (w/w) % and 22.6 (w/w) % and the reference foam without PCM.

In DSC analyses, the effect of the PCM content can directly be observed in terms of enthalpies and phase change peaks. The phase change temperatures of the particles inside the composite are very close to the original PCM. Additionally, the measured and calculated phase change enthalpy values are almost the same which means that the PCM content stays as a chemically inert material during foaming and it has its net thermal effect on heat absorption enhancement of the foam samples.

It is interesting to notice that eventhough the melting process succeeds in one single step; the freezing is divided into regions and concluded after subsequent steps. However, this problem is figured out by increasing the PCM content of the composites. So that, more closely packed PCM particles tend to initiate phase change of the adjacent particles more easily and the lag of thermal response is minimized. It is meaningful to suggest that working with PCM compositions above 10.0 (w/w) % is favorable in order to be able to ignore the thermal lag during cooling.

In addition to the enhancement of the heat absorption capacity at the phase change temperatures, the improvement in the total heat absorption capacity of the composites with respect to the reference foam in the temperature range of 4°C and 87°C has also been investigated in this research. According to the calculated results, the total heat absorption capacity is improved up to 34 % and it is directly proportional to the PCM content. This means that approximately 30 % thinner foam blocks can be used to maintain the same insulation performance. It can be mentioned that the heat absorption capacity of one of the most common insulation materials has been successfully improved in this research and it has been proven that PCMs can be incorporated into polyurethane rigid foam formulations to improve their thermal properties. It is quite possible to use other PCMs with different phase change temperatures and enthalpies to produce composites which have distinct heat absorption intervals and sensitive for different application temperatures of insulation.

In addition to the DSC analyses of the composites, the thermogravimetric analyses of the samples show that the PCM content decreases the thermal durability of the material. As the PCM content increases up to 22.6 (w/w) %, the onset decomposition temperature decreases by 27°C with respect to the reference foam. The decrease in the thermal stability of the composites can be prevented by use of fire preservative additives in formulations.

Besides the thermal properties of the measured samples, the homogeneous distribution of the PCM content throughout the polymer matrix is a very important property to observe uniform thermal response in foam blocks when pilot scale production is to be discussed according to the modified foam formulation. The success of the modified synthesis method and the validity of the presented thermal values for larger scale production depend on the homogeneous distribution of the material inside the polymer matrix. Hence, optical microscope and SEM images are presented in the thesis in order to clarify this issue.

According to the optical microscope images, the PCM content is distributed homogeneously at x400 magnification. The main particle size distribution is determined with the help of the SEM images at x2000 magnification and it is clearly seen that the distributed fine particles have diameters between 2 µm and 4 µm in general.

The particle size distribution does not depend on the amount of the PCM content with respect to the SEM images because the main particle size distributions are almost the same on the images. However, the fine distribution of the particles is a great advantage to increase the thermal response area of the PCM particles which is provided by the modified synthesis method.

The modified synthesis method of PU – PCM composites is a very effective way of overcoming the drawbacks of using solid state PCMs which melt during the exothermic foaming reactions in laboratory. Proper blowing and surface formation during foaming provide good surface appearance of the synthesized composites compared to the reference foam. However, it may not be necessary to use such a modified method in industry. Heated molds are used intensively for production of foams which can be kept at elevated temperatures. It worths trying pilot scale production by using a basic formulation with moderate PCM content inside a heated mold which is kept at a temperature above the melting point of the PCM. In this way, it might be possible to load the thermal energy needed to melt the PCM to the reaction medium from a secondary source and the inhibition of the reaction kinetics might be prevented. A new research project can be submitted with cooperation of university and industry for pilot scale production of modified insulation materials and value added new product development.

This part of the research can be considered as an introduction to PU – PCM composites with enhanced thermal properties. Further investigations with other PCMs or PCM mixtures can be conducted with different foam formulations to obtain composites with different thermal and structural properties.





## REFERENCES

- Abe, Y., Takahashi, Y., Kanari, K., Kamimoto, M., Sakamoto, R., and Ozawa, T.,** 1986. Molten salt latent thermal energy storage for load following generation in nuclear power plants, Proceedings of 21st Intersociety Energy Conversion Engineering Conference, San Diego, California, USA, 856-861.
- Abhat, A.,** 1983. Low temperature latent heat thermal energy storage: heat storage materials, *Solar Energy*, **30**, 313-332.
- Alkan, C., Kaya, K., and Sari, A.,** 2008. Preparation and thermal properties of ethylene glycol distearate as a novel phase change material for energy storage, *Materials Letters*, **62**, 1122-1125.
- ASTM D2766-95,** 1995. Standard test method for specific heat of liquids and solids, *ASTM International*, United States.
- ASTM E793-06,** 2006. Standard test method for enthalpies of fusion and crystallization by differential scanning calorimetry, *ASTM International*, United States.
- Bailey, J., Mulligan J., Liao, C., Guceri, S., and Reddy, M.,** 1976. Research on solar energy storage sub-system utilizing the latent heat of phase change of paraffin hydrocarbons for the heating and cooling of the buildings, Report to the National Science Foundation, North Carolina University, USA.
- Barrett, A. G. M., and Braddock, D. C.,** 1997. Scandium(III) or lanthanide(III) triflates as recyclable catalysts for the direct acetylation of alcohols with acetic acid, *Chemical Communications*, **4**, 351-352.
- Baykut, F., and Aydın, A.,** 1969. The synthesis and physical properties of the homologous series of fatty acids' esters, *Revue De La Faculte Des Sciences De L'Universite D'Istanbul*, **Serie C**, 119-148.
- Bellettre, J., Sartre, V., Biais, F., and Lallemand, A.,** 1997. Transient state study of electric motor heating and phase change solid-liquid cooling, *Appl. Thermal Eng.*, **17**, 17-31.
- Biswar, D. R.,** 1977. Thermal energy storage using sodium sulphate decahydrate and water, *Solar Energy*, **19**, 99-100.
- Blanchard, L. A., and Brennecke, J. F.,** 2001. Esterification of acetic acid with ethanol in carbon dioxide, *Green Chemistry*, **3**, 17-19.

- Bourdeau, L. E.**, 1980. Study of two passive solar systems containing phase change materials for thermal storage, Proceedings of the fifth national passive solar conference, 297-301.
- BS-EN ISO 11358**, 1997. Thermogravimetry (TG) of polymers-general principles, *International Organization for Standardization*, Switzerland.
- Cabeza, L. F., Castellon, C., Nogues, M., Medrano, M., Leppers, R., and Zubillaga, O.**, 2007. Use of microencapsulated PCM in concrete walls for energy savings, *Energy and Buildings*, **39**, 113-119.
- Camp, D., and Jenkins, I. D.**, 1989. Mechanism of the Mitsunobu esterification reaction. 1. The involvement of phosphoranes and oxyphosphonium salts, *Journal of Organic Chemistry*, **54**, 3045-3049.
- Cao, Q., and Liu, P.**, 2006. Hyperbranched polyurethane as novel solid-solid phase change material for thermal energy storage, *European Polymer Journal*, **42**, 2931-2939.
- Cedeno, F. O., Prieto, M. M., Espina, A., and Garcia, G. R.**, 2001. Measurements of temperature and melting heat of some pure fatty acids and their binary and ternary mixtures by differential scanning calorimetry, *Thermochimica Acta*, **369**, 39-50.
- Chandra, S., Kumar, R., Kaushik, S., and Kaul, S.**, 1985. Thermal performance of a non A/C building with PCM thermal storage wall, *Energy Convers Manage*, **25**, 15-20.
- Chaurasia, P. B. L.**, 2000. Phase change material in solar water heater storage system, Proceedings of the 8<sup>th</sup> International Conference on Thermal Storage.
- Chernova, I. K., Filimonova, E. I., Bychkov, B. N., Soloven, V. V., and Koshel, G. N.**, 1996. Preparation of oleic acid based on aliphatic acids of thallic oil, *Khim. Khim. Tekhnol.*, 117-118.
- Collier, R. K., and Grimmer, D. P.**, 1979. The experimental evaluation of phase change material building walls using small passive test boxes, Proceedings of the 3<sup>rd</sup> national passive solar conference, San Joseph, CA.
- Demharter, A.**, 1998. Polyurethane rigidfoam, a proven thermal insulating material for applications between +130°C and -196°C, *Cryogenics*, **38**, 113-117.
- Dillon, J. G.**, 1989. *Infrared spectroscopic atlas of polyurethanes*, Technomic Publishing, PA, USA.
- Dinçer, I., and Rosen, M. A.**, 2002. Thermal Energy Storage, Systems and Applications, John Wiley & Sons, Chichester, UK.
- Dyer, J. R.**, 1965. *Applications of absorption spectroscopy of organic compounds*, Prentice-Hall, USA.

- Dyke, C. A., and Bryson, T. A.,** 2001. Esterification of carboxylic acids with boron trichloride, *Tetrahedron Letters*, **42**, 301-303.
- Enibe, S. O.,** 2002. Performance of a natural circulation solar air heating system with phase change material energy storage, *Renewable Energy*, **27**, 69-86.
- Farid, M.** 1986. Solar energy storage with phase change, *Journal of Solar Energy Research*, **4**, 11-29.
- Farid, M. M., and Kanzawa, A.,** 1989. Thermal performance of a heat storage module using PCMs with different melting temperatures-mathematical modeling, *Journal of Solar Energy Engineering*, **111**, 152-157.
- Farid, M. M., Kim, Y., and Kanzawa, A.,** 1990. Thermal performance of heat storage module using PCMs with different melting temperatures-experimental, *Journal of Solar Energy Engineering*, **112**, 125-131.
- Farid, M. M., and Khalaf, A. N.,** 1994. Performance of direct contact latent heat storage units with two hydrated salts, *Solar Energy*, **52**, 179-189.
- Farid, M. M., Hamad, F. A., and Abu-Arabi, M.,** 1998. Phase change cool storage using dimethyl-sulfoxide, *Energy Conversion and Management*, **39**, 819-826.
- Farid, M. M., Khudhair, A. M., Razack, S. A. K., and Al-Hallaj, S.,** 2004. A review on phase change energy storage: materials and applications, *Energy Conversion and Management*, **45**, 1597-1615.
- Feldman, D., and Shapiro, M. M.,** 1989. Fatty acids and their mixtures as phase change materials for thermal energy storage, *Solar Energy Materials*, **18**, 201-216.
- Feldman, D., Shapiro, M. M., and Banu, D.,** 1986. Organic phase change materials for thermal energy storage, *Solar Energy Materials*, **13**, 1-10.
- Feldman, D., Banu, D., and Hawes, D.,** 1995. Low chain esters of stearic acid as phase change materials for thermal energy storage in buildings, *Solar Energy Materials and Solar Cells*, **36**, 311-322.
- Fischer, E., and Speier, A.,** 1895. Darstellung der ester, *Chemische Berichte*, **28**, 3252-3258.
- Fouda, A. E., Despault, G. J., Taylor, J. B., and Capes, C. E.,** 1984. Solar storage system using salt hydrate latent heat and direct contact heat exchange-II, characteristics of pilot operating with sodium sulfate solution, *Solar Energy*, **32**, 57-65.
- Ghoneim, A. A., Kilein, S. A., and Duffie, J. A.,** 1991. Analysis of collector – storage building walls using phase change materials, *Solar Energy*, **47**, 15-20.

- Gibbs, B., and Hashain, S.,** 1995. DSC study of technical grade phase change heat storage materials for solar heating applications, Proceedings of the 1995 ASME/JSME/JSEJ International Solar Energy Conference, Part 2.
- Grochowski, E., Hilton, B. D., Kupper, R. J., and Michejda, C. J.,** 1982. Mechanism of the triphenylphosphine and diethyl azodicarboxylate induced dehydration reactions – the central role of pentavalent phosphorous intermediates, *Journal of the American Chemical Society*, **104**, 6876-6877.
- Gurke, T.,** 2002. New advances in polymeric MDI, EuroCoat 2002, Spain, Barcelona.
- Hadjieva, M., Stoykov, R., and Filipova, T.,** 2000. Composite salt-hydrate concrete system for building energy storage, *Renewable Energy*, **19**, 111-115.
- Hasnain, S. M.,** 1998. Review on sustainable thermal energy storage technologies, Part 1: heat storage materials and techniques, *Energy Convers Mng*, **39**, 1127-1138.
- Hawes, D. W., Feldman, D., and Banu, D.,** 1993. Latent heat storage in building materials, *Energy Buildings*, **20**, 77-83.
- Heckenkamp, J., and Baumann, H.,** 1997. Laetenwaermespeicher, *Sonderdruck aus Nachrichten*, **11**, 1075-1081.
- Himran, S., Suwono, A., and Manssori, G.,** 1994. Characterization of alkanes and paraffin waxes for application as phase change energy storage medium, *Energy Sources*, **16**, 117-128.
- Hong, H., Kim, S. K., and Kim, Y. S.,** 2004. Accuracy improvement of T-history method for measuring heat of fusion of various materials, *Int. J. Refrig.*, **27**, 360-366.
- Hong, Y., and Xin-shi, G.,** 2000. Preparation of polyethylene-paraffin compounds as a form stable solid-liquid phase change material, *Solar Energy Materials and Solar Cells*, **64**, 37-44.
- Ishihara, K., Ohara, S., and Yamamoto, H.,** 1996. 3,4,5-trifluorobenzeneboronic acid as an extremely active amidation catalyst, *Journal of Organic Chemistry*, **61**, 4196-4197.
- Ismail, K., and Concalves, M. M.,** 1999. Thermal performance of a PCM storage unit, *Energy Conversion and Management*, **40**, 115-138.
- Jurinak, J. J., and Khalik, S. I.,** 1979. On the performance of air-based solar heating systems utilizing phase change energy storage, *Solar Energy*, **24**, 503-522.
- Kadaba, P. K.,** 1971. Convenient method of esterification of unsaturated organic acids using a boron trifluoride etherate-alcohol reagent, *Synthesis*, **6**, 316-317.

- Kakuichi, H., Yamazaki, M., Yabe, M., Chihara, S., Terunuma, Y., and Sakata, Y.,** 1998. A Study of Erythrol as Phase Change Material, Proceedings of the 2nd workshop IEA annex 10, phase change materials and chemical reactions for thermal energy storage, Sofia, Bulgaria.
- Kauranen, P., Peippo, K., and Lund, P. D.,** 1991. An organic PCM storage system with adjustable melting temperature, *Solar Energy*, **46**, 275-278.
- Kedl, R. J., and Stovall, T. K.,** 1989. Activities in support of the wax-impregnated wallboard concept, Thermal energy storage activity review, New Orleans, Louisiana, USA, US Department of Energy.
- Kenisarin, M., and Mahkamov, K.,** 2007. Solar energy storage using phase change materials, *Renew. Sus. Energy Rev.*, **11**, 1913-1965.
- Khurana, J. M., Sahoo, P. K., and Maikap, G. C.,** 1990. Sonochemical esterification of carboxylic-acids in presence of sulfuric acid, *Synthetic Communications*, **20**, 2267-2271.
- Kimura, H., and Kai, J.,** 1984. Phase change stability of  $\text{CaCl}_2 \cdot 6\text{H}_2\text{O}$ , *Solar Energy*, **33**, 557-563.
- Kissock, J. K., Hamming, J. M., Whitney, T. I., and Drake, M. L.,** 1998. Testing and simulation of phase change wallboard for thermal storage in buildings, Proceedings of international solar energy conference, 45-52.
- Knowler, T.,** 1983. Proportioning composites for efficient-TSWs, *Solar Energy*, **31**, 319-326.
- Lacroix, M.,** 1993. Numerical simulation of a shell and tube latent heat thermal energy storage unit, *Solar Energy*, **50**, 357-367.
- Lane, G. A.,** 1980. Low temperature heat storage with phase change materials, *Int. J. Ambient Energy*, **1**, 155-168.
- Lane, G. A.,** 1983. Solar Heat Storage: Latent Heat Materials, Volume I- Background and Scientific Principles, CRC Press, Florida.
- Lane, G. A.,** 1992. Phase-change materials for energy storage nucleation to prevent supercooling, *Solar Energy & Solar Materials*, **27**, 135-160.
- Li, J. H., Zhang, G. E., and Wang, J. Y.,** 1991. Investigation of a eutectic mixture of sodium acetate trihydrate and urea as latent heat storage, *Solar Energy*, **47**, 443-445.
- Li, W. D., and Ding, E.,** 2007. Preparation and characterization of a series of diol di searates as phase change materials, *Materials Letters*, **61**, 4325-4328.
- Liao, X., Raghavan, G. S. V., and Yaylayan, V. A.,** 2002. A novel way to prepare n-butylparaben under microwave irradiation, *Tetrahedron Letters*, **43**, 45-48.

- Lindner, F.**, 1996. Waermespeicherung mit salzen und salzhydraten, *Ki Luft- und Kaeltechnik*, **10**, 462-467.
- Magerramov, M. N.**, 1995. Thermal esterification of carboxylic acids with alcohol, *Russian Journal of Applied Chemistry*, **68**, 291-293.
- Markley, K.**, 1961. *Fatty Acids Part 2*, Interscience Publishers, New York.
- Maruoka, N., and Akiyama, T.**, 2003. Thermal stres analysis of PCM encapsulation for heat recovery of high temperature waste heat, *J. Chem. Eng. Japan*, **36**, 794-798.
- Mehling, H., Cabeza L. F.**, 2008. *Heat and cold storage with PCM: An up to date introduction into basics and applications*, Springer, Berlin, Germany.
- Mettawee, E. B. S., Assassa G. M. R.**, 2006. Experimental study of a compact PCM solar collector, *Energy*, **31**, 2958-2968.
- Mitsunobu, O.; Yamada, Y.**, 1967. Preparation of esters of carboxylic and phosphoric acid via quaternary phosphonium salts, *Bull. Chem. Soc. Japan*, **40**, 2380-2382.
- Morrison, D. J., Khalik, S. I.**, 1978. Effects of phase change energy storage on the performance of air –based and liquid-based solar heating systems, *Solar Energy*, **20**, 57-67.
- Naumann, R., Emons, H. H.**, 1989. Results of thermal analysis for investigation of salt hydrates as latent heat-storage materials, *J. Thermal Analysis*, **35**, 1009-1031.
- Neises, B., Steglich, W.**, 1978. Simple Method for the Esterification of Carboxylic Acids, *Angewandte Chemie International Edition*, **17** 522–524.
- Neeper, D. A.**, 2000. Thermal dynamics of wallboard with latent heat storage, *Solar Energy*, **68**, 393-403.
- Nudelman, A., Bechor, Y., Falb, E., Fischer, B., Wexler, B. A., and Nudelman, A.**, 1998. Acetyl chloride-methanol as a convenient reagent for: A) quantitative formation of amine hydrochlorides b) carboxylate ester formation c) mild removal of N-t-Boc-protective group, *Synthetic Communications*, **28**, 471-474.
- Oertel, G.**, 1985. *Polyurethane Handbook*, Macmillen Publishing Co. Inc., New York.
- Otera, J.**, 2003. *Esterification: Methods, reactions and applications*, Wiley-VCH Verlag, Weinheim.
- Ozonur, Y., Mazman, M., Paksoy, H. O., and Evliya, H.**, 2006. Microencapsulation of coco fatty acid mixture for thermal energy storage with phase change material, *International Journal of Energy Research*, **30**, 741-749.

- Pal, D., Joshi, Y.,** 1996. Application of phase change materials for passive thermal control of plastic quad flat packages: a computational study, *Numer. Heat Transfer, Part A*, **30**, 19-34.
- Prakash, J., Garg, H. P., and Datta G.,** 1985. A solar heater with a built-in latent heat storage, *Energy Convers. Manage.*, **25**, 51-56.
- Randall, D., Lee, S.,** 2002. *The Polyurethanes Book*, Wiley, New York.
- Raymond B., Seymour G. B., and Kauffman J.,** 1992. Polyurethanes: A Class of Modern Versatile Materials, *Journal of Chemical Education*, **69**, 909.
- Regin, F. A., Solanki, S. C., and Saini, J. S.,** 2008. Heat transfer characteristics of thermal energy storage system using PCM capsules: A review, *Renewable and Sustainable Energy Review*, **12**, 2438-2458.
- Reid, E. E.,** 1953. Esterification, *Industrial and Engineering Chemistry*, **45**, 1936-1943.
- Riahi M.,** 1993. Efficiency of heat storage in solar energy systems, *Energy Conversion and Management*, **34**, 677-685.
- Robinson, P.,** 2003. Practical Specific Heat Determination by Power Compensation DSC, Perkin Elmer technical note, Seer Green, UK.
- Royon, L., Guiffant, G., and Flaud, P.,** 1997. Investigation of heat transfer in a polymeric phase change material for low level heat, *Energy Conversion*, **38**, 517-524.
- Ryu, H. W., Woo, S. W., Shin, B. C., and Kim, S. D.,** 1992. Prevention of subcooling and stabilization of inorganic salt hydrates as latent heat storage materials, *Solar Energy Materials and Solar Cells*, **27**, 161-172.
- Saitoh, T., Hirose, K.,** 1986. High performance of phase change thermal energy storage using spherical capsules, *Chemical Engineering Communications*, **41**, 39-58.
- Salzer, I. O., Sircar, A. K.,** 1990. Phase change material for heating and cooling of residential buildings and other applications, *Proceedings of 25<sup>th</sup> intersociety energy conservation engineering conference*, 236-243.
- Sari, A., Kaygusuz, K.,** 2001. Thermal energy storage system using stearic acid as a phase change material, *Solar Energy*, **71**, 365-371.
- Sari, A.,** 2003. Thermal characteristics of a eutectic mixture of myristic and palmitic acids as phase change material for heating applications, *Appl. Therm. Eng.*, **23**, 1005-1017.
- Sari, A.,** 2003. Thermal reliability test of some fatty acids as PCMs used for solar thermal latent heat storage applications, *Energy Conversion and Management*, **44**, 2277-2287.

- Sarı, A., Sarı, H., and Onal, A.,** 2004. Thermal properties and thermal reliability of eutectic mixtures of some fatty acids as latent heat storage materials, *Energy Conversion and Management*, **45**, 365-376.
- Sarı, A.,** 2005. Eutectic mixtures of some fatty acids for low temperature solar heating applications: thermal properties and thermal reliability, *Appl Therm. Eng.*, **25**, 2100-2107.
- Sarı, A., Kaygusuz, K.,** 2008. Preparation and thermal properties of capric acid/palmitic acid eutectic mixture as a phase change energy storage material, *Materials Letters*, **62**, 903-906.
- Sharma, A., Sharma, S. D., and Buddhi D.,** 2002. Accelerated thermal cycle test of acetamide, stearic acid and paraffin wax for solar thermal latent heat storage applications, *Energy Conversion and Management*, **43**, 1923-1930.
- Sharma, A., Tyagi, V. V., Chen, C. R., and Buddhi, D.,** 2009. Review on thermal energy storage with phase change materials and applications, *Renewable and Sustainable Energy Reviews*, **13**, 318-345.
- Sowa, F. J., Nieuwland, J. A.,** 1936. Organic Reactions with Boron Fluoride.1 XII. The Preparation of Esters of Aromatic Acids, *Journal of American Chemical Society*, **58**, 271-272.
- Stark, P.,** 1990. PCM-impregnated polymer microcomposites for thermal energy storage, *SAE Transactions*, **99**, 571-588.
- Suppes, G. J., Goff, M. J., and Lopes, S.,** 2003. Latent Heat Characteristics of Fatty Acid Derivatives Pursuant Phase Change Material Applications, *Chemical Engineering Science*, **58**, 1751 – 1763.
- Swamy, K. C. K., Kumar, N. N. B., Balaraman, E., and Kumar, K. V. P. P.,** 2009. Mitsunobu and Related Reactions: Advances and Applications, *Chemical Reviews*, **109**, 2551-2651.
- Swet, C. J.,** 1980. Phase change storage in passive solar architecture, Proceedings of the fifth national passive solar conference, 282-286.
- Szycher, M.,** 1999. *Szycher's Handbook of Polyurethanes*, CRC Press, New York.
- Telkes, M.,** 1952. Nucleation of super saturated inorganic salt solution, *Indust. Eng. Chem.*, **44**, 1308.
- Telkes, M.,** 1975. Thermal storage for solar heating and cooling, Proceedings of the Workshop on Solar energy Storage Subsystems for the Heating and Cooling of Buildings, Charlottesville, USA.
- Tyagi, V. V., Buddhi, D.,** 2007. PCM Thermal Storage in Buildings: A State of Art, *Renewable and Sustainable Energy Review*, **11**, 1146 – 1166.



- Url-1** < <http://www.rubitherm.de/>>, accessed at 21.11.2009.
- Url-2** < <http://www.sofrigam.com/>>, accessed at 21.11.2009.
- Url-3** <<http://news.uns.purdue.edu/UNS/html4ever/010607.Revankar.solar.html>>, accessed at 21.11.2009.
- Url-4** <<http://www.nrel.gov/vehiclesandfuels/energystorage/pdfs/techbr.pdf>>, accessed at 21.11.2009.
- Url-5** < <http://www.epsltd.co.uk/>>, accessed at 21.11.2009.
- Url-6** < <http://www.climator.com/>>, accessed at 21.11.2009.
- Url-7** <<http://en.wikipedia.org/wiki/Ester>>, accessed at 20.01.2010.
- Vakilaltojjar, S. M., and Saman, W.**, 2001. Analysis and modeling of a phase change storage system for air conditioning applications, *Applied Thermal Engineering*, **21**, 249-263.
- Wang, X. C., Niu, J. L., and van Paassen A. H. C.**, 2008. Raising evaporative cooling potentials using combined cooled ceiling and MPCM slurry storage, *Energy and Buildings*, **40**, 1691-1698.
- Zalba, B., Marin, J., Cabeza, L., and Mehling, H.**, 2003. Review on thermal energy storage with phase change: materials, heat transfer analysis and applications, *Applied Thermal Engineering*, **23**, 251-283.
- Zhang, Y., and Jiang, Y.**, 1999. A simple method, the T-History method, of determining the heat of fusion, specific heat and thermal conductivity of phase change materials, *Meas. Sci. Technol.*, **10**, 201-205.
- Zhao, X. , Wang, Y., Wang, S., Yang, H., and Zhang, J.**, 2002. Synthesis of MDI from Dimethyl Carbonate over Solid Catalysts, *Industrial & Engineering Chemistry Research*, **41**, 5139–5144.



## **APPENDICES**

### **APPENDIX A.1:** Supplementary Results of the Analyses of the Other High-Chain Fatty Acid Esters

## APPENDIX A.1

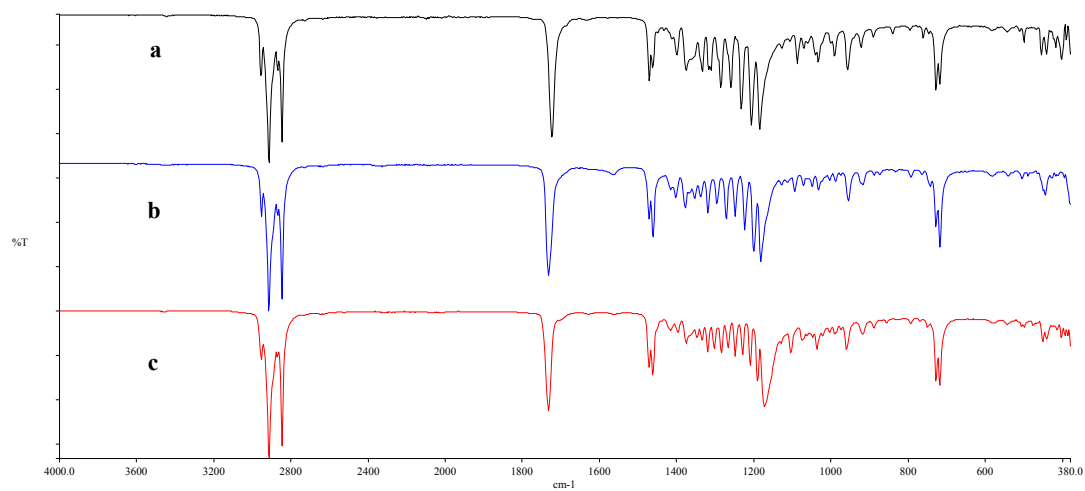


**Figure A.1 :** FT-IR spectra of (a) 14 – 13, (b) 14 – 15 and (c) 14 – 19.

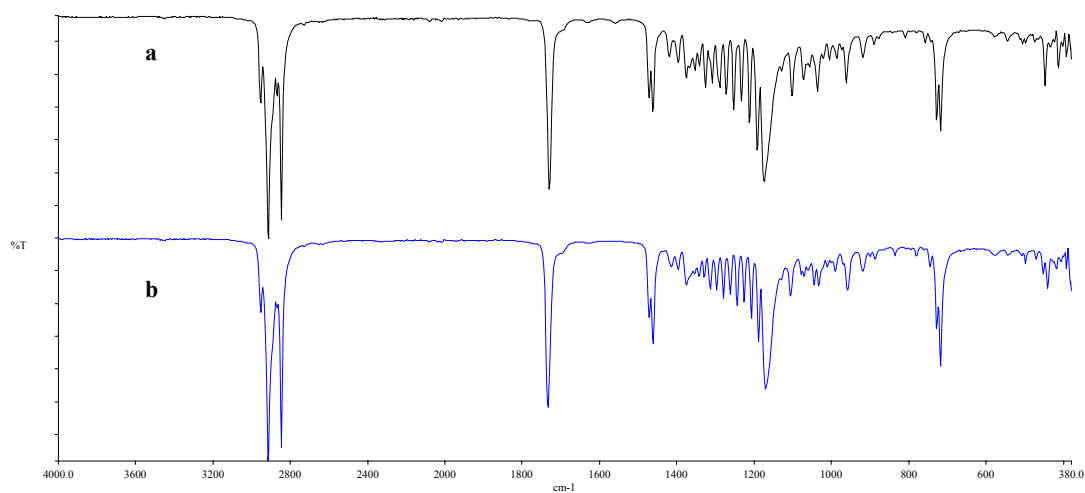


**Figure A.2 :** FT-IR spectra of (a) 14 – 18 and (b) 14 – 20.

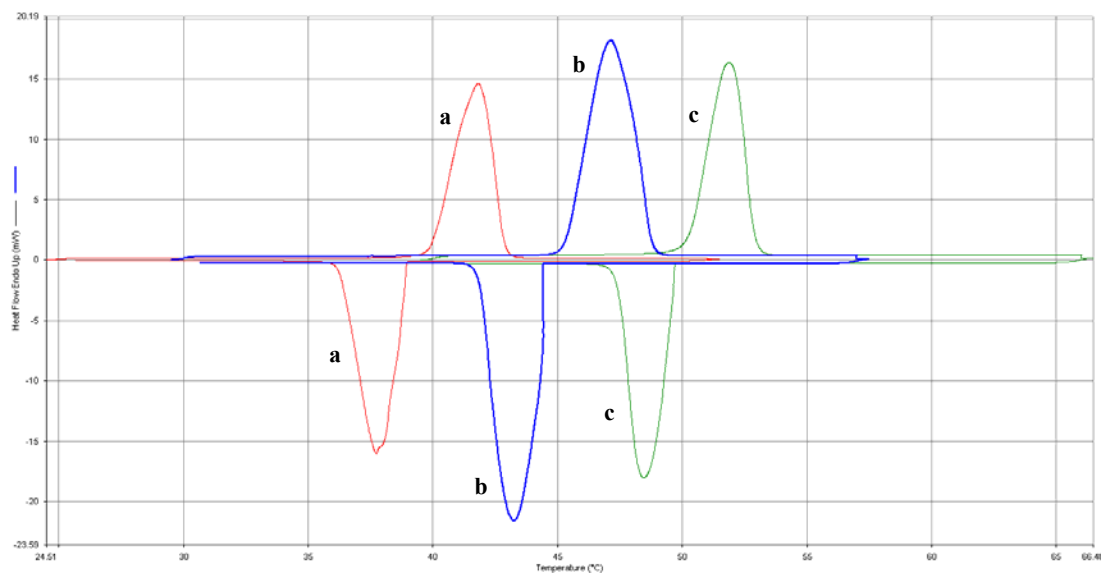


**Figure A.3 :** Heat flow graphs of (a) 14 – 13, (b) 14 – 15 and (c) 14 – 19.

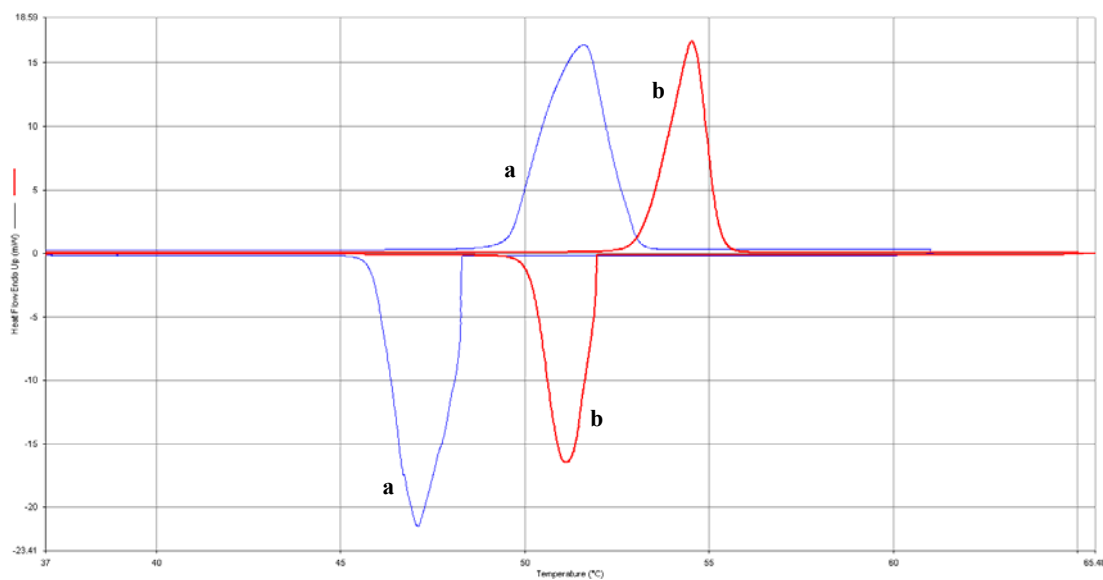


**Figure A.4 :** Heat flow graphs of (a) 14 – 18 and (b) 14 – 20.

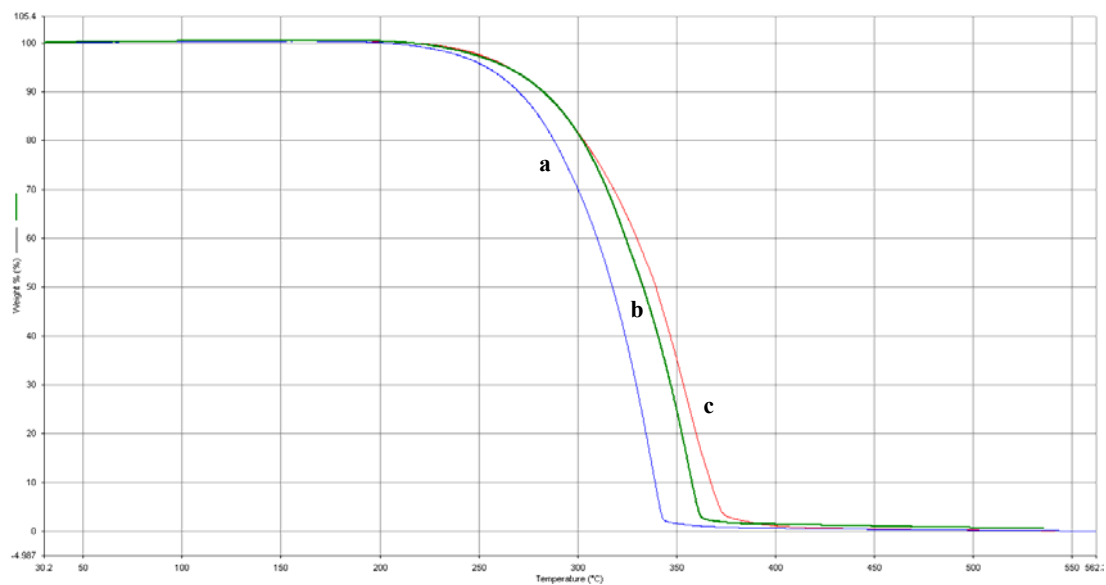


**Figure A.5 :** Thermal decomposition graphs of (a) 14 – 13, (b) 14 – 15 and (c) 14 – 19.

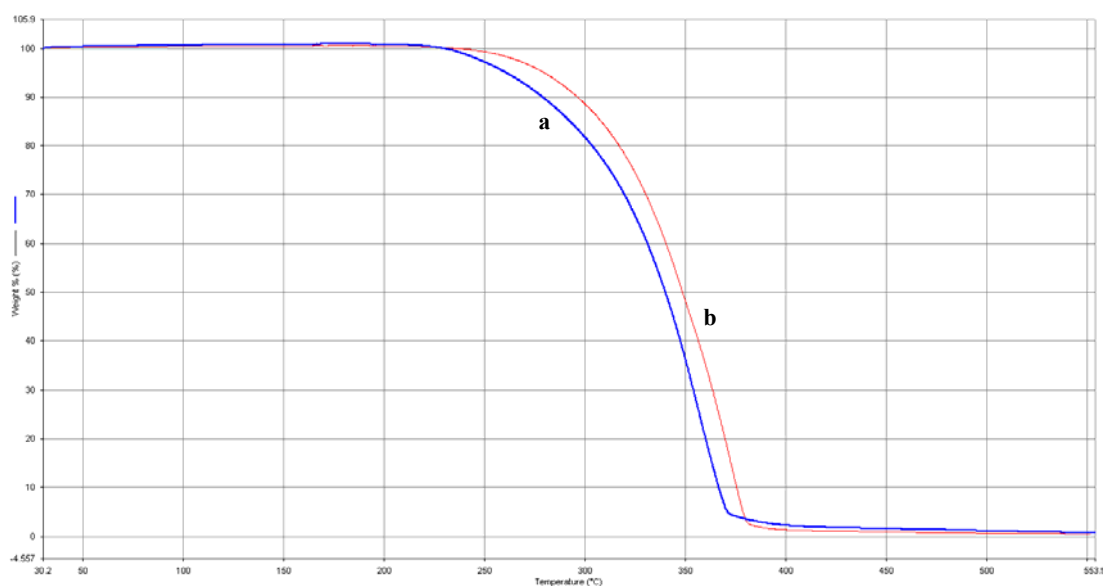


**Figure A.6 :** Thermal decomposition graphs of (a) 14 – 18 and (b) 14 – 20.

## CURRICULUM VITA



**Candidate's full name:** Ahmet Alper AYDIN

**Place and date of birth:** Istanbul, 1981

**Permanent Address:** Ulus Vadi Konutları B1 Blok D13, Öztöpüz Cad.  
34340 Ulus / Istanbul

### Universities and Colleges attended:

2003 – 2005	MSc	Istanbul Technical University Chemical Engineering
2003 – 2005	MSc	Marmara University Engineering Management
1999 – 2003	BSc	Istanbul Technical University Chemical Engineering

### Publications:

- 1) Garaevaa, S. R., **Aydın, A. A.**, Aydın, A., Yalçın, B., Fatullaevaa, P. A., Medzhidovc, A. A., “*Composition, Properties, and Application of Products Formed in Oxidation of Polyethylene by Nitric Acid*”, *Russian J. Appl. Chemistry*, 83, 97-101, (2010).
- 2) Christian, M., Ilberg, V., **Aydın, A. A.**, Titze, J., Friess, A., Jacob, F., Parlar, H., “*New Gushing Mechanism Proposed by Applying Particle Size Analysis and Several Surfactants*”, *BrewingScience*, 62, 100-107, (2009).

**3) Aydın, A. A.,** Erciyes, A. T., Okutan, H., “*Sulfur Dioxide Solubility in Heat Transfer Oil in the Temperature Range of (293.15 to 313.15)K: Experimental Results and Related Correlations*”, *J. Chem. Eng. Data*, 51, 1289-1293, **(2006)**.

**4) Aydın, A.,** Kaki, E., **Aydın, A. A.,** “*Gold Leaching by Use of an N,N'Disubstituted Thiourea*”, *Sep. Sci. & Tech.*, 36, 3239 – 3251, **(2001)**.

#### **International Presentations:**

**1) Christian, M.,** Ilberg, V., Titze, J., **Aydın, A. A.,** Jacob, F., Parlar, H., New Cognitions on the Gushing Phenomenon, 32<sup>nd</sup> EBC Congress, 10-14 May 2009, Hamburg, Germany.

**2) Christian, M.,** Ilberg, V., Titze, J., **Aydın, A. A.,** Jacob, F., Parlar, H., New Cognitions on Gushing Characteristics of Malt, First International Symposium for Young Scientists and Technologists in Malting, Brewing and Distilling, 6-7 November 2008, Cork, Ireland.